Molecular Control of Pyramidal Neuron Fate Determination in the Developing Neocortex

PhD Thesis

in partial fulfilment of the requirements
for the degree "Doctor of Philosophy (PhD)/Dr. rer. nat."
in the Neuroscience Program
at the Georg August University Göttingen,
Faculty of Biology

Submitted by

Srinivas Parthasarathy

born in

Chennai, India

Göttingen, 2014

Declaration

This thesis has been written independently and with no other sources and aids than quoted.

Srinivas Parthasarathy

28th March 2014, Göttingen.

TABLE OF CONTENTS

TABLE OF FIGURES

ACKNOWLEDGMENTS

There are so many people who were responsible for making sure things turned out the way they did, and to them I owe a debt of gratitude.

Firstly, none of this would have happened (and I mean this in the nicest way possible!) without the support of my supervisor- Prof. Victor Tarabykin. Having spent close to half a decade working with him, I probably have taken all that he did and does for me, granted. For the great supervision he provided, for never letting his excitement levels drop and most importantly, for supporting me at every stage of my PhD- Thank you Victor!

Considering that a PhD student spends more than half his day in the lab, life would have been extremely boring and hard, had it not been for the great people I encountered in the lab- Anjana, for supporting and mentoring me during my initial steps; Manu- for being an inspiration to all who strive to be a perfectionist in the lab; Ingo- for being a storehouse of patience and possessing a godly nature of going out of the way to help anyone; Kuo- for all our fun filled moments, Marta for all the great advice and support and everyone else in the lab over the years whom I've greatly enjoyed working with.

I would also like to thank Roman, Denis, Jutta and Marni for all the technical and administrative support they have extended to me over the years. I would also like to acknowledge everyone in the Institute for Cell and Neurobiology, for providing a great collaborative environment to work in. I would specially like to thank Ele, for being a very special friend- I'll miss our coffee breaks!!

My PhD wouldn't have been half as special without my association with the Boehringer Ingelheim Fonds. My heartfelt gratitude to the entire BIF team for supporting my PhD so generously, believing in my project, making me feel so special and most importantly organizing our BIF meetings, which according to me are the golden standard for any kind of scientific meeting.

A warm note of thank you to Prof.Michael Hörner, Sandra Drube and the neuroscience program for talking such good care of us. I would also like to thank my thesis committee members-Dr.Judith Stegmüller and Dr.Till Marquardt for their invaluable suggestions and time.

Finally, the person whom I would like to thank the most for making this entire journey so memorable- Swathi. I'm so glad you decided to join the lab when you did! Science would have probably seen new lows had it not been for the support I found in you. Living away from home, I found the greatest friend in you one could ask for. We literally shared almost every single waking moment with each other during the last four years- and for that one reason alone, I'd say a PhD wasn't that hard!!

Most importantly, my family- who has probably still not made me feel I live away from home and will always be my biggest support! My dad for inspiring me to be a workaholic (and yes that's a good thing), my mom for still spending her day thinking if I'm fine, my grandmother for teaching me that learning never ends and my sister- apart from all that she means to me….for giving us our biggest bundle of joy- my lil nephew Ranga!

And last and most importantly- my Acharyan HH the 45th jeeyar of Sri Ahobilam Mutt. I long to see his smile everyday that I live!

ABSTRACT

The pyramidal neurons of the neocortex, which form the neural substrate for our higher cognitive abilities, arise from a single layer of neuroepithelium lining the dorsal ventricles. It has been of immense interest to study how cell fate specification within the developing cortex dictates the generation of these numerous classes of pyramidal neurons from a small pool of cortical progenitors.

Others and we had previously shown that postmitotic neurons signal back to their progenitors and instruct the timing of cell fate switch. This process governs both the switch from producing one neuronal type to the other and from neurogenesis to gliogenesis. We have previously shown that Fgf9 controls the switch from neurogenesis to gliogenesis. While a similar mechanism governing the switch from deep layer to upper layer neuronal production was predicted, the precise molecular pathway was not shown.

In this thesis, we show that the neurotrophin Ntf3, signals back to cortical progenitors and initiates the shift from deep to upper layer cell fate. It does so by shifting the ratio of apical progenitors to basal progenitors, which in turn govern the production of cortical neurons.

We go on to show that the effect of Ntf3 is most likely mediated by the truncated- Non Catalytic isoform of TrkC- NC-TrkC. NC-TrkC, to our knowledge, is the first molecule to show an expression pattern that parallels the timing of deep layer neurogenesis. Through gain-of-function experiments, we show that *NC-TrkC* expression tilts neurogenesis in favor of deeper layer neurons. We also show that the effect of NC-TrkC is most likely through the negative regulation of ERK signaling. We provide further evidence that signaling via the binding site for the signaling molecule Shc, on NC-TrkC is important for its role in cell fate determination. Further, we show a novel interaction between NC-TrkC and the BMP class I receptor BMPRIA. These receptors interact *in vitro* and *in vivo.* The genetic programs controlled by them interact to govern neuronal fate during corticogenesis.

Finally, we study the role of a family of transneuronal cytokines-Cbln, as molecules that function in parallel to Ntf3 in controlling neuronal fate switch in the cortex. We show that over-expression of the Cbln family members can also alter the proportions of apical and basal progenitors, thereby providing insights into new modes of signaling between postmitotic neurons and their progenitors.

INTRODUCTION

1. Cortical Development

The mammalian neocortex is a six-layered structure that is considered to be responsible for our higher cognitive abilities. Within the neocortex hundreds of different cell subtypes are arranged into specific neuronal networks that are engaged in receiving, processing and responding to complex stimuli. The neocortex consists of two major neuronal subtypes- excitatory projection neurons and inhibitory interneurons. While interneurons are born in the ganglionic eminence, cortical projection neurons arise from progenitors lining the dorsal aspects of the lateral ventricles. These progenitors give rise to the different cortical layers sequentially. During this process, later born neurons must migrate past earlier born neurons to occupy their final position in the cortex, thus giving rise to the 'inside first-outside last' cortex (Angevine and Sidman, 1961; Rakic, 1974). The various layers of the cortex show a high degree of heterogeneity with respect to their functions. This correlates to the fact that these neurons also show great variation with respect to their molecular and morphological characteristics (Fishell and Hanashima, 2008). However, such a diverse group of neurons are born from a relatively homogenous progenitor population. Thus, how progenitors undergo successive fate restriction to generate the entire repertoire of cortical neurons, has invited detailed study and research over the last two decades.

1.1 Types of Progenitors

The developing cortex can be sub-divided into the ventricular zone (VZ), subventricular zone (SVZ), Intermediate zone (IZ) and the cortical plate (CP). The earliest born cortical neurons form the preplate. Subsequently born neurons split the preplate to form the outer marginal zone and the inner subplate. The subplate comprises of a group of transient neuronal populations, which are mostly important

for their pioneering function in early axonal guidance (McConnell et al., 1989).

1.1.1 Ventricular zone

The ventricular zone is the primary progenitor pool for the developing neocortex. The primitive cortical VZ comprises of neuroepithelial cells. These early neuroepithelial cells, owing to their interkinetic nuclear movement, give the appearance of a pseudo-stratified structure. With the beginning of neurogenesis, neuroepithelial cells give birth to radial glial cells which in-turn serve as the main progenitor population for the cortex. Radial glial cells maintain certain epithelial like characteristics in addition to developing astroglial features. The epithelial characteristics include the maintenance of strong apical-basal polarity, interkinetic nuclear movement and the expression of epithelial markers such as the intermediate filament- Nestin. Radial glial cells also undergo mitotic division with their nuclei at the apical surface, similar to neuroepithelial cells. However, unlike neuroepithelial cells, their interkinetic nuclear migration does not span the entire apical-basal length of the cell. Their astroglial features include the expression of the glial fibrillary acidic protein (GFAP), brain lipid binding protein (BLBP), the Ca^{2+} binding protein S100ß and the astrocyte specific glutamate transporter GLAST (Götz and Huttner, 2005).

Radial glial progenitors also undergo either symmetric or asymmetric division. Symmetric divisions give rise to two progenitors, thus increasing the progenitor pool. Symmetric divisions arise as result of a vertical (perpendicular to the apical surface) cleavage plane. Asymmetric divisions on the other hand give rise to a progenitor and a neuron (Iacopetti et al., 1999; Miyata et al., 2001; Noctor et al., 2004; Götz and Huttner, 2005).

Radial glial progenitors serve as the source for all projection neurons, oligodendrocytes and astrocytes that inhabit the future cortex (Malatesta et al., 2000; Anthony et al., 2004). These radial glial cells

have been shown to not only generate neurons, but also provide a scaffold for the young neuron to migrate on (Rakic, 2003). Retroviral lineage tracing experiments showed that radial glia give rise to clones of neurons that migrate along the radial glial process, giving rise to radial columns (Noctor et al., 2001). Radial glia are marked by the expression of the transcription factor Pax6 (Heins et al., 2002; Englund et al., 2005a). Pax6 promotes the asymmetric and hence neurogenic cell division of apical progenitors, which is supported by the finding that the number of neurons in the cortex are reduced by half in the Pax6 mutant (Heins et al., 2002).

1.1.2 Subventricular Zone

The cortical subventricular zone (SVZ) harbors another type of progenitor termed as basal or intermediate progenitors. Radial glial progenitors give rise to these basal or subventricular zone progenitors, thereby serving as the direct or indirect source of all cortical neurons. These basal progenitors have also been shown to contribute to neurogenesis (Haubensak et al., 2004; Noctor et al., 2004). While basal progenitors are present from the very beginning of neurogenesis, they are believed to contribute more towards the production of upper layer neurons (Tarabykin et al., 2001; Haubensak et al., 2004; Zimmer et al., 2004; Arnold et al., 2008). However, it has also been shown that they are capable of producing all the different layers of the cortex (Kowalczyk et al., 2009). Basal progenitors undergo symmetric divisions, giving rise to two neuronal cells (Haubensak et al., 2004; Noctor et al., 2004). Thus, basal progenitors are believed to help increase the number of neurons produced from a single apical progenitor by acting as an intermediate amplification step (Götz and Huttner, 2005). The proportion of basal progenitors has increased with mammalian and primate evolution and is believed to be one of the reasons for the increase in the size of the neocortex seen in higher

primates (Martínez-Cerdeño et al., 2006; Nonaka-Kinoshita et al., 2013b; Stahl et al., 2013).

Basal progenitors are marked by the expression of the non-coding RNA *SVET1* and the transcription factor Tbr2 and Cux2 (Tarabykin et al., 2001; Zimmer et al., 2004; Englund et al., 2005). Inactivation of the Tbr2 gene leads to a reduction in the number of basal progenitors and a concomitant reduction in the number of cortical upper layer neurons (Arnold et al., 2008).

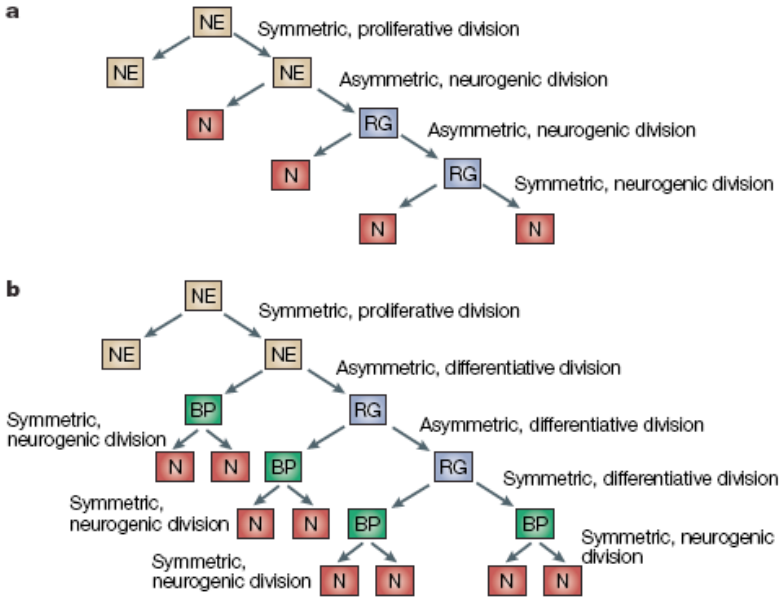

Figure 1. Lineage tree of Neurogenesis.
Adapted from (Götz and Huttner, 2005). During cortical development neuroepithelial cells (NE) give rise to radial glial (RG) cells, which in turn give rise to neurons. Alternatively, RG cells give rise to basal progenitors (BP), which serve to amplify the number of neurons generated per RG cell.

1.2 Progenitor Cell fate switch

Similar to all progenitor populations, cortical progenitors too loose their multi-potency over time. As development progresses, cortical progenitors become more restricted with respect to the types of cells they can produce. Individual cortical progenitors cultured *in vitro* can

faithfully recapitulate the entire sequence of corticogenesis (Shen et al., 2006). This suggests that successive fate restriction is hardwired into a progenitor cell. Cortical progenitors also show an increase in cell cycle length with progression of neurogenesis, suggesting that the cell cycle length and neural cell fate are intertwined (Takahashi, 1995). Interestingly, progenitors briefly over-expressing a constitutively active form of the Notch receptor at early stages, leading to increased cycling of progenitors, skip the production of deep layers and start generating upper layer neurons (Mizutani and Saito, 2005).

Transplantation experiments showed that when younger cortical progenitors are transplanted into an older brain, they adapt to producing neurons appropriate to their new environment (Desai and McConnell, 2000). This would suggest that environmental cues also dictate the ability of a progenitor to produce one neuronal subtype over another. However, consistent with the progressive fate restriction theory, older progenitors when transplanted into an younger environment, do not adapt and continue to produce late born upper layer neuron (Desai and McConnell, 2000). Thus, collectively it is well established that while cortical progenitors undergo self programmed fate restriction, environmental cues influence this process to a large extent.

More recent work has even suggested the presence of lineage specific progenitors, as compared to the multi-potent progenitor theory. Using genetic fate mapping, Cux2 was shown to label upper layer neuron specific radial glial cells (Franco et al., 2012). These progenitors were shown to undergo symmetric divisions during early cortical development, thus increasing the progenitor pool, and undergoing neurogenic divisions during mid-late corticogenesis (Franco et al., 2012). However, work by others has contradicted this finding, wherein Cux2 positive radial glial cells were shown to generate all the different layers of the cortex (Guo et al., 2013). This work also showed that the transcription factor Fezf2 marks radial glial progenitors that also give

rise to cortical neurons of all layers and then subsequently to glia (Guo et al., 2013).

Work from our lab suggested that cortical postmitotic neurons signal back to the progenitors thereby forming a negative feedback loop (Seuntjens et al., 2009). We proposed that neurons within each cortical layer signal back to the progenitors, instructing them to change their fate and start producing the next layer of neurons. This would ensure that neurons of a particular kind are not over-produced, thereby laying the foundation for the generation of the different layers at the right time and in the right amount.

While, others and we had shown the presence of such signals initiating the switch from neurogenesis to gliogenesis, no formal evidence was provided for the existence of such a mechanism for controlling inter-layer fate switch during neurogenesis (Barnabé-Heider et al., 2005; Seuntjens et al., 2009).

In this study, we have looked at the Neurotrophin Ntf3 and it's role in cortical feedback signaling and cell fate determination.

1.3 Cortical Cell Identity

The different layers of the neocortex express a unique set of transcription factors that govern the appropriate maturation of these neurons. The six layers of the cortex can be divided into the following classes:

a) **Layer VI**: Layer VI neurons mostly project to the thalamus. They express markers such as Sox5, Tbr1 and FoxP2. These neurons are largely born between E11.5 and E13.5 in the mouse, with the peak of production being E12.5.

b) **Layer V Cortico-fugally projecting neurons**: Principle output neurons of the cortex. Express the layer markers Ctip2, ER81 and are easily recognized by their large cell body and long apical dendrite. Layer V neurons mostly project to the spinal cord, optic tectum

(superior colliculus), principle and spinal trigeminal nuclei and the striatum. These neurons are born between E12.5 and E14.5 in the mouse, with the peak of production being E13.5.

c) **Layer V Callosally Projecting Neurons**: These neurons also occupy layer V, but project interhemispherically via the corpus callosum. These neurons do not express the marker Ctip2, but instead express the transcription factor Satb2. They are born at the same time as layer V cortico-fugal projection neurons.

d) **Layer IV**: The principle input layer for the cortex, which receives connections from the thalamus. They express the layer marker Rorß and are different in morphology from the rest of the cortical neurons. These neurons are born between E13.5 and E14.5 in the mouse.

e) **Layer II-III**: These neurons are the last-born neurons of the cortex. They are generated between E14.5 and E16.5, with E15.5 being the peak of upper layer neuronal production. They express markers such as Brn1, Brn2, Cux1, Cux2 and Satb2. These neurons primarily project interhemispherically through the corpus callosum and to other cortical areas intrahemispherically.

f) **Layer I**: Also called the molecular layer or the marginal zone is a largely cell free layer. It is also the only cortical layer born outside the cortex. The apical dendrites of cortical neurons terminate here and branch extensively. This layer is occupied by Cajal-Retzius cells that act as a source of Reelin, which plays an important role in controlling migration of cortical neurons.

2. Sip1 controls cortical feedback signaling

Sip1 or Smad-interacting-protein-1 was identified as a postmitotic specific transcription repressor. Sip1 was shown to interact with the activated Smads and *SIP1* mutations have been implicated in the Mowat-Wilson syndrome (Verstappen et al., 2008). *Sip1* mutants fail to develop beyond E9.5 and show defects in neural tube closure and

defective cranial neural crest cell migration (Van de Putte et al., 2003). *Sip1* conditional mutants (crossed to either Nex-Cre or Emx1-Cre) showed a reduction in deeper layer cortical neurons and an increase in upper layer neurons. BrdU birth-dating experiments showed that this was a result of a premature end of deep layer neuronal production coupled to precocious upper layer neuronal generation. This was followed with a premature end of neurogenesis and an early onset of gliogenesis (Seuntjens et al., 2009). Thus Sip1 was hypothesized to be a postmitotic specific transcription factor controlling cortical feedback signaling. In the absence of *Sip1*, these signals are heightened prematurely, leading to an early cell fate switch. Indeed, Sip1 was shown to regulate the expression of *Fgf9*, which signals from postmitotic neurons to progenitors instructing the shift from neurogenesis to gliogenesis. Fgf9 coated agarose beads, when ectopically placed within the cortical plate, lead to an enhanced number of Olig2 positive oligodendrocytic precursors. Similarly, Sip1 was shown to regulate the expression of *Ntf3*, a well-characterized neurotrophin. Since *Sip1* mutants showed an upregulation of *Ntf3* expression coinciding with the shift from deep layer to upper layer neurogenesis, it was hypothesized that Ntf3 acts as a feedback signal during neurogenesis. Although no formal experiment validating the presence of such cortical feedback signaling during neurogenesis was performed (Seuntjens et al., 2009).

In this current work, we investigated the role of Ntf3 and the signaling pathway downstream that causes a shift from deep layer to upper layer neurogenesis.

3. Neurotrophin Signaling

Neurotrophins are a class of small-secreted molecules that have profound influence on a large variety of neuronal functions. Neurotrophins and their receptors are relatively new in evolution and cannot be found in *D.melanogaster* and *C.elegans*. This paved way for

the thinking that these molecules are not essential for the development of neuronal circuitry. Indeed, deletion of the neurotrophins does not affect early development in mammals (Chao, 2003). The neurotrophin family primarily consists of Nerve growth factor (NGF), Brain-derived-neurotrophic factor (BDNF), Neurotrophin factor 3 (Ntf3) and Neurotrophin factor 4(NT-4). Each of the family member binds to a specific Tropomyocin related kinase (Trk) receptor with maximum affinity and to a lesser extent with one or more of the other receptors. Trks are a family of receptor tyrosine kinases with NGF binding to TrkA, BDNF and NT-4 to TrkB and Ntf3 to TrkC (Cordon-Cardo et al., 1991; Klein et al., 1991; Lamballe et al., 1991; Soppet et al., 1991). While TrkA is largely expressed in the Peripheral nervous system (PNS), TrkB and TrkC are expressed within the CNS (Klein et al., 1990; Martin-Zanca et al., 1990; Lamballe et al., 1991). In addition, the Trk receptors interact with another receptor termed p75-NTR. Interaction of Trk receptors with p75-NTR can alter their binding affinity for neurotrophins (Chao, 2003).

Neurotrophin signaling begins upon ligand binding to its cognate Trk receptor, which leads to receptor dimerization (Lamballe et al., 1991; Jing et al., 1992; Lemmon and Schlessinger, 1994). Upon dimerization, the receptors autophosphorylate specific tyrosine residues, which serve as docking stations for downstream effector molecules. The classical Neurotrophin-Trk signaling involves the recruitment and phosphorylation of either the downstream adaptor molecule Shc or PLC-γ. These in-turn activate the PI3K or ERK pathways (Chao, 2003).

Trk receptor mediated signaling has been shown to be important in the context of the developing cortex. Over-expression of dominant negative TrkB or TrkC leads to a decrease in progenitor proliferation of cortical progenitors (Bartkowska et al., 2007). TrkB mutant mice also display migration defects in the cortex. While single mutants for the Shc or Plc-γ binding site does not display major defects, cortical neurons

carrying mutations in both these sites, show defects similar to the TrkB knock-out (Medina et al., 2004).

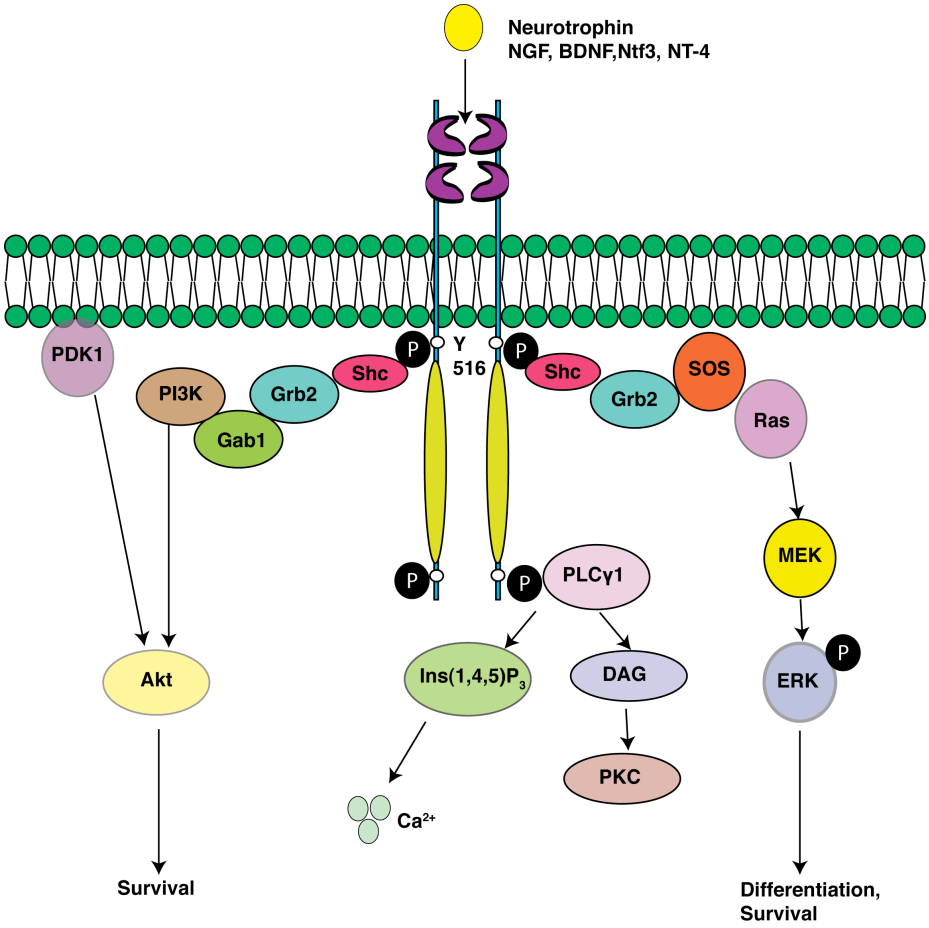

Figure 2. General scheme for Trk mediated intracellular signaling.
Modified from (Chao, 2003; Minichiello, 2009). Ligand binding induces receptor dimerization leading to autophosphorylation of the receptors. Phosphorylation of the tyrosine at residue 516 (in TrkC) leads to recruitment of ShcA. Phosphorylation of Shc1 in turn leads to the activation of the Akt or ERK pathway. Alternatively, phosphorylated Trk(s) recruit Plcγ1 and thereby activate the PKC or the Ins(1,4,5)P_3 pathways.

The identification of alternate splice variants of the Trk receptors has further fuelled interest in understanding the signaling cascade downstream of these receptors (Klein et al., 1990; Middlemas et al., 1991; Fenner, 2012). Splice variants of TrkB and C have been reported, in each case lacking the intracellular kinase domain (Tsoulfas et al., 1993; Valenzuela et al., 1993). Interestingly, the

number of alternate splice variants for TrkC and TrkB has increased with mammalian evolution, suggesting that the fine control of signaling cascades downstream of these receptor-isoforms might play an important role.

While these receptors bind to their neurotrophin partner with the same affinity as the full-length receptors, they are incapable of initiating a signaling cascade. This hence encouraged the idea that these receptors act as dominant negative isoforms, impairing the classical signaling pathways (Dorsey et al., 2012; Yanpallewar et al., 2012). However, a plethora of recent work has shown that these receptors not only initiate signaling cascades; they are also most often different from the classical signaling pathways (Rose et al., 2003; Esteban et al., 2006; Carim-Todd et al., 2009; Renn et al., 2009; Fenner, 2012). In addition, owing to the lack of a catalytic domain, research into the possibility of these receptors employing different signaling molecules has lead to the discovery of new binding partners (Esteban et al., 2006). Additionally, in some systems the expression pattern of the different isoforms is non-overlapping, which is further suggestive of the divergent functions of the full length and truncated isoforms (Menn et al., 1998, 2000). In some systems the different isoforms have also been shown to modulate each other's expression levels. For example, excitotoxicity in hippocampal neurons leads to the downregulation of the full length *TrkB* and an increase in the expression of the truncated *TrkB* (Gomes et al., 2012).

In the current study we focus on the role of Ntf3 and the truncated TrkC isoforms- NC-TrkC (Non catalytic-TrkC) in cortical neuronal fate switch.

3.1 Shc interaction with TrkC

Ligand dependent receptor autophosphorylation of TrkC at tyrosine 516 leads to the recruitment of the downstream adapter molecule Src homologous and collagen-like adaptor protein (Shc). Although some results suggest that Shc maybe constitutively bound to the Trk receptors and only a conformational change occurs upon the phosphorylation of Y516 (De Vries et al., 2010). Three *shc* genes, namely *ShcA*, *ShcB*, *ShcC* have been identified in mammals (Ravichandran, 2001). Three different isoforms of ShcA are found- p66, 52 and 46. Though, initially considered to be ubiquitously present, more recent work has shown that both *ShcA* mRNA and protein are down-regulated upon neuronal differentiation and is replaced by *ShcC* in postmitotic neurons (Conti et al., 2001). *ShcA* expression pattern within the developing cortex coincides with the proliferative neurogenic ventricular zone, thus suggesting an important role in controlling corticogenesis (Conti et al., 1997). ShcA contains an SH2-phosphotyrosine binding domain and a PTB domain, which also binds phosphotyrosines. Further, phosphorylation of ShcA on different Tyrosines and Serine/ Threonine leads to the initiation of downstream signaling cascades. The site of phosphorylation has been linked to the diversification of the downstream signaling cascade initiated (Zheng et al., 2013). Interestingly, recent work showed that ShcA is additionally phosphorylated on Serine 29, upon EGFR stimulation. This Serine phosphorylation however occurs a little later than the Tyrosine phosphorylation initiated by the receptor itself (Zheng et al., 2013). This raises the question as to whether receptor tyrosine kinases (of which the Trks are a subclass) may also interact with other Serine/Threonine kinases, which could be responsible for this Serine phosphorylation.

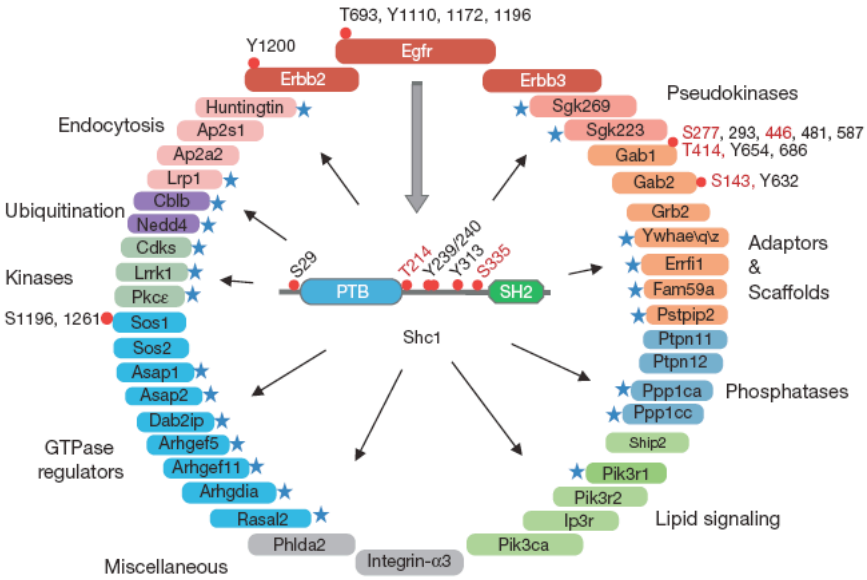

Figure 3. ShcA protein interactome
(adapted from (Zheng et al., 2013)). Receptor Tyrosine kinase activation leads to the recruitment and phosphorylation of ShcA. ShcA in-turn interacts and regulates a wide range of proteins with diverse functions. ShcA is also phosphorylated on multiple Tyrosines and Serine/Threonines, which are believed to modify the function and targets of ShcA.

4. BMP signaling and BMP receptors

An important part of the work presented in this thesis focused on the role of NC-TrkC in regulating cell fate decision in the cortex. Since, NC-TrkC does not have any intracellular kinase domain, we wondered if it could interact with other receptors that could serve as co-receptors. Amongst the family of proteins we studied, we found an interaction between NC-TrkC and the BMP class I receptor BMPRIA.

BMPs are members of the TGFß protein family of extracellular ligands. The TGFß superfamily also includes, apart from the BMPs, TGFß and Activin subfamilies. Each of these extracellular ligands bind to two types of receptors- Class I (ALK2, ALK3/BMPRIA and ALK6/BMPRIB) and Class II (BMPRII, ACTRIIA, ACTRIIB) (Liu and Niswander, 2005). These receptors belong to the class of receptor Serine-Threonine kinases. Upon ligand binding, Class I receptors heterotetramerize with Class II receptors, which in turn now phosphorylate and activate the

Class I receptors. Activated Class I receptors now recruit downstream effectors called R-Smads (receptor activated- Smads) and phosphorylate these in turn. The activated R-Smads multimerize with Co-Smad (common mediator Smad/Smad4) and translocate to the nucleus, where they regulate gene expression. Bmp signaling employs Smads 1, 5, 8 while TGFß signaling uses Smad 2 and 3. Inhibitory Smads 6 and 7 compete with R-Smads for binding to the receptor, thereby modulating the downstream signaling pathway (Liu and Niswander, 2005; Anderson and Darshan, 2008; Guo and Wang, 2009).

During early embryogenesis, BMP signaling needs to be blocked for neural induction. Later, BMP signaling has been shown to be necessary for the development of dorsal neural structures. The roof plate that forms post the closure of the neural tube, acts as one of the main sources of BMPs (Liu and Niswander, 2005). This dorsal BMP signaling is also necessary for the development of neural crest cells, which give rise to the PNS, amongst other cellular populations (Dickinson et al., 1995). The roof plate and dorsal neural tube derived BMPs have been shown to play a critical role in the dorso-ventral patterning of the spinal cord (Nguyen et al., 2000). Ectopic over-expression of constitutively active forms of the BMP class I receptors in the ventral spinal cord has been shown to induce dorsal cell identities (Timmer et al., 2002).

Bmp signaling has also been shown to play an important role within the developing cortex. Bmp signaling was shown to promote cell death and inhibit the proliferation of early cortical precursors *in vitro* (Mabie et al., 1999).

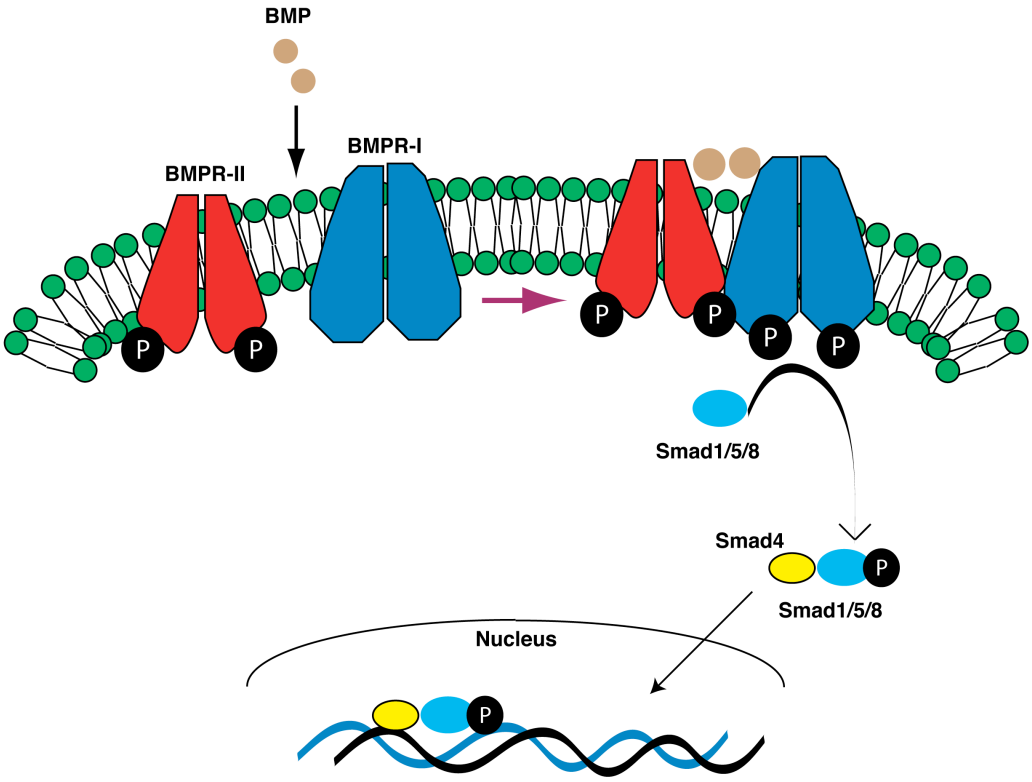

Figure 4. General scheme for BMP signaling.
Modified from (Anderson and Darshan, 2008). Ligand binding leads to the multimerization of BMPR class II and I. Class II receptors then phosphorylate Class I receptors which leads to the recruitment and phosphorylation of R-Smads 1/5/8. Activated R-Smads now bind to the Co-Smad (Smad4) and translocate to the nucleus to affect gene regulation.

Transgenic mice that express a constitutively active form of BMPRIA showed that signaling via the IA receptor leads to the generation of dorsalized precursor. Signaling via BMPRIB was however shown to lead to mitotic arrest and differentiation (Panchision et al., 2001). BMPRIA null mutants have a shortened cell-cycle length in the ventral SVZ (Samanta et al., 2007). Meningial BMP7 is also known to inhibit the formation of the corpus callosum (Choe et al., 2012).

Here, we study the role of the BMP class I receptor BMPRIA in cortical development and the interaction of the pathways governed by NC-TrkC and BMPRIA.

5. Cbln family of Transneuronal cytokines

In this current study, we also investigated if factors apart from the up-regulation of *Ntf3* in the *Sip1* mutant cortex could also be responsible for the enhanced feedback signaling seen in these mutants. We found through microarray analysis that a member of the transneuronal cytokine-*Cbln4* was upregulated in the *Sip1* mutant cortex (Nityanandam, 2009). Cbln4 belongs to a family of four-transneuronal cytokines: Cbln1-Cbln4. These molecules belong to the C1q/tumor necrosis factor (TNF) superfamily (Bodmer et al., 2002; Kishore et al., 2004). While Cbln1, 2 and 4 are secreted; Cbln3 is localized to the endoplasmic reticulum (ER). Cbln3 is secreted only in conjugation with one of the other three family members. All four members form homo and heterodimers and are secreted as glycoproteins (Iijima et al., 2007). Cbln1 is the only family member with well-characterized functions. Cbln1 acts as a ligand for the GluR∂2 receptor and functions as both a pre and postsynaptic organizer (Matsuda et al., 2010). Cbln1 is also known to bind to Nrxn1, thus mediating the trans-synaptic interaction of GluR∂2 and Neurexins (Uemura et al., 2010). However, the function of these molecules at earlier stages of development is largely unknown. Cbln1, 2 and 4 expression has been detected as early as embryonic day 10-13 in the mouse (Miura et al., 2006).

Cbln4 has been shown to function as a ligand for the Netrin1 receptor-DCC (Wei et al., 2012). Cbln4 competes with Netrin1 for DCC binding, thus making it an important molecule that could aid in axon guidance in the developing brain and spinal cord (Wei et al., 2012).

Here, we investigated if the Cbln family can influence cell fate switch in the developing cortex. We also developed a full length E14.5 cDNA library to screen for new receptors for Cbln4.

MATERIALS AND METHODS

1. Mouse mutants

All mouse experiments were carried out in compliance with German law and according to the guidelines approved by the Bezirksregierung Braunschweig or Landesamt für Gesundheit und Soziales, Berlin. Both male and female mouse embryos were used. Sip1 conditional mutants carried a loxP flanked exon 7 crossed to either Nex or Emx1-Cre (Gorski et al., 2002; Higashi et al., 2002; Goebbels et al., 2006). Ntf3 mutant was kindly provided by Dr.Michael Sendtner, University of Würzburg. *Sip1-Ntf3* double mutants were generated by crossing $Sip1^{loxP/+}Nex^{Cre/wt}$ $Ntf3^{+/-}$ parents. The day of vaginal plug was considered as E0.5

2. Genotyping

Tail tissue was digested in 0.3ml Lysis buffer (100mM Tris- HCl pH8.5, 5mM EDTA, 200mM NaCl, 0.2% SDS, 100µg/ml Proteinase K) at 55°C for 2hrs to overnight. Strands of hair were removed by centrifugation at 9000 rpm for 5 minutes. The DNA in the supernatant was precipitated by adding 300µl of isopropanol, followed by vigorously mixing and centrifugation at 13000 rpm for 15 minutes. The DNA precipitate was washed in 80% ethanol, air dried and re-suspended in 100 to 200µl sterile distilled water.

All PCR reactions were prepared in a final volume of 20µl containing the following:

10x Buffer (Genecraft) -	2µl
10mM dNTPs (Invitrogen) -	0.4µl
10nmol/ml Forward/Reverse primers -	0.4µl each
GoTAQ polymerase (Promega) -	0.1µl

Template DNA -	1µl
ddH2O -	13µl

The following primer sequences and reactions were used-

1. *Sip1*-floxed and wildtype alleles

Forward- 5' TGGACAGGAACTTGCATATGCT 3'

Reverse- 5' GTGGACTCTACATTCTAGATGC 3'

Amplification program-

94°C- 10"

59°C- 20"

72°C- 40"

31 cycles; wildtype allele yields a product of ~450bp and the floxed Sip1 allele yields a product of ~600bp.

2. *Cre* allele (for both Emx1-IRES-Cre and Nex-Cre)

Forward- 5' TCGATGCAACGAGTGATGAG 3'

Reverse- 5' TTCGGCTATACGTAACAGGG 3'

Amplification program-

94°C- 10"

55°C- 30"

72°C- 40"

30 cycles; presence of at least one Cre allele yields a product of ~500bp.

3. Tissue processing

Pregnant females were sacrificed by first anesthetizing with Avertin followed by cervical dislocation. Newborn pups were sacrificed by decapitation. Brains (E15.5 onwards) or whole heads (E12.5-E14.5) were fixed in 4% PFA for 4-8 hrs (E12.5-E15.5) or overnight (E16.5 onwards). Thereafter, the tissue was washed twice in 1X PBS. Following this, the tissue was either processed for cryo sectioning or paraffin sectioning. For cryoprotection, the brains were incubated in

15% and 30% sucrose (5-8 hours each), followed by embedding in OCT (TissueTek) on dry ice. The brains were then sectioned on a Leica cryotome. Alternatively, the brains were passed through a series of ethanol solutions (30%-100%) to progressively dehydrate the tissue. Following which, the brains were incubated in toluol for 6 hours. This was followed by two Paraplast wax incubations for 6-8 hours each at 60°C. The brains were then embedded in paraplast and sectioned into 10µm thick sections using a Leica microtome.

4. Immunohistochemistry

For immunohistochemistry, paraffin sections were dewaxed in xylol. Subsequently, the sections were rehydrated by passing through a descending series of ethanol concentrations. They were then washed in 1X PBS for 10mins, prior to heat mediated antigen retrieval. Using a microwave, the sections were boiled for 3mins in a preheated 0.96% antigen unmasking solution (Vector Labs). The solution was them allowed to cool to 50°C, which was followed by heating again for 3mins in the unmasking solution. After the sections cooled to room temperature, the slides were rinsed in 1X PBS for 10mins. They were then incubated in a blocking solution (2% BSA + 0.3% TritonX-100 in 1X PBS) for 1hr at room temperature (RT) to block all non- specific binding sites on the tissue. Primary antibodies were prepared in the same solution and incubated overnight at 4°C. This was followed by four rounds of 2+3+5+10 min washes in 1X PBS. The sections were then incubated in Alexa or Dylight Fluor- tagged secondary antibodies (1:500 in blocking solution, Molecular Probes or Jackson immunoresearch) for 45-60mins at RT. The slides were then washed twice in 1X PBS for 10mins per wash and incubated either in Hoechst dye 33342 (SIGMA, 1:500) or Draq5 (1:1000, ebiosciences) for 10min and mounted in a fluorescent mounting medium (DAKO Cytomation). For immunostaining of BrdU, the slides were pretreated by incubating

them in pre-warmed 2N HCl at 37°C for 30mins, followed by neutralization in borate buffer (0.1M $Na_2B_4O_7$, pH 8.5). After two washes in PBS, the slides were incubated in blocking solution and processed as described above.

For chromogenic immunohistochemistry using alkaline phosphatase coupled secondary antibodies, the tissue sections were first subjected to antigen retrieval by boiling them for 3mins in a preheated 0.96% antigen unmasking solution (Vector Labs). This was done to ensure inactivation of endogenous alkaline phosphatase. After the washes that follow incubation in the secondary antibody, the sections were washed twice with AP reaction buffer (100mM Tris pH 9.5, 100mM NaCl, 50mM $MgCl_2$ and 0.05% Tween-20). This was followed by addition of alkaline phosphatase substrate (NBT/BCIP, Roche, 1:50 in AP reaction buffer) until the desired staining intensity was reached. The sections were then washed twice in PBS and mounted in an aqueous mounting media.

5. List of Primary Antibodies

Following is the list of Primary antibodies used:

Antigen	Source Species	Dilution	Company
BMPRIA	Rabbit	1:500 WB	Abcam
BrdU	Rat	1:200	Abcam
BrdU	Mouse	1:200	Milipore
Brn2	Goat	1:200	Santa Cruz
Cre	Mouse	1:200	Sigma
Ctip2	Rat	1:250	Abcam
Cux1	Rabbit	1:100	Santa Cruz
ERK1/2	Rabbit	1:1000 WB	Cell Signaling
GFP	Goat	1:500	Rockland

GFP	Chicken	1:1000	Abcam
HA	Mouse	1:500 WB	Sigma
Myc-tag	Mouse	1:2000 WB 1:200 IP	Cell Signaling
p-Smad1/5/8	Rabbit	1:1000 WB 1:100 IHC	Cell Signaling
p-TrkA (490)/TrkB(516)	Rabbit	1:1000 WB	Cell Signaling
Pax6	Rabbit	1:300	Milipore
Phospho-ERK1/2	Rabbit	1:1000 WB 1:100 IHC	Cell Signaling
pTyrosine	Mouse	1:1000 WB	Santa Cruz
Satb2	Rabbit	1:1000/1:300	Generated in the lab
Shc	Rabbit	1:1000 WB	Cell Signaling
Smad1	Rabbit	1:1000 WB	Cell Signaling
Sox5	Goat	1:200	Santa Cruz
Tbr1	Rabbit	1:200	Abcam
Tbr2	Rabbit	1:150	Abcam
TrkC	Rabbit	1:1000 WB 1:100 IHC	Cell Signaling
TrkC-T1	Rabbit	1:100 IP	Rockland

Dylight (Jackson Immunoresearch) or Alexa (Molecular probes) coupled secondary antibodies were used at a dilution by 1:500. HRP linked secondary antbodies (Jackson Immunoresearch) were used for western blot analysis at a dilution of 1:5000.

6. Image Acquisition and Analysis

Images were procured on a Zeiss or leica-SL confocal system. Images were processed using Fiji and Adobe photoshop. Statistical analysis was done using Excel and Graphpad Prism. Student's t-test was used for

measuring statistical significance. Data is presented as mean ± standard deviation, unless specified. Two-tailed student's T-test was used for determining statistical significance.

7. Plasmids

E17.5 telencephalon specific first strand cDNA was used as a template for PCR amplification. Alternatively, P3 genomic DNA was used for cloning promoter sequences.
All clones were verified by DNA sequencing.

The following primers were used for cloning the fragments used for making the anti-sense probe used in *in-situ* hybridization:

GENE	**Forward Primer (5'-3')**	**Reverse Primer (5'-3')**
NC-TrkC	GGGTCTTTTCAAACATAGACAATCA	CTGGAGGAGGCCAGGTTTTTACTT
FL-TrkC	AAGCCAGACACATATGTTCAGCACAT	GCGGCCGCCTACAGATCCTCTTCTGAGA TGAGTTTTTGTTCTCCGCCAAGAATGTCC AGGTAGATCGGG
NC-TrkB	GGGTAGCTGAGATAAAGGAAAGACA	GGGTGGACTTTGAAAGCAATCGTTA
FL-TrkB	ATTATTGGAATGACCAAGATTCCTGT	AATGCCAGAAGCGAGTTAATACTGT
BMPRIA	TCGAATTCGCCGCCACCATGACTCAGCT ATACACTTACATCA	TAGCGGCCGCCTACAGATCCTCTTCTGA GATGAGTTTTTGTTCACCACCAATCTTTAC ATCCTGGGATTCAACC
Cbln1	CGAGGGAGAGGCGTAGTGGCCCGG	GGATGAGGACGCCGTTGCTGGCGG
Cbln2	CCGTAAGGGCTCAGAACGAC	TTAAGGCTACACACACACAG
Cbln4	ATCATCATCTTCCCCTCTGGGGATAT	TGATCTGTGAAACTTTGTGTCTGTCC

The following primers were used for cloning the Promoter sequences used in the luciferase assays:

GENE	**Forward Primer (5'-3')**	**Reverse Primer (5'-3')**
Ntf3	ATCGAATTCCTCTCAGCCTTAACCGGTG GGTGCA	ATCGGATCCTTCGGTCATTCAGTCTCGCC CACCC
Cbln4	ATCGAATTCAAGGCCTGGCAAGCTTTTC TGTTTT	ATCGGATCCCTGCCAAGGTCTGAGGTCA CTTGA

The following primers were used for cloning the full-length cDNA constructs:

GENE	**Forward Primer (5'-3')**	**Reverse Primer (5'-3')**
NC-TrkC	GATATCGCCGCCACCATGGATGTCTCTC TTTGCCCAGCC	ACCTCGAGAAAGCCATGACGTCCTTTGCT GAAAT
NC-TrkC ΔECD	CTGGGCACGGCCAACCAG	GCAAGCCAGCACGGAGCC
NC-TrkC ΔICD	CTCAAGCTTCGAATTCTG	TGATGGTGTAGTGATGCC
NC-TrkC Y516F	GAACCCCCAGTTTTTCCGTCAGG	TCAATGACTGGGATGCGG
NC-TrkB	GAATTCGCCGCCACCATGTCGCCCTGG CTGAAGTGGCATG	ACGAGCTCCCCATCCAGTGGGATCTTAT GAAACA
BMPRIA	TCGAATTCGCCGCCACCATGACTCAGCT ATACACTTACATCA	TAGCGGCCGCCTACAGATCCTCTTCTGA GATGAGTTTTTGTTCACCACCAATCTTTAC ATCCTGGGATTCAACC
Ntf3	AATTATTTAAATTGCCATGGTTACTTCTG CCACGATCT	GGACAGATGCCAATTCATGTTCTTCC
Cbln1-EGFP	ATTAAGATCTATGCTGGGCGTCGTGGAG CTG	GGCCGGTCGACTGGAGGGGAAACACGA GGAATC
Cbln2	AGTTGAATTGAGCCCAGATGCCCGCGC CTGG	GTTAGCGGCCGCCTGGTGGCTCTGAGTC TATAGAGGAAAA

Cbln4-EGFP	ATTAAGATCTATGGGCTCCGCGCGCCGGGCG	GGCCGGTCGACTGTAGAGGAAACACCAGAAAGC
Cbln4-AP	AGCTGCTAGCATGGGCTCCGCGCGCCGGGCGCTG	AGCTTCCGGACGATAGAGGAAACACCAGAAAGCCAGAA
Ntf3-AP	AGCTGCTAGCATGGTTACTTCTGCCACGATCTT	AGCTTCCGGACGATGTTCTTCCAATTTTTCTCGACAA
Smad1	TCGGTACCGCCGCCACCATGAATGTGACCAGCTTGTTTTCATTCACA	ATGCGGCCGCTTAAGACACGGATGAAATAGGATTGTGGGG
p66-ShcA	TCGAATTCGCCGCCACCATGGATCTTCTACCCCCCAAGCCGA	TAGCGGCCGCCTACGCATAATCCGGCACATCATACGGATACACTTTCCGATCCACGGGTTGCTGT
p52-ShcA	GAATTCGCCGCCACCATGAACAAGCTGAGTGGAGGCGGCG	TAGCGGCCGCCTACGCATAATCCGGCACATCATACGGATACACTTTCCGATCCACGGGTTGCTGT
Sip1 fragment 1	TCGATATCGCCGCCACCATGAAGCAGCCGATCATGGCGGATG	GAAAGCTTCCCGGGCCCTATTCCCCTGC
Sip1 fragment 2	GCAGGGGAATAGGGCCCGGGAAGCTTTC	TAGCGGCCGCCTACAGATCCTCTTCTGAGATGAGTTTTTGTTCACCACCTTCCATGCCATCTTCCATATTGTCT

The NC-TrkC ΔICD, ΔECD, Y516F clones were generated by using the Q5 site directed mutagenesis kit (NEB). All PCR products were amplified using either Phusion polymerase or Q5 hot-start polymerase (NEB). The NC-TrkC ΔECD and ΔICD deletion constructs lacked amino acids 33-383 and 393-614 of the mouse NC-TrkC protein sequence respectively (Takahashi et al., 2011).

Cre recombinase was subcloned into a *NeuroD1* promoter plasmid (a kind gift from Dr. Gordon Fishel, NYU). A *mCherry* coding region followed by *polyA* sequence was amplified using primers carrying the 34bp *loxP* sequence. The resulting PCR product was cloned upstream of the multiple cloning site of pCAGIG (Addgene). This plasmid thus

allowed the expression of a gene of interest only upon Cre mediated recombination.

GFP fusion of Cbln1 and Cbln4 was cloned by inserting the Cbln1 and Cbln4 ORF into pEGFP-N1 (Clontech). The entire sequence was then subcloned into a pCAG vector (Addgene).

8. *In-utero* electroporation

The procedure was carried out as described earlier (Saito, 2006). Time mated pregnant females were anesthetized using Isofluran inhalation. During the entire procedure the animal was placed on a heating pad to prevent heat loss. Tamgesic was administered subcutaneously as a painkiller. Hair around the abdomen was shaved off with a regular shaver. The skin was cleaned two to three times with 70% ethanol and then an Iodine solution to minimize the risk of infections. A 30mm incision was made into the skin and then the abdominal wall along the midline. Carefully without damaging any blood vessels and organs, embryos from either side of the uterine wall were pulled out with the help of blunt forceps. Embryos were continuously bathed with a warm solution of Penicillin (1000 units/ml)-Streptomycin (1000µg /ml) to prevent the embryos from drying and to minimize chances of infection. The plasmid solution mixed with fast green was injected into the lateral ventricles with the help of a picospritzer (WPI). Plasmid solution was injected until visual confirmation of the blue solution in the ventricle was achieved. Electroporation was carried out by applying 6 electric pulses of 35V each, 50ms duration and 950ms interval. Post injection and electroporation, embryos were returned into the abdomen and the abdominal cavity was flushed three times with the Penicillin-Streptomycin solution. The muscle was carefully sutured and surgical staples were used to staple the skin. The animals were allowed to recover and then returned to their cage and kept under observation.

9. Cell Transfection and Stimulation

Cells were cultured in DMEM+10%FBS+1%P/S. Cells were split one day prior to transfection and the media was changed to DMEM+10%FBS. Cells were transfected with lipofectamine 2000 (Invitrogen) according to the manufacturer's protocol. 12 hours post transfection, the media was changed to Optimem+ 1% P/S (no serum) and the cells were kept in this media for 12-16 hours prior to stimulation. Cells were stimulated with EGF (Peprotech, 100 ng/ml) or Ntf3 (Peprotech, 50ng/ml) or BMP-4 (Invitrogen, 10ng/ml).

10. shRNA generation and Validation

shRNA clones targeting the following sequences of mouse BMPRIA were cloned into pSuper.Retro.Neo.GFP (Oligoengine):

1) GCTGTCTGTATAGTTGCTATG
2) GCTAGCTGGTTTAGAGAAACA
3) GGACTCAGCTGTATTTGATTA
4) GCCTAGCTGTTAAATTCAACA

Targeting sequences were designed using the Block-IT RNAi Designer (Invitrogen). The loop sequence used was TCTCTTGAA. Positive clones were transfected along with a Myc-tagged BMPRIA expression construct in HEK293T cells using lipofectamine 2000 (invitrogen). Four days post transfection, cells were lysed in 50mM Tris-HCl pH 7.5, 150mM NaCl, 1mM EDTA, 1% Triton X-100, 1x protease inhibitor cocktail (Sigma) and pepstatin. Lysates were centrifuged for 20 minutes at 12000g, 4°C. Protein concentration was measured using the BCA assay kit (Thermo scientific). 30µg protein was loaded on a SDS-PAGE gel and transferred onto a PVDF membrane. Anti-Myc antibody and anti-GAPDH antibodies were used to measure the relative amount of BMPRIA. A scrambled shRNA was used as the control.

11. Luciferase Assay

Cbln4 and Ntf3 enhancer regions were cloned upstream of a Gaussia luciferase coding sequence (Thermo scientific). This was then co-transfected with a CMV promoter driven Alkaline phosphatase in COS or HEK293T cells using lipofectamine 2000 according to the manufacturers protocol (Invitrogen). Supernatant from the cells was collected 48-72h post transfection. The gaussia luciferase and Alkaline phosphatase mediated luminescence was detected using the secrete pair DUAL luminescence kit (GeneCopoeia) and read using a Glomax luminometer (Promega). Data was collected from three independent experiments, each probed in triplicates and presented as the relative luminescence ratio (Gaussia luciferase: Alkaline phosphatase).

12. Western Blotting and Immunoprecipitation

Cultured cells or fresh cortical tissue were lysed either in Flag buffer (50mM Tris pH7.5, 100mM NaCl, 1mM EDTA, 1% v/v Triton X-100) or RIPA buffer (50mM Tris pH7.5, 150mM NaCl, 1%NP-40, 0.5% Sodium deoxycholate, 0.1% SDS) containing 1x protease inhibitor cocktail (SIGMA) and PhosphoStop (Roche). The samples were then centrifuged for 20 minutes at 14000 at 4°C. The protein concentration was estimated using the BCA protein assay kit (Thermo Scientific). The samples were denatured by boiling for 5 minutes at 95°C in 1x SDS loading buffer and equal amounts of protein were separated by SDS-PAGE. The protein samples were then transferred onto a PVDF transfer membrane (Immobilon-P, Milipore). The membrane was subsequently blocked for one hour in 3% BSA in TBST (TBS + 0.5% Tween-20), followed by overnight incubation in the primary antibody at 4°C. The following day, the membranes were washed in TBST and incubated for one hour in peroxidase coupled secondary antibodies (Jackson Laboratory). Chemiluminescence (ECL western blotting detection

reagent, Perkin Elmer) was used for visualizing the protein bands. The chemiluminescence was captured using the Image lab software on a ChemiDoc XRS+ detector (Bio-Rad). For stripping, the membranes were washed three times in PBS followed by two-ten minute washes in the stripping buffer (25mM glycine-HCl pH 2, 1% (w/v) SDS). The membranes were then equilibrated in 1M Tris pH 6.8 followed by three PBS washes. After blocking the membranes in 5% BSA in TBST, they were incubated overnight with the primary antibody.

For Immunoprecipitation, after lysis, the samples were pre-cleared using 20µl of ProteinG sepharose beads (GE) for one hour at 4°C on a rotor. The samples were then briefly centrifuged and the required antibody was added to the supernatant and incubated for 2 hours at 4°C on a rotor. The antigen-antibody complex was captured by adding 20µl of pre-washed ProteinG sepharose beads for 1 hour at 4°C on a rotor. The samples were briefly centrifuged and washed four times in lysis buffer and once in TBS. After removing as much of the buffer as possible, 20µl of 2.5X SDS loading buffer was added to each sample and boiled for five minutes at 95°C. Alternatively, the proteins were eluted from the beads using a glycine elution buffer (Thermo scientific).

13. *In-situ* Hybridization

For cloning probes used in *in-situ hybridization*, PCR fragments were either amplified using GoTaq (Promega) or Phusion Polymerase (NEB). Whenever Phusion polymerase was used, an additional 'A' tailing step was done with GoTaq for one hour at 72°C. Amplicons were cloned into a pGEMT vector (Promega) following the manufacturers protocol. After verifying the directionality of the insert, the vector was linearized and the anti-sense probe was generated using either the T7, T3 or Sp6 RNA polymerases (Roche). The *in-vitro* transcription consisted of the following components:

10X Transcription buffer	2 µl
Polymerase	2 µl
DIG RNA labeling mix	2 µl
Linerarized Plasmid	1-2 µg
RNase inhibitor	2 µl
DEPC-H_2O	variable

Total Volume	20 µl

After incubation for 2 hours at 37°C, the sample was treated with DNase for 30 minutes, followed by overnight precipitation of the RNA using LiCl. The RNA probe was finally dissolved in 20µl DEPC-H_2O. 1µl was used for running on an agarose gel to verify the size of the RNA product.

For the *in situ* hybridization 12-14µm thick cryosections were used. The sections were fixed in 4% PFA followed by two 5 minute PBS washes. The sections were then subjected to Proteinase-K treatment (2-3 minutes, 37°C, 20µg/ml) to permeabilize the cells in order to allow for better probe penetration. The Proteinase-K activity was inhibited by washing the sections in 0.2% glycine in PBS. Following this, the slides were rinsed in PBS and post-fixed in 4% PFA/ 0.2% Glutaraldehyde in PBS for 20 minutes at RT. After washing the slides twice in PBS, the sections were incubated for 2 hours in hybridization buffer (50% formamide, 5X SSC pH 7.0, 1% Boehringer block, 2.5mM EDTA, 0.1% Tween-20, 0.1% CHAPS, 0.1mg/ml Heparin, 100µg/ml Yeast RNA, 50µg/ml Salmon sperm DNA and 1x Denhardt's solution) at 65°C. After the prehybridization step, the slides were incubated in the anti-sense probe (diluted in hybridization buffer) at 65°C for 16-20 hours. The following day, the slides were washed in 2X SSC pH4.5 (20X SSC= 3M NaCl and 300mM Trisodium citrate), followed by an RNase treatment for 30 minutes at 37°C (20µg/ml in 0.5M NaCl, 10mM Tris pH 7.5). The slides were then rinsed in 2X SSC pH 4.5, followed by three washes of 30 minutes each in 2X SSC pH4.5/ 50% formamide at

65°C. The slides were then washed twice in KTBT (50mM Tris pH 7.5, 150mM NaCl, 10mM KCl and 1% Triton X-100) before blocking in 20% sheep serum prepared in KTBT. Anti-DIG Alkaline phosphatase conjugated antibody (Sheep, Roche, 1:1000) was added and the slides were incubated overnight at 4°C. The next day, the slides were washed in KTBT, followed by three washes in NTMT (100mM Tris pH 9.5, 100mM NaCl, 50mM $MgCl_2$ and 0.05% Tween-20). The colorimetric reaction was developed by adding the alkaline phosphatase substrate - NBT/BCIP (1:50, Roche) prepared in NTT (100mM Tris pH 9.5, 100mM NaCl, and 0.05% Tween-20) to the slides. The reaction was stopped by washing the slides in PBST (PBS + 0.1% Triton X-100) and progressively dehydrating the slides in Ethanol. The slides were mounted using Eukitt mounting medium.

14. AP staining of Sections and Cells

AP tagged constructs were expressed transiently in HEK293T cells. The media was changed 24 hours post transfection. Thereafter, the media was collected 5-6 days later and checked for Alkaline phosphatase activity using NBT-BCIP as a substrate. The recombinant proteins were also run on a SDS-PAGE gel and blotted to verify the size of the fusion proteins. AP fusion staining was carried out as described earlier (Flanagan et al., 1990; Flanagan and Cheng, 2000; Brennan and Fabes, 2003). For AP-fusion protein binding on tissue, fresh-frozen (unfixed) tissue was sectioned using a Leica cryostat. Sections were mounted on slides and stored inside the cryostat to avoid air-drying. Subsequently, the sections were fixed in dry ice cooled 100% methanol for 8-10 minutes and then washed three times in PBS with 4mM $MgCl_2$. Sections were then blocked in PBS (containing $MgCl_2$) with 10% FBS for one hour at room temperature. Varying dilutions of the AP-fusion protein were made in the blocking solution and added to the

sections. After incubating the sections in the AP-fusion protein for two hours, the sections were washed five times for five minutes each in 1X PBS. The bound AP-fusion protein was fixed for 90 seconds with 4% PFA, 60% acetone and 20mM HEPES pH 7.0. The slides were washed for three more times in 1X PBS and then the endogenous phosphatases were inactivated by heating the slides in a water bath at 65°C for 100 minutes. After washing the slides in PBS, they were washed twice in the AP reaction buffer (100mM Tris pH 9.5, 100mM NaCl, 5mM $MgCl_2$). NBT-BCIP substrate (Roche) was then added to the slides and they were incubated at room temperature until the desirable color was attained.

For AP-fusion protein staining on cells, COS-7 cells were used. The cells were washed in HBHA (0.137M NaCl, 5.4mM KCl, 0.25mM Na_2HPO_4, 0.44mM KH_2PO_4, 1.3mM $CaCl_2$, 1.0mM $MgSO_4$, 4.2mM $NaHCO_3$, 0.5mg/ml BSA) buffer, followed by incubation of the AP-fusion protein for 90 minutes at room temperature. The cells were then washed in HBHA five times and then fixed for 15 seconds in 4% PFA, 60% acetone and 20mM HEPES pH 7.0. The cells were then washed three times in HBS (0.137M NaCl, 5.4mM KCl, 0.25mM Na_2HPO_4, 0.44mM KH_2PO_4, 1.3mM $CaCl_2$, 1.0mM $MgSO_4$, 4.2mM $NaHCO_3$) for five minutes each, followed by heat inactivation for two hours at 65°C. The cells were then washed in AP reaction buffer. NBT-BCIP substrate (Roche) was then added to the cells and they were incubated at room temperature until the desirable color was attained. The reaction was stopped by fixing the cells in 4% PFA.

15. cDNA library synthesis

E14.5 cortices were used for RNA isolation. RNA was isolated using Trizol reagent following the manufacturer's protocol (Invitrogen). The quality of the RNA was assessed using agarose gel-electrophoresis. 500µg of total RNA was used for purifying mRNA using the Fast track

MAG mRNA isolation kit (Invitrogen) following the manufacturer's protocol. 10µg of purified mRNA was used for preparing the cDNA library. The cDNA library was made using the SuperScript Full Length cDNA library construction Kit II (Invitrogen) following the manual provided. The kit allowed a size exclusion chromatography separation of the cDNA molecules to enrich for larger insert size. Accordingly, two separate cDNA libraries were prepared in the entry vector- pDONR 222. 24-30 random clones were selected and digested using the enzyme BsrGI to estimate the average insert size. Upon complete quality check of the cDNA library, the clones were grown briefly and DNA was isolated. 25ng of the cDNA library in the entry vector pDONR 222 was transferred into the destination vector pDEST 40 using the gateway LR recombination reaction (Invitrogen). The clones were again screened randomly to confirm the successful shuttling of the cDNA library from the entry vector into the destination vector.

RESULTS

1. Mosaic deletion of *Sip1* in young cortical neurons phenocopies the *Sip1* mutant.

We have previously demonstrated that deletion of *Sip1* in young neocortical neurons changes the proportion of deep layer versus upper layer neurons (Seuntjens et al., 2009). In order to test whether this effect is cell intrinsic or cell extrinsic we decided to employ *in utero* electroporation (IUE). We electroporated a plasmid encoding *GFP-IRES-Cre*, that expresses *Cre* recombinase together with *GFP*, into the lateral ventricles of E12.5 $Sip1^{fl/fl}$ and $Sip1^{fl/wt}$ mouse embryos. To see if this relatively low efficiency deletion of *Sip1* would replicate the phenotype of $Sip1^{fl/fl}$:Nex^{Cre} mutants we performed immunohistochemistry with the layer V marker Ctip2. Like in $Sip1^{fl/fl}$:Nex^{Cre}, the proportion of Ctip2 cells had decreased in $Sip1^{fl/fl}$ as compared to the control (Figure5A). Interestingly, within the electroporated region where the loss of Ctip2 positive cells was observed, GFP positive cells did not show a preference to being Ctip2 positive or negative. This shows that Sip1 affects cortical cell fate not due to its cell intrinsic action but through cell extrinsic mechanisms. This data demonstrates that IUE, despite its relatively low cell targeting efficiency can be used to study cell extrinsic effects. On the other hand it also shows that *Sip1* affects cortical cell fate not due to its cell intrinsic action but through cell extrinsic mechanisms.

2. *Ntf3* is upregulated in the *Sip1* mutant cortex.

We have previously shown that upon loss of *Sip1* in the developing cortex, there is an ectopic upregulation of *Ntf3* in the cortical plate (Figure 5B,(Seuntjens et al. 2009)). This upregulation correlates to the premature generation of upper layer neurons in the *Sip1* mutant. We had also shown through Chromatin immunoprecipitation (ChIP) assay

that Sip1 directly binds to the *Ntf3* promoter region (Seuntjens, et al. 2009). In order to investigate the functionality of this binding we performed a luciferase assay. A 1.7 Kb fragment of the *Ntf3* enhancer region (Figure 5C) was inserted into a plasmid encoding the gaussia luciferase gene and co-transfected into COS-7 cells with a plasmid encoding *Sip1* cDNA.

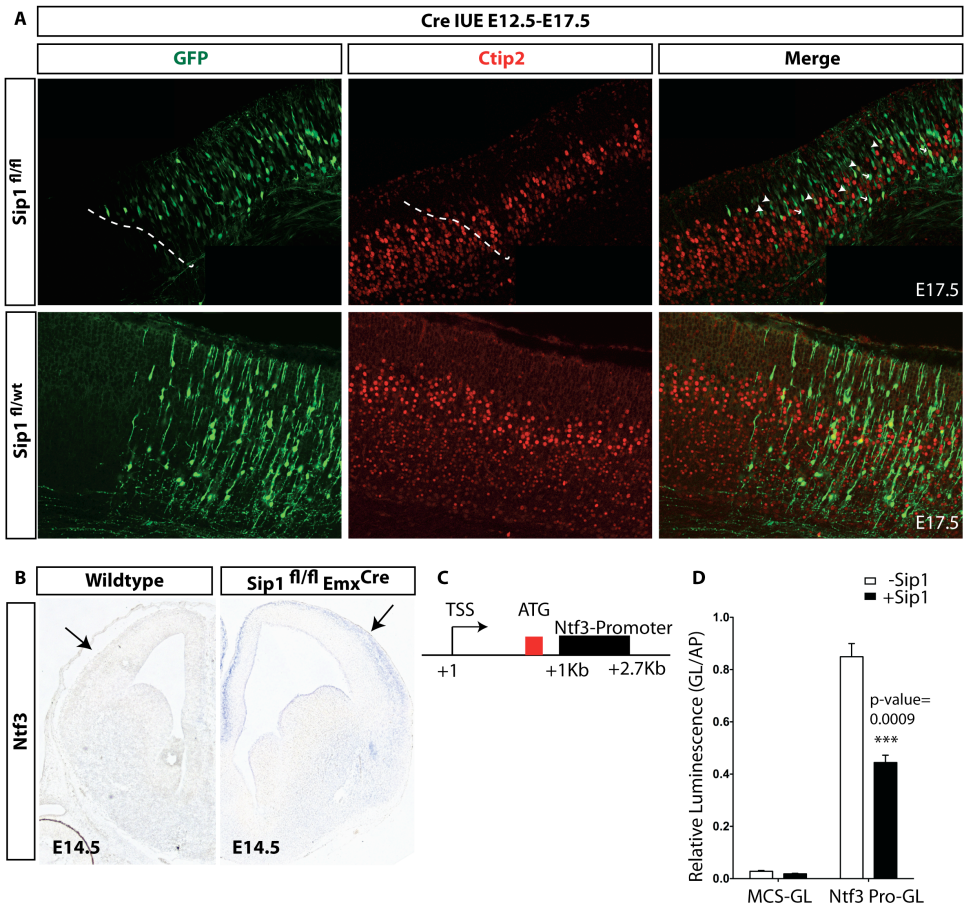

Figure 5. *Ntf3* is upregulated in the *Sip1* mutant cortex
(A) *In utero* electroporation of *Cre* in *Sip1*$^{fl/fl}$ and *Sip1*$^{fl/wt}$ embryos at E12.5. Proportion of Ctip2 positive cells decreased within the electroporated region of *Sip1*$^{fl/fl}$ embryos at E17.5, while no difference was observed in *Sip1*$^{fl/wt}$ embryos. Filled arrowheads point to GFP+/Ctip2+ and arrows point to GFP+/Ctip2- cells **(B)** *In situ* hybridization shows that *Ntf3* is upregulated in the *Sip1* mutant cortex at E14.5, while no expression can be detected in the wildtype. **(C)** Scheme showing the *Ntf3* enhancer region used for the luciferase assay **(D)** Luciferase assay shows that upon co-transfection of *Sip1*, the transcription of luciferase driven by the *Ntf3* enhancer element reduced by 1.9 fold (n=3, relative luminescence without Sip1= 0.85 ± .05 as compared to 0.44 ± 0.03 with Sip1, p-value= 0.0009).

We observed a decrease in transcription activity of the *Ntf3* enhancer by 1.9-fold (Figure 5D, n=3, p-value= 0.0009). These results indicate that Sip1 can directly repress *Ntf3* transcription.

3. Ntf3 promotes an increase in the basal progenitor population.

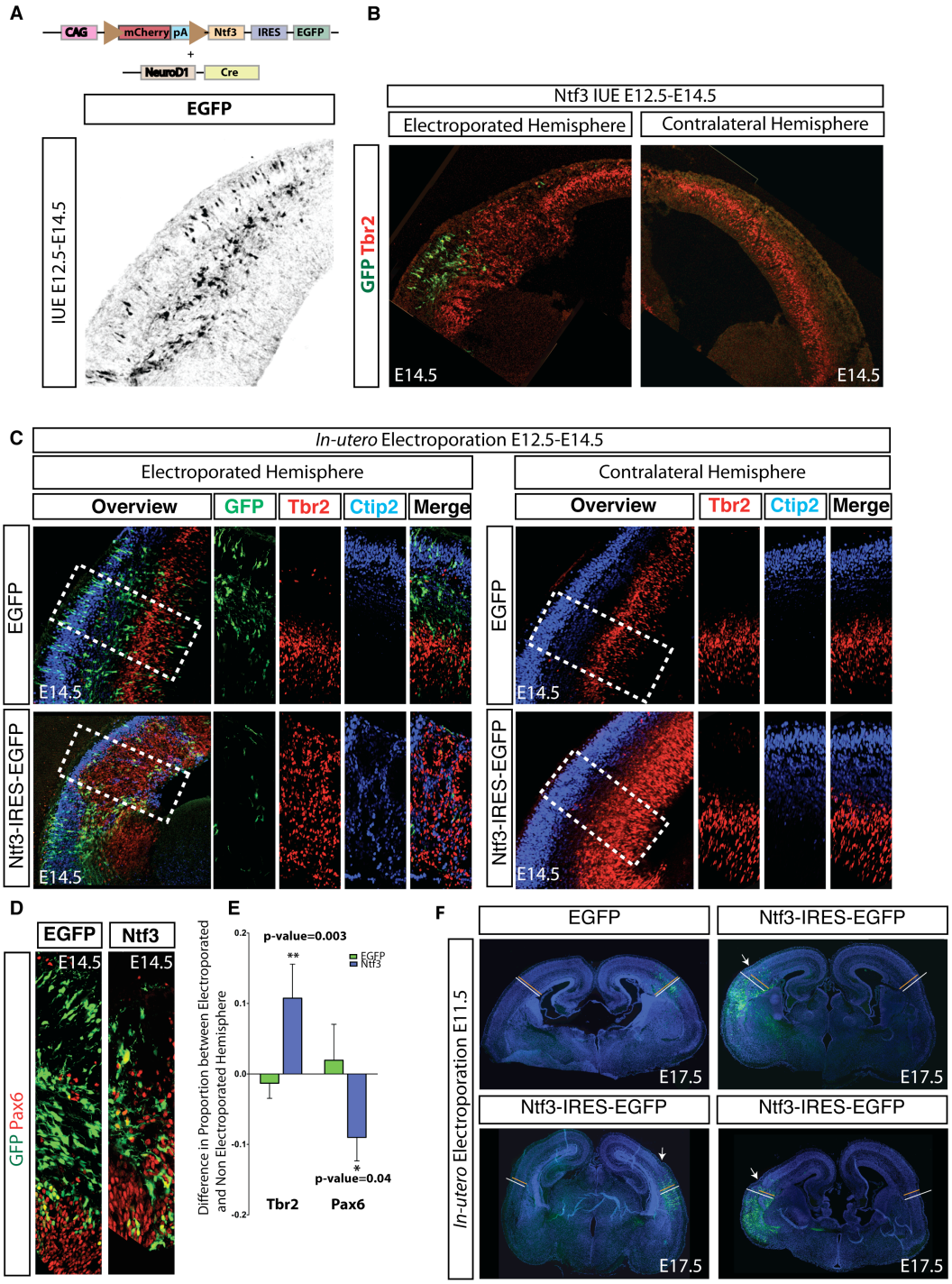

Figure 6. Ntf3 promotes an increase in the basal progenitor and decrease in apical progenitor population.
(A) Plasmid system for restricting expression to postmitotic neurons. A postmitotic neuron specific promoter (*NeuroD1*) drives *Cre* expression. Cre mediated recombination switches expression from *mCherry* to *Ntf3* and *EGFP*. A representative image shows that GFP expression is largely restricted to postmitotic neurons (B) Overview image showing that upon *Ntf3* over-expression, Tbr2+ basal progenitor population is expanded (C) Electroporation of *GFP* does not lead to any change in the size or distribution of Tbr2+ and Ctip2+ cells. Over-expression of *Ntf3* leads to an expansion of Tbr2+ cells. Ctip2+ cells are displaced, probably due to a secondary effect of this increase in Tbr2+ cells. The contralateral hemisphere serves as an internal control. (D) Pax6+ cells are also displaced and reduced in number in *Ntf3* over-expression brains (E) Differences in the proportion of Tbr2+ and Pax6+ cells in a radial unit of the cortex between electroporated and non-electroporated hemisphere (10.75 ± 4.8% higher Tbr2+ cells in the electroporated hemisphere upon *Ntf3* over expression compared to -1.3 ± 2.1% in *EGFP* electroporations, n=5, p-value= 0.003; 9 ± 3.3% lesser Pax6+ cells in the electroporated hemisphere upon *Ntf3* over expression compared to 1.9 ± 5.1% in control plasmid electroporations, n=3, p-value=0.04). All electroporation were done at E12.5 and analyzed at E14.5. (F) Radial expansion of the cortex on *Ntf3* over-expression. White and orange bars indicate the thickness of the electroporated and non-electroporated hemisphere respectively. The bars were placed parallel to the apical process of the cells. Arrows indicate the physical fold in the cortical plate highlighting the expansion.

To study if the upregulation of *Ntf3* in the *Sip1* mutant has any effect on the proportion of apical and basal progenitors, we decided to over-express *Ntf3* in the wildtype cortex. In order to restrict the expression of *Ntf3* to postmitotic neurons, we designed a plasmid system using the Cre-loxP system. In this plasmid *Ntf3-IRES-eGFP* cassette was preceded by a *mCherry-polyA* sequence flanked by *loxP* sites. The *Cre* recombinase used here was driven by the postmitotic specific *NeuroD1* promoter, which switches expression from *mCherry* to *Ntf3* and *EGFP* specifically in postmitotic neurons (Figure6A). EGFP expression verified that most of the recombined cells were indeed postmitotic (Figure 6A). In order to avoid variations that arise from comparing different medio-lateral and rostro-caudal levels while analyzing electroporated brains, we performed all analysis as the difference between the electroporated and non-electroporated hemispheres at the same medio-lateral and rostro-caudal level. We firstly looked at any possible effects of *Ntf3* over expression on the ratio of apical and basal progenitors. To do so, we electroporated wildtype E12.5 embryos

and analyzed the brains at E14.5. We noticed that upon *Ntf3* over expression there was a vast expansion of the number of Tbr2 positive basal progenitors and correspondingly on the size of the SVZ (Figure 6B, C, E 10.75 ± 4.8% higher Tbr2 positive cells in the electroporated hemisphere upon *Ntf3* over expression compared to -1.3 ± 2.1% in control plasmid electroporations, n=5 each, p-value= 0.003). Interestingly, there was also a decrease in the Pax6 positive apical progenitor population on Ntf3 over-expression (Figure 6D, E; 9 ± 3.3% lesser Pax6 positive cells in the electroporated hemisphere upon *Ntf3* over-expression compared to 1.9 ± 5.1% in control plasmid electroporations, n=3 each, p-value=0.04). Interestingly, the expansion of Tbr2 positive SVZ was not always found to be restricted to the electroporated region of the cortical plate but expanded into the regions flanking the electroporation site as well (Figure 6B, C). Following the expansion in Tbr2 positive progenitors, we also observed a radial expansion of the cortex (Figure 6F). Since in all these experiments *Ntf3* expression was restricted to postmitotic neurons, the changes in apical or basal progenitor populations are most likely a result of feedback signaling from postmitotic neurons to the progenitors.

4. Ntf3 promotes upper layer neurogenesis at the expense of deep layer neurons.

The above results show that *Ntf3* promotes a shift from apical to basal progenitor production. Consequently, this might lead to an increase in upper layer production at the expense of deeper layer neurons (Arnold et al. 2008). In order to test this hypothesis, we over-expressed *Ntf3* in postmitotic neurons at E11.5 and analyzed the brains at E17.5. We observed a decrease in Ctip2 positive layer V neurons in the *Ntf3* electroporated regions (Figure 7A). When analyzed, *Ntf3* electroporated brains showed a 3.4 ± 1.35% decrease in Ctip2 cells compared to the

contralateral hemisphere, while *EGFP* electroporated brains did not show any difference (-0.05 ± 1.2%) between electroporated and non-electroporated hemispheres (Figure 7B, C, n=5, p-value=0.003).

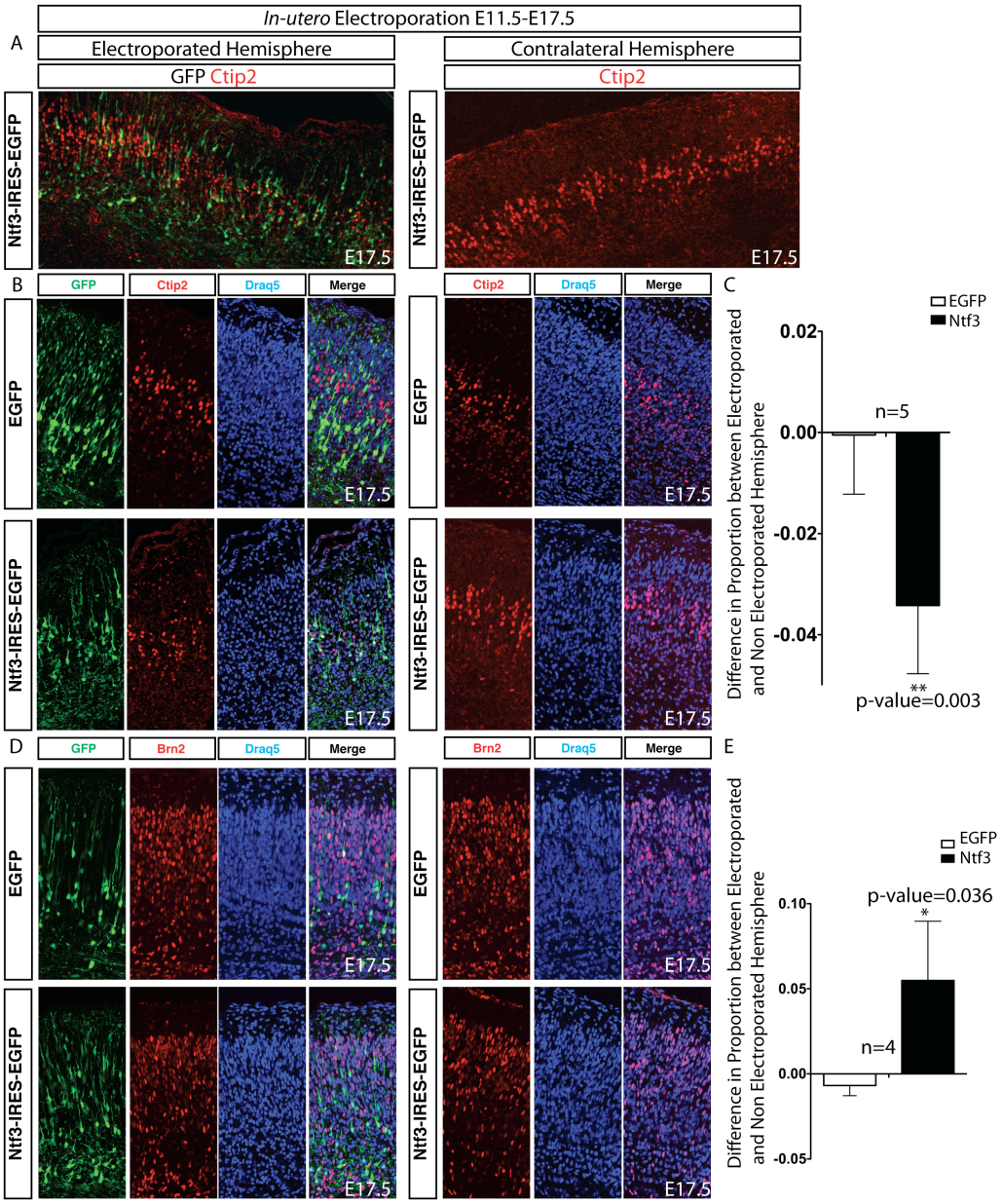

Figure 7. *Ntf3* promotes upper layer neurogenesis at the expense of deep layer neurons

(A) Decline in Ctip2 numbers within the *Ntf3* electroporated hemisphere **(B-C)** *Ntf3* overexpression leads to a 3.4 ± 1.35% decrease in deep layer Ctip2+ cells compared to the non-electroporated hemisphere, while *EGFP* expression does not alter the proportion (-0.05 ± 1.2%), n=5, p-value=0.003 **(D-E)** *Ntf3* electroporated brains show a 5.4 ± 3.47% increase in Brn2+ Upper layer neurons while *EGFP* does not affect the proportion (-0.68 ± .6%, n=4 each, p-value=0.036).

We also observed a 5.4 ± 3.47% increase in Brn2 positive upper layer neurons in *Ntf3* electroporated hemispheres compared to *EGFP* electroporation (-0.68 ± .6%, Figure 7D, E n=4, p-value=0.036).

5. Deletion of *Ntf3* increases the number of layer VI neurons but the *Ntf3-Sip1* compound mutant does not rescue *Sip1* mutant phenotype.

We have previously reported that in the absence of *Sip1*, cortical progenitors precociously produce upper layer neurons at the expense of deep layer neurons (Seuntjens et al. 2009). To investigate if this phenotype can be reverted on *Ntf3* deletion, we generated *Sip1-Ntf3* compound mutants. We compared the proportion of the different cortical layers between the wildtype, *Ntf3* single mutant, *Sip1* single mutant and *Sip1-Ntf3* compound mutant. We did not find any significant difference in the proportions of Satb2 positive (layer II-V), Ctip2 positive (layer V), Brn2 positive (layer II-IV) and Sox5 positive (layer VI) cells between *Sip1* single and *Sip1-Ntf3* double mutants (Figure 8A-D, all p-value ≥ 0.05). Further, we did not find any difference between wildtype and *Ntf3* mutants with respect to the proportion of Satb2, Brn2 and Ctip2 positive populations (Figure 8A, B, D). Interestingly, we noticed an increase in the Sox5 positive layer VI population in *Ntf3* mutants compared to wildtype controls (36.5 ± 2.9% in *Ntf3* mutants compared to 29.3 ± 2.3% in wildtype controls, n=3, p-value= 0.029; student's t-test). This might suggest that *Ntf3* indeed plays an important role in cortical lamination in the wild type scenario.

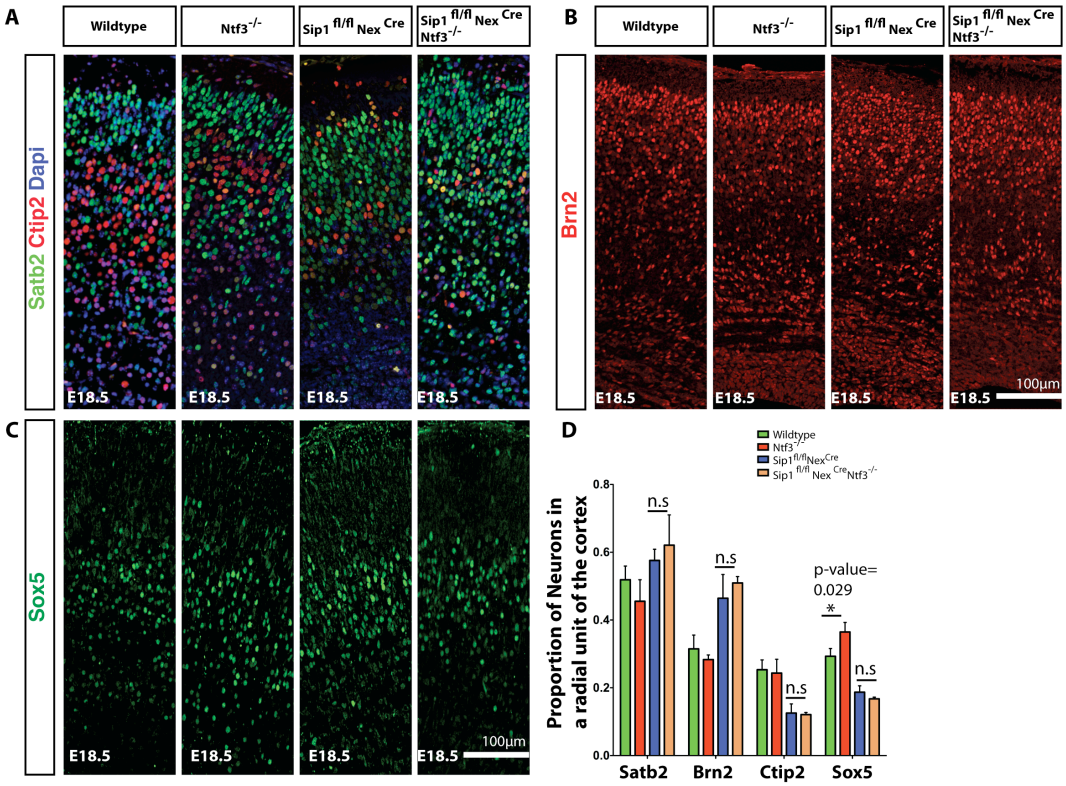

Figure 8. Deletion of *Ntf3* from the *Sip1* mutant cortex does not rescue the *Sip1* mutant phenotype.

(A) Satb2 and Ctip2 immunohistochemistry marking upper layer and layer V cells in wildtype, *Ntf3*$^{-/-}$, *Sip1*$^{fl/fl}$;*Nex*^{Cre} and *Sip1-Ntf3* double mutants. The decrease in Ctip2 cells in *Sip1* mutants is not restored in the *Sip1-Ntf3* double mutant. Similarly the increase in Satb2+ cells is also not restored. Another upper layer marker (**B**) Brn2 and layer VI marker **(C)** Sox5 also confirm that the excessive production of upper layer neurons at the expense of deep layer neurons in the *Sip1* mutant is not restored in the *Sip1-Ntf3* double mutant. **(D)** n=3 for wildtype, *Sip1* mutant and *Ntf3* mutant, n=2 for *Sip1-Ntf3* double mutants. The differences between *Sip1* mutant and *Sip1-Ntf3* double mutant are not significant for any of the layer markers. The proportion of Sox5+ cells is higher in *Ntf3* mutant compared to wildtype (36.5 ± 2.9% in *Ntf3* mutant compared to 29.3 ± 2.3% in wildtype controls, p-value= 0.029).

6. Localizing the receptors for Ntf3 in the developing cortex

To understand how Ntf3 functions as a feedback signaling molecules, it was essential to locate the cognate receptor. To study the location of possible receptors of Ntf3, we made an *Ntf3-alkaline phosphatase* (AP) fusion construct (Figure 9A). We then transfected this construct in HEK293T cells and collected the supernatant, which was enriched in Ntf3-AP recombinant protein (Figure 9A). In order to verify the

biological activity of the AP fused Ntf3, we used this recombinant protein to immunoprecipitate two known Ntf3 receptors- TrkC and TrkB.

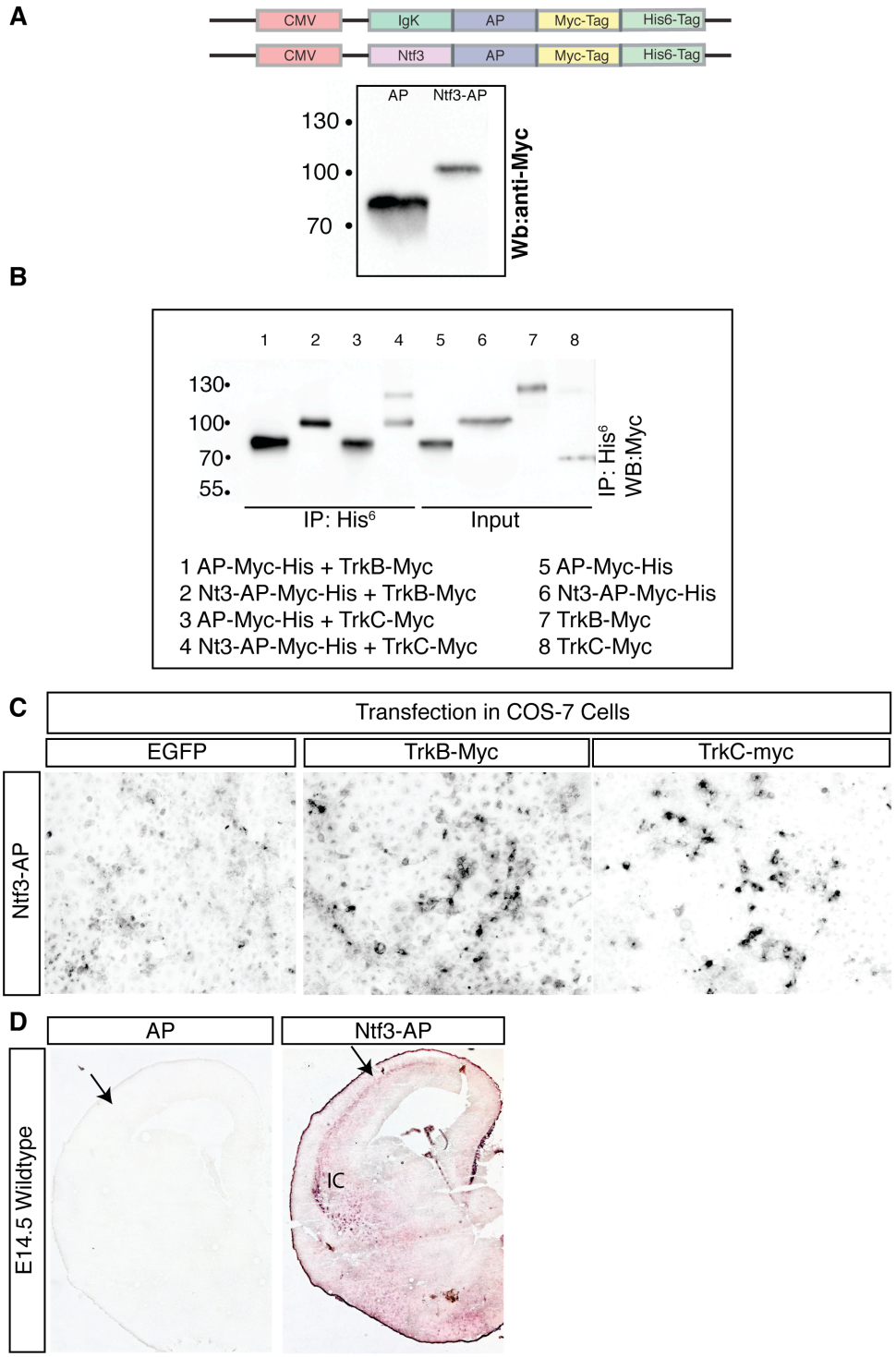

Figure 9. Localizing the receptors for Ntf3 in the developing cortex
(A) Scheme showing the design of the *Ntf3-Alkaline phosphatase* fusion plasmid construct. The plasmids were transfected in HEK293T cells and six days post

transfection the supernatant was analyzed by western blot to validate the expression of the recombinant protein. Ntf3-AP as visualized by using a Myc tag antibody, can be seen running higher than untagged AP **(B)** for validating the binding ability of recombinant Ntf3-AP, the protein enriched supernatant was mixed with myc tagged TrkC or TrkB containing cell lysates. The samples were immunoprecipitated with a His tag antibody and probed for the presence of TrkC or TrkB using a Myc tag antibody. Ntf3-AP but not untagged AP could bind to TrkC (lanes 3-4). TrkB fails to co-immunoprecipitate with both AP and Ntf3-AP (lanes1-2) **(C)** To validate the ability of Ntf3-AP to bind to its receptors in the native state, Ntf3-AP or AP alone was over layed on TrkB or TrkC transfected COS-7 cells. In this case, Ntf3-AP could bind to both receptors **(D)** E14.5 sections were incubated with AP or Ntf3-AP to identify the location of the receptors in the developing cortex. Ntf3-AP marks the intermediate zone and fibers entering the internal capsule (IC).

Indeed, Ntf3-AP could bind to TrkC but not to TrkB (Figure 9B). However, since Ntf3 is also known to bind to TrkB at higher concentrations, we performed an *in vivo* binding assay. Here, *TrkC* and *TrkB* plasmids were transfected in COS7 cells and the Ntf3-AP recombinant protein was allowed to bind to the receptors in their native state. As expected, Ntf3-AP did bind to TrkB but with much lower affinity as compared to TrkC (Figure 9C). Finally, in order to visualize the location of the Ntf3-receptor, we incubated E14.5 sections with the Ntf3-AP recombinant protein and used the enzymatic activity of AP to visualize the location of the receptor. While we observed a strong signal from the intermediate zone, no staining could be seen in the germinal zone of the cortex (Figure 9D). We however, could not rule out the possibility that the receptor was inaccessible to the exogenous ligand used here.

7. Expression of *TrkC* and *TrkB*

Since from the previous experiment, we could not conclusively identify the location of the receptor, we decided to study the expression pattern of the known Ntf3 receptors- TrkC and TrkB. At first, we limited our study to the full-length isoforms of both receptors. We performed *in situ* hybridization at E14.5 with probes against the full-length *TrkC* and *TrkB* mRNAs (*FL-TrkC, FL-TrkB*). Since *Ntf3* over-expression at E12.5 showed that it affects the ratio of apical to basal

progenitors (Figure 6), we assumed that Ntf3 had to act through receptors located on neocortical progenitors. To our surprise, we did not find any expression of either *TrkC* or *TrkB* within the germinal zone of the developing cortex (Figure 10A,B).

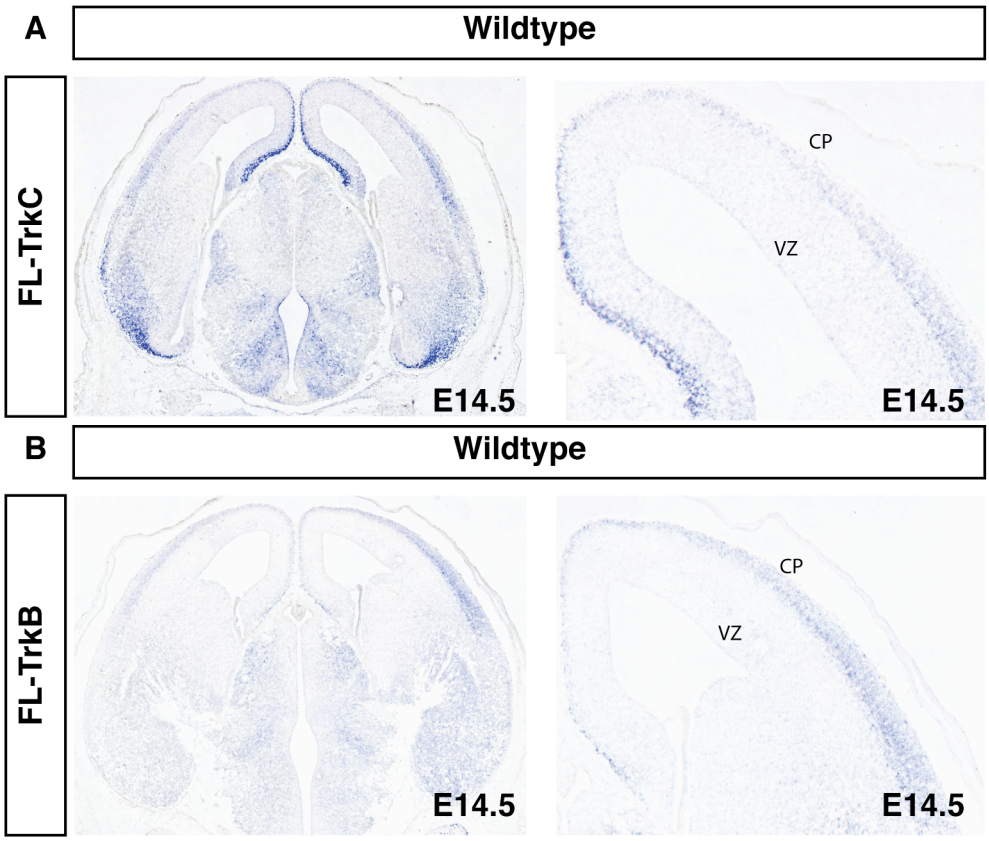

Figure 10. Expression of *TrkC* and *TrkB*
(A) *In situ* hybridization using a probe targeting the *FL-TrkC* mRNA at E14.5 shows that *TrkC* is not expressed in the ventricular zone. Expression of *FL-TrkC* is confined to the postmitotic cortical plate. **(B)** Expression of *FL-TrkB* is also confined to the cortical plate, with no detectable expression within the cortical germinal zone. VZ=ventricular zone, CP=cortical plate

8. Expression of Non-Catalytic (NC) TrkC and TrkB

Since full length- *TrkC* and *TrkB* mRNAs are not expressed in progenitors, our search for a putative Ntf3 receptor expressed within the ventricular zone lead us to study the expression of the alternate splice variants of *TrkC* and *TrkB* receptors. Both *NTRK3 (TrkC*) and *NTRK2 (TrkB)* genes have been shown to also produce alternate truncated isoforms, which lack the intracellular kinase domains

(Valenzuela et al., 1993). These Non-catalytic isoforms also have a distinct 3' UTR, suggesting differential post-transcriptional control. Using riboprobes specifically targeting the truncated isoforms, we observed that *NC-TrkC* and *NC-TrkB* were expressed in the ventricular zone of the developing cortex (Figure 11).

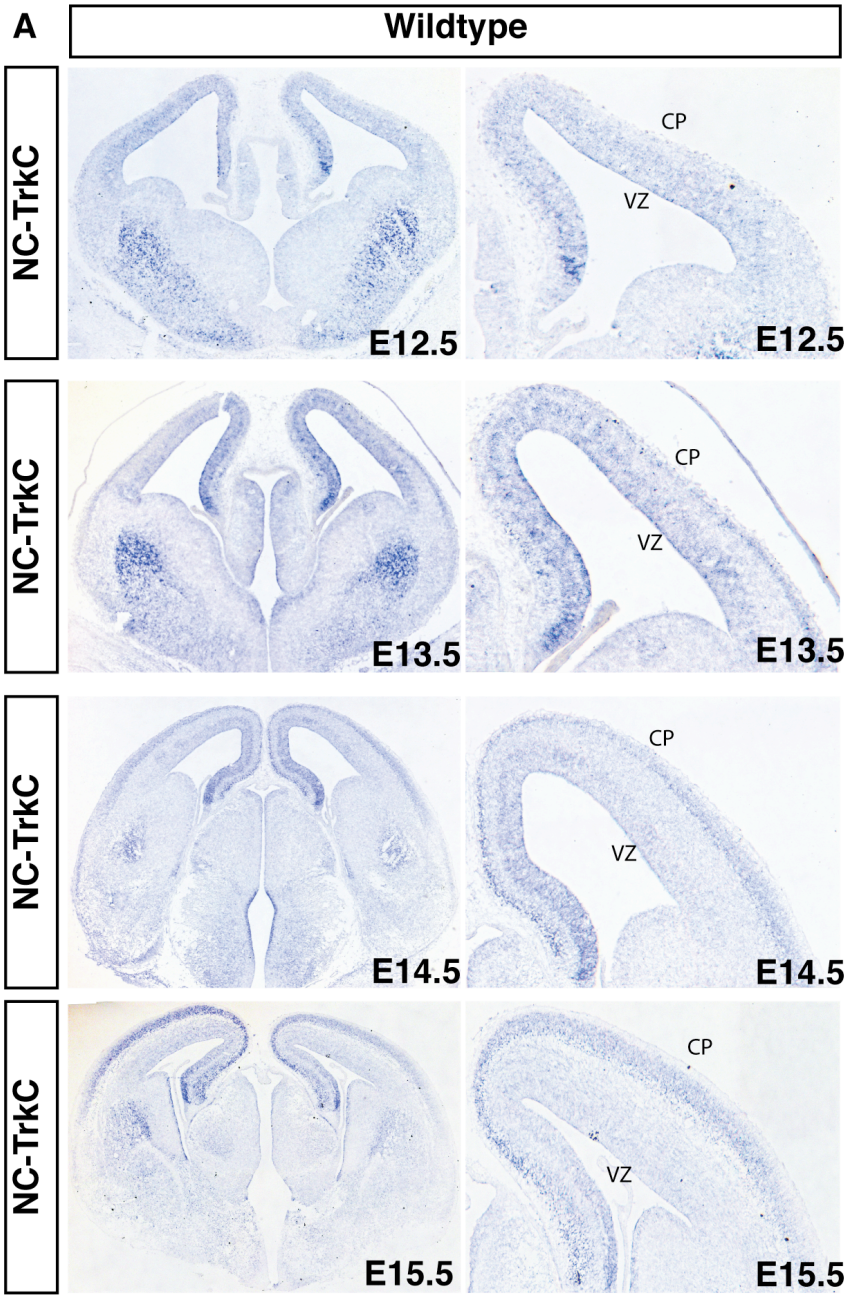

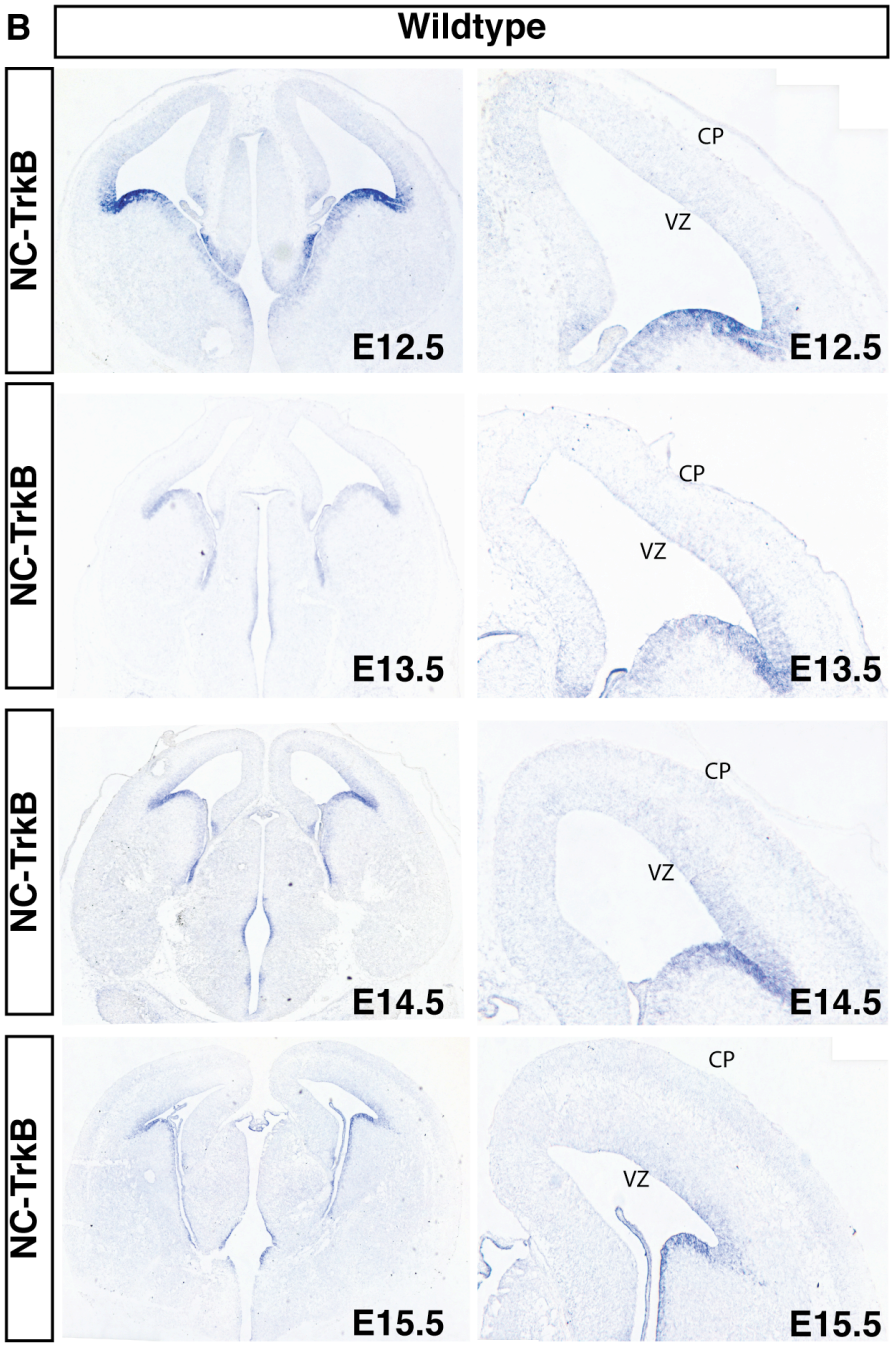

Figure 11. Expression of *NC-TrkC* and *NC-TrkB*

(A) *In situ* hybridization using a probe targeting *NC-TrkC* at various stages of development. At E12.5 and 13.5, *NC-TrkC* is expressed in the VZ. At E13.5, expression can also be seen in the young cortical plate. At E14.5, the expression of *NC-TrkC* follows a high medial-low lateral expression in the VZ, while the cortical plate expression remains uniform. At E15.5, expression of *NC-TrkC* is lost in the VZ whereas the cortical plate signal is still present. **(B)** Expression pattern of *NC-TrkB* from E12.5-15.5. Unlike *NC-TrkC*, *NC-TrkB* expression within the postmitotic cortical plate is never detected. Expression within the VZ is restricted to the lateral boundary, at the junction of the pallium-subpallium ventricular zones. This expression is constant during the developmental stages studied. VZ=ventricular zone, CP=cortical plate

While *NC-TrkC* was also expressed in the cortical plate, *NC-TrkB* was restricted to the germinal zone (Figure 11A,B). Unlike *NC-TrkB*, which showed a constant pattern of expression throughout early development (Figure 11B), the expression pattern of *NC-TrkC* was highly dynamic. While *NC-TrkC* was expressed strongly in the ventricular zone at E12.5 and E13.5, its expression showed a high medial-low lateral expression at E14.5 and reduced to undetectable levels by E15.5 (Figure 11A). The combination of the presence of *NC-TrkC* expression in the ventricular zone cells and its highly dynamic expression pattern made *NC-TrkC* an interesting gene to study in the context of cell fate switch in the developing cortex.

9. NC-TrkC protein is also absent from the E15.5 ventricular zone

In order to further establish the dynamic expression pattern of NC-TrkC, we used an antibody that identifies both isoforms of TrkC. Similar to the mRNA expression pattern, TrkC immmunostaining was observed at the ventricular zone of E13.5 but not E15.5 neocortex (Figure 12A-B). Further, western blot analysis of E13.5 to E15.5 cortical protein lysates, clearly shows that while at E13.5 NC-TrkC (Figure 12C, lower band) dominates over FL-TrkC (Figure 12C, upper band), by E15.5 this ratio is reversed (Figure 12 C, D, ratio of NC-TrkC to FL-TrkC at E13.5= 2.25±0.9 compared to 0.299±0.012 at E15.5, p-value=0.003). Thus, we went on study the role of NC-TrkC in cell fate determination in the developing cortex.

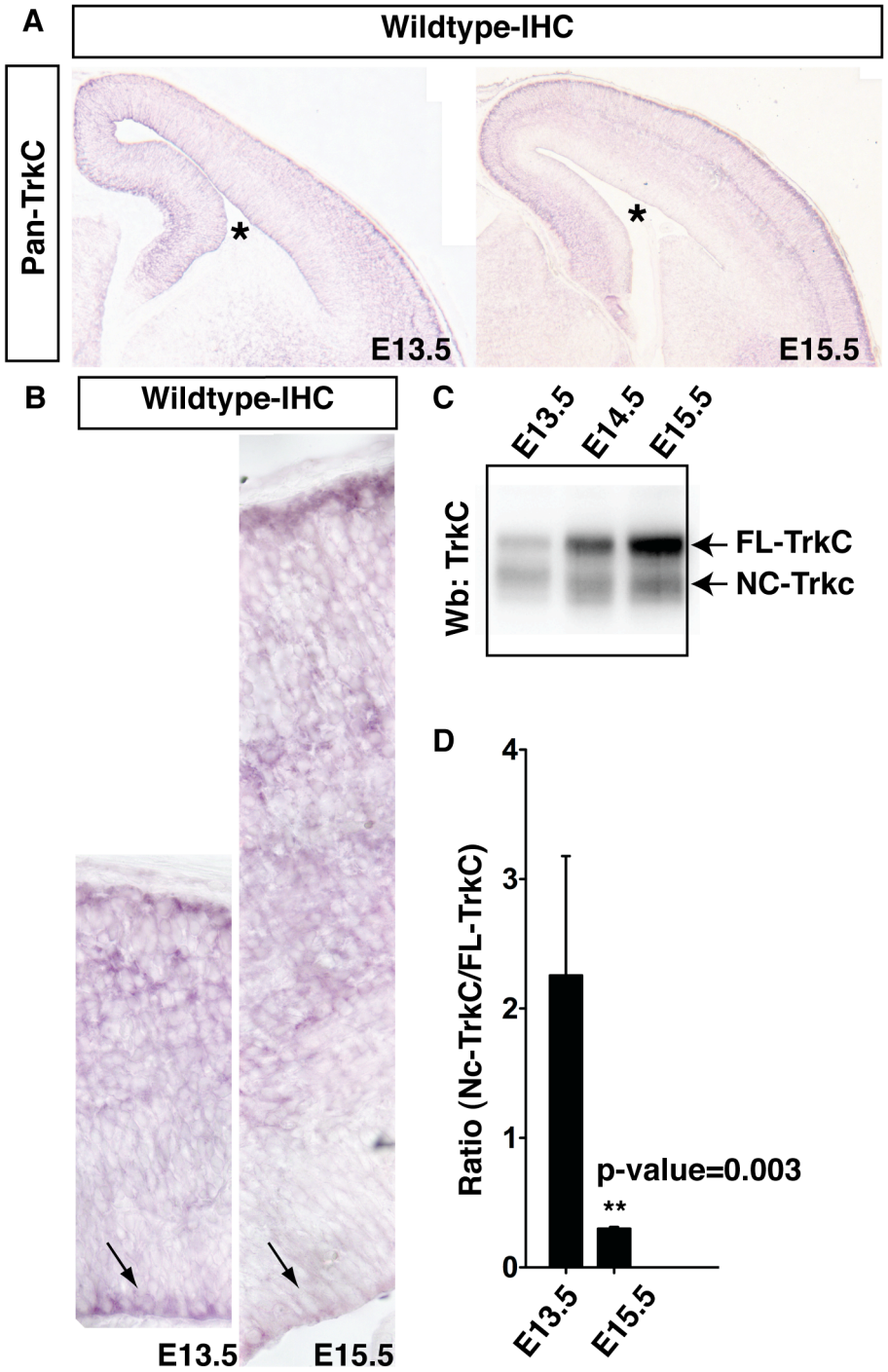

Figure 12. Ratio of NC-TrkC to FL-TrkC shifts from E13.5 to E15.5

(A) Immunohistochemistry against TrkC shows that at E13.5, TrkC is expressed strongly in the VZ and weakly in the cortical plate. At E15.5, the expression of TrkC in the cortical plate is high and the signal in the VZ is below detection **(B)** Higher magnification images of the developing cortex at E13.5 and E15.5 show the presence of TrkC expression in the VZ at E13.5 but not E15.5 (arrows) **(C)** Western blot analysis of E13.5, 14.5 and 15.5 cortical lysates shows the presence of the two isoforms of TrkC and their relative abundance **(D)** At E13.5 NC-TrkC dominates over FL-TrkC while the ratio is reversed by E15.5 (ratio of NC-TrkC to FL-TrkC at E13.5= 2.25±0.9 compared to 0.299±0.012 at E15.5, p-value=0.003).

10. Over-expression of *NC-TrkC* leads to over-production of deep layer neurons at the expense of upper layer neurons

In order to study the function of NC-TrkC in cortical cell fate determination, we over-expressed the receptor at E12.5 in cortical progenitors. The cDNA was followed by an *IRES-EGFP* sequence allowing us to study the fate of these cells. When we looked at the location of the *NC-TrkC* expressing cells four days after the injection, we observed that a vast majority of these GFP positive postmitotic cells were located in the deeper layers of the cortex, as compared to *GFP* only electroporations. On studying the molecular identity of these GFP positive cells, we observed an increase in the number of GFP positive cells that were also positive for layer VI (Tbr1) or layer V (Ctip2) markers upon *NC-TrkC* over-expression as compared to *GFP* alone over-expression (Figure 13A, B; Tbr1: 21.2±4.9% from n=8 control versus 30.1±3.8% from n=5 *NC-TrkC* over-expression; p-value=0.004. Ctip2: 21.4±6.5% from n=8 control versus 35±4.8% from n=8 *NC-TrkC* over-expression; p-value=0.0003). This increase in deeper layer markers was coupled with a decrease in the number of GFP positive cells also positive for an upper layer marker-Cux1 (Figure 13A, B; 42.2±5.4% from n=6 control versus 29.1±6.2% from n=6 *NC-TrkC* over-expression; p-value=0.003). These results thus suggested that NC-TrkC could program cortical progenitors to favor the production of deeper layer neurons at the expense of upper layer neurons.

Of the two-tyrosine binding sites present in the FL-TrkC- Shc binding site and Plc-γ binding site, NC-TrkC only possesses the *Shc* binding site- Y516. The tyrosine at this position upon phosphorylation leads to the recruitment of Shc, thus initiating downstream signaling.

We hence asked if this tyrosine (Y516) and its phosphorylation were necessary for the NC-TrkC mediated control over cortical cell fate. We

introduced a mutated variant of *NC-TrkC* carrying a tyrosine to phenylalanine mutation at the 516th position (Y516F) in cortical progenitors via *in utero* electroporation at E12.5. When we analyzed these brains we observed that NC-TrkC Y516F had no influence on cell fate. GFP positive cells co-localized with Tbr1, Ctip2 and Cux1 to the same extent as control GFP positive cells (Figure 13A, B; Tbr1: 21.2±4.9% from n=8 control versus 19.1±5.1% from n=6 *NC-TrkC Y516F* over-expression; Ctip2: 21.4±6.5% from n=8 control versus 26.5±3.1% from n=6 *NC-TrkC Y516F* over-expression; Cux1: 42.2±5.4% from n=6 control versus 42.4±5.6% from n=6 *NC-TrkC Y516F* over-expression; all p-values >0.05).

Next, we asked whether the extracellular domain of NC-TrkC was important for its role in cell fate determination. Our interest was based on the lack of *Ntf3* expression in the cortex during early development. To answer this, we introduced an extracellular domain-lacking mutant of *NC-TrkC* (ΔECD-NC-TrkC) in E12.5 cortical progenitors by *in utero* electroporation. We found that the over-expression of Δ*ECD-NC-TrkC* resulted in the same phenotype as that achieved when the full length *NC-TrkC* was over-expressed. The proportion of GFP+ cells that co-labeled with Ctip2 and Tbr1 was significantly higher than that in control electroporations, while those that were Cux1+ was lowered (Figure 13A, B; Tbr1: 21.2±4.9% from n=8 control versus 29.8±4.1% from n=5 ΔECD-*NC-TrkC* over-expression, p-value=0.007; Ctip2: 21.4±6.5% from n=8 control versus 39.8±4.3% from n=5 ΔECD-*NC-TrkC* over-expression, p-value<0.0001; Cux1: 42.2±5.4% from n=6 control versus 29.2±5.3% from n=5 ΔECD-*NC-TrkC* over-expression, p-value=0.003; all p-values between Nc-TrkC and ΔECD-NC-TrkC over-expression >0.05)

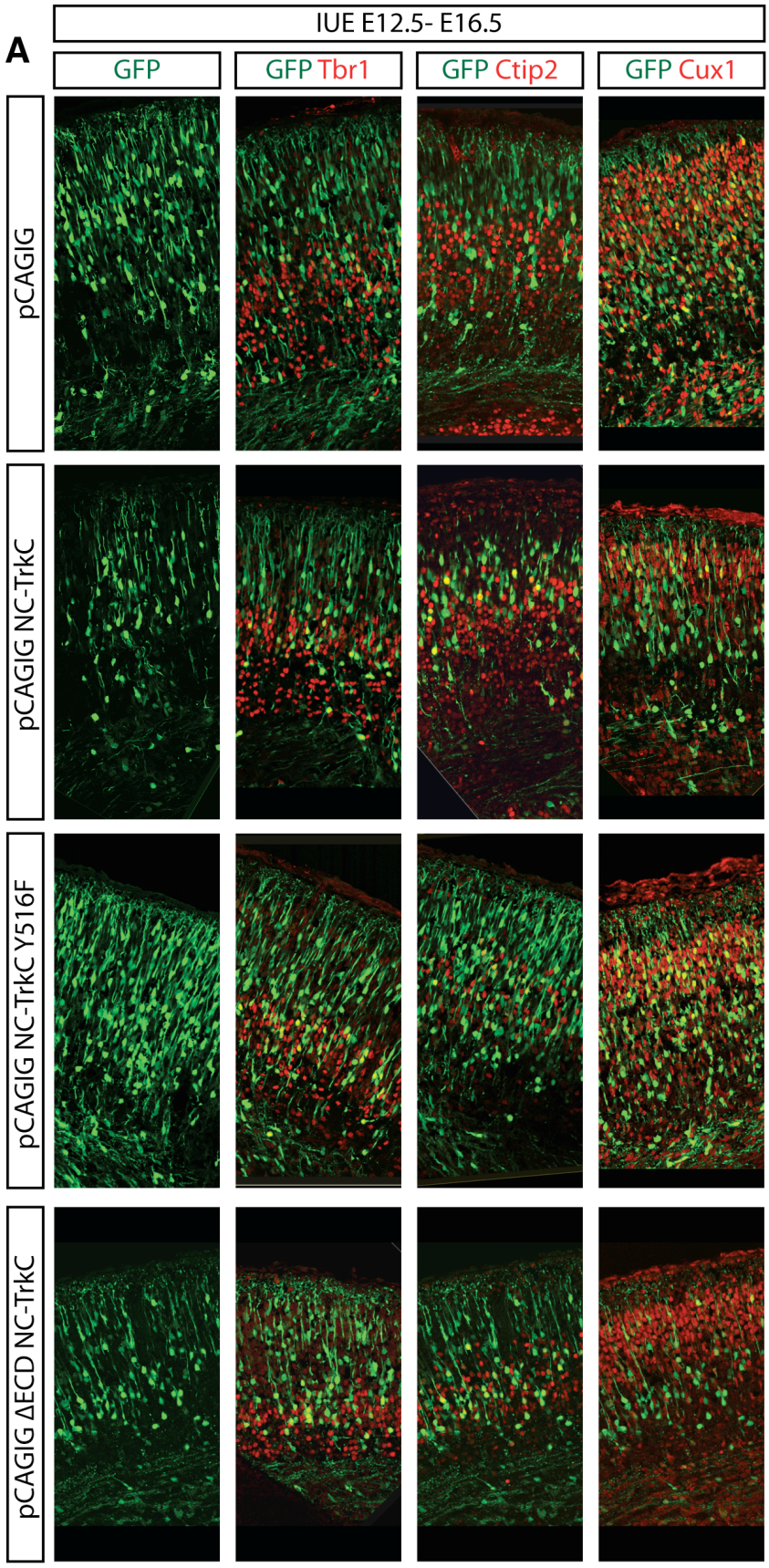
A
IUE E12.5- E16.5
GFP
GFP Tbr1
GFP Ctip2
GFP Cux1
pCAGIG
pCAGIG NC-TrkC
pCAGIG NC-TrkC Y516F
pCAGIG ΔECD NC-TrkC

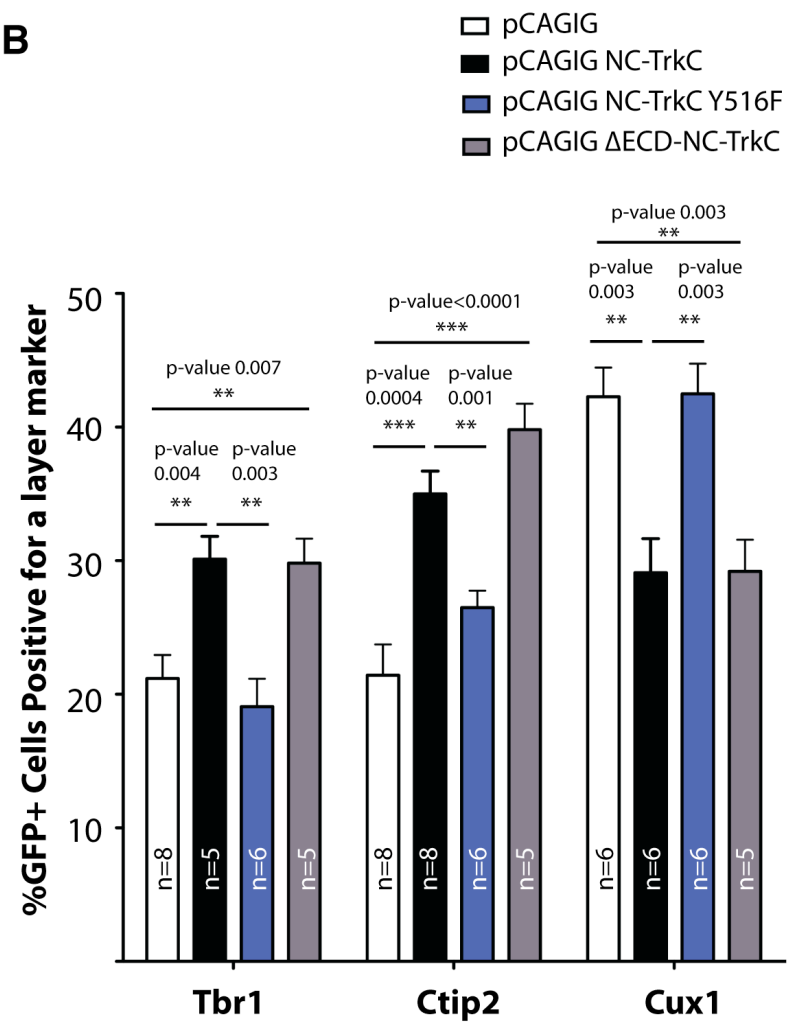

Figure 13. *NC-TrkC* over-expression leads to an increase in deeper layer production.

(A) Series of *in utero* electroporations (IUE) wherein the empty vector, *NC-TrkC*, *NC-TrkC Y516F* or ΔECD NC-TrkC were over-expressed at E12.5 and the brains analyzed at E16.5. With the over-expression of *NC-TrkC*, cortical progenitors produce more Tbr1+ and Ctip2+ deep layer neurons and lesser Cux1+ upper layer neurons. Over-expression of the mutated *NC-TrkC* Y516F abolishes this effect. The over-expression of the Δ*ECD NC-TrkC* mutant, where the entire extracellular domain has been deleted, also leads to an increased production of Tbr1+ and Ctip2+ cells, while leading to a decrease in the number of Cux1+ cells. **(B)** Percentage of GFP positive cells that were either positive for the deeper layer marker Tbr1 or Ctip2 or upper layer marker Cux1. P-values and number of samples analyzed are labeled within the figure. Error bars indicate mean± S.E.M.

11. *NC-TrkC* and pERK1/2 share opposing expression domains in the developing neocortex

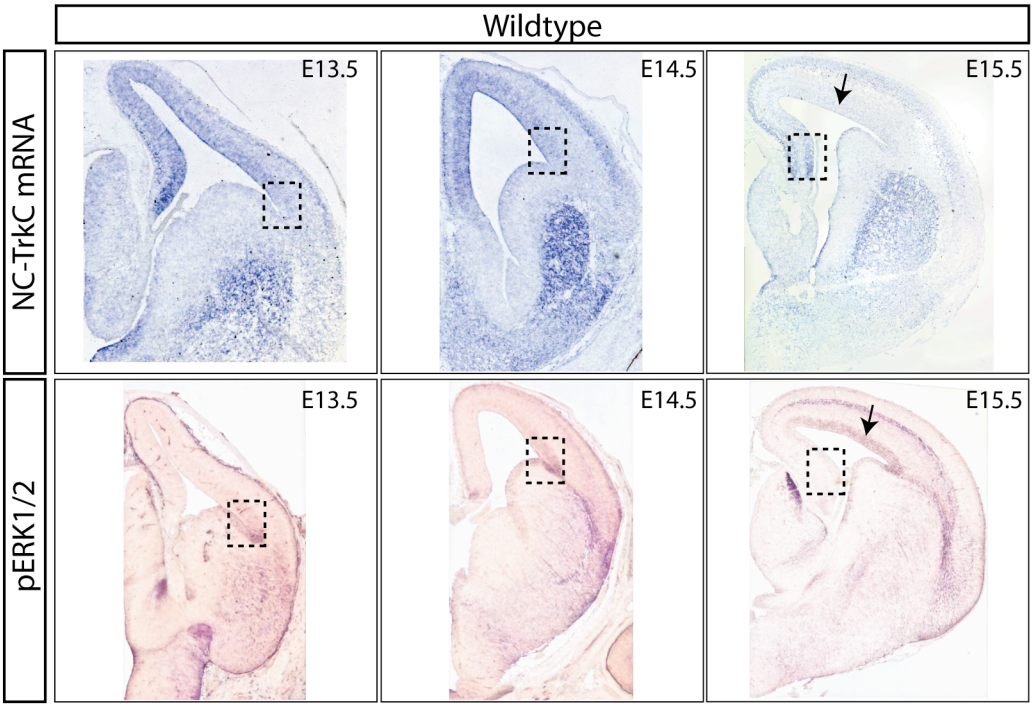

Figure 14. Comparison of *NC-TrkC* and p-ERK1/2 expression patterns.
At E13.5 *NC-TrkC* is expressed throughout the cortical VZ whereas pERK1/2 is only present at the very lateral edge. At E14.5 when the expression of *NC-TrkC* recedes from the lateral boundary of the VZ, pERK1/2 extends further medially. At E15.5, when *NC-TrkC* expression is completely lost from the VZ (arrow), pERK1/2 is present uniformly throughout the cortex (arrow). Also, at E15.5 when expression of *NC-TrkC* persists in the hippocampal anlage, pERK1/2 is not present.

One of the products of activation of receptor tyrosine kinases is the activation of the MAP kinase pathway (phosphorylation of ERK1/2). We asked if the presence of the NC-TrkC could be a negative regulator of such a pathway, thereby dampening ERK1/2 mediated signaling. The deletion of *ERK1/2* is also known to cause an increase in the number of deeper layer neurons and a decrease in upper layer neuronal populations (Pucilowska et al., 2012). Since this is phenocopied by the over-expression of *NC-TrkC*, we had further reasons to believe that NC-TrkC could negatively regulate ERK1/2 signaling. We studied the expression pattern of phosphorylated-ERK1/2 from E13.5-15.5 and compared it to the expression of *NC-*

TrkC. We found that the expression pattern of *NC-TrkC* and pERK1/2 were opposing at all stages (Figure 14). At E13.5 *NC-TrkC* was expressed throughout most of the cortical VZ, barring the lateral most edge. Interestingly, at the same stage pERK1/2 is present only within this small region (Figure 14; left column). At E14.5, when *NC-TrkC* follows a high medial-low lateral expression, pERK 1/2 extends further medially (Figure 14; middle column). At E15.5, when *NC-TrkC* expression is completely lost from the cortical VZ, pERK1/2 is present throughout the VZ (Figure 14; right column). This mutually exclusive pattern of *NC-TrkC* and pERK1/2 expression raised the question if NC-TrkC could negatively regulate ERK signaling.

12. NC-TrkC negatively regulates ERK signaling *in vitro*

To study if NC-TrkC could prevent ERK phosphorylation, we transfected HEK293T cells with *NC-TrkC*. To activate the MAP kinase pathway in HEK293T cells, we stimulated the cells with 100ng/ml EGF and lysed the cells at varying time points. Over-expression of NC-TrkC lead to a decrease in the p-ERK1/2 levels at all stages analyzed (Figure 15A). Phosphorylation of NC-TrkC at Tyr516 (Y516F, Shc binding site) could also be seen as a result of EGF mediated transactivation, as reported earlier (Figure 15A, (Puehringer et al., 2013)). To further investigate if signaling via the Y516 was necessary for the NC-TrkC mediate negative regulation of ERK signaling, we transfected the *NC-TrkC Y516F* mutant in HEK293T cells. Again, we observed a significant decrease in the amount of pERK1/2 when the wildtype NC-TrkC was expressed in comparison to the mutated NC-TrkC (Figure 15B). This suggests that phosphorylation and/or signaling via Y516 is important for the negative regulation of ERK signaling by NC-TrkC.

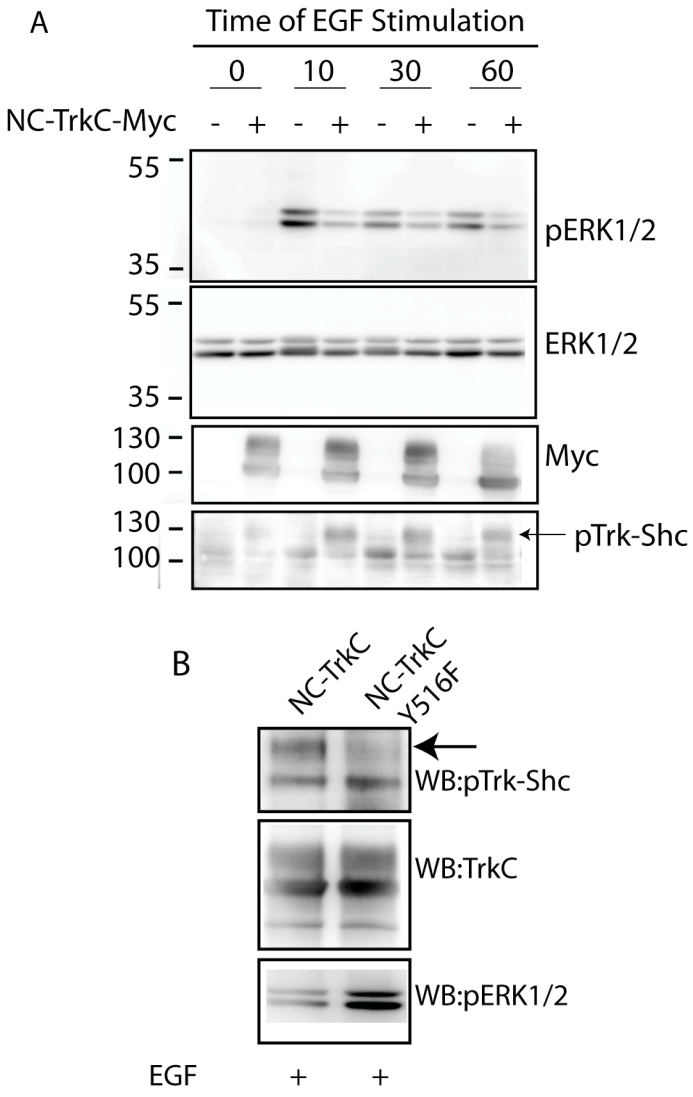

Figure 15. NC-TrkC negatively regulates ERK signaling *in vitro*
(A) HEK293T cells transfected with *NC-TrkC* were stimulated with EGF and the cells were harvested at different time points. Probing the blots for pERK1/2 shows that expression of *NC-TrkC* leads to a decrease in pERK1/2 levels. This effect was consistent throughout all the time points studied. EGF activation also leads to the phosphorylation of the TrkC Shc binding site **(B)** Decrease in p-ERK1/2 levels upon *NC-TrkC* transfection as compared to pERK1/2 levels in *NC-TrkC Y516F* mutant over-expressing cells.

13. NC-TrkC interacts with BMPRIA both *in vivo* and *in vitro*

The above data thus clearly highlights the important role played by NC-TrkC in cortical cell fate determination. We then investigated the signaling pathway activated downstream of NC-TrkC. Since, Nc-TrkC

does not possess any kinase domain in the carboxy terminal of the protein, we wondered if the receptor could interact with other membrane proteins that could serve as co-receptors. In a completely serendipitous experiment, we observed that NC-TrkC could interact with the BMP class I receptor-BMPRIA. We over-expressed an EGFP tagged version of *NC-TrkC* along with a myc tagged version of *BMPRIA* in HEK293T cells (Figure 16A). 24 hours post transfection, the cells were harvested without stimulation or after stimulation with either Ntf3 or BMP-4 or both. After immunoprecipitation using an antibody against EGFP or Myc, we observed that NC-TrkC and BMPRIA co-immunoprecipitated (Figure 16A). The interaction was not affected by addition of either the NC-TrkC ligand-Ntf3 or the BMPRIA ligand-BMP4 (Figure 16A). This suggests a constitutive interaction between the two receptors. To verify if these two receptors also interact *in vivo*, we immunoprecipitated NC-TrkC from E13.5 cortical lysates using an antibody specific to this isoform. When we probed for BMPRIA, we indeed observed a specific band at the predicted molecular weight of BMPRIA (Figure 16B). NC-TrkC was visualized using a pan-TrkC antibody (Figure 16B). The presence of a single band confirms the specificity of the immunoprecipitating antibody for the NC-TrkC isoform.

To further test the interaction of these two receptors, we cultured E13.5 cortical progenitors and transfected them with the tagged versions of these two receptors. A co-localized pixel map shows that the two receptors show a near complete over-lapping domain of expression (Figure 16C).

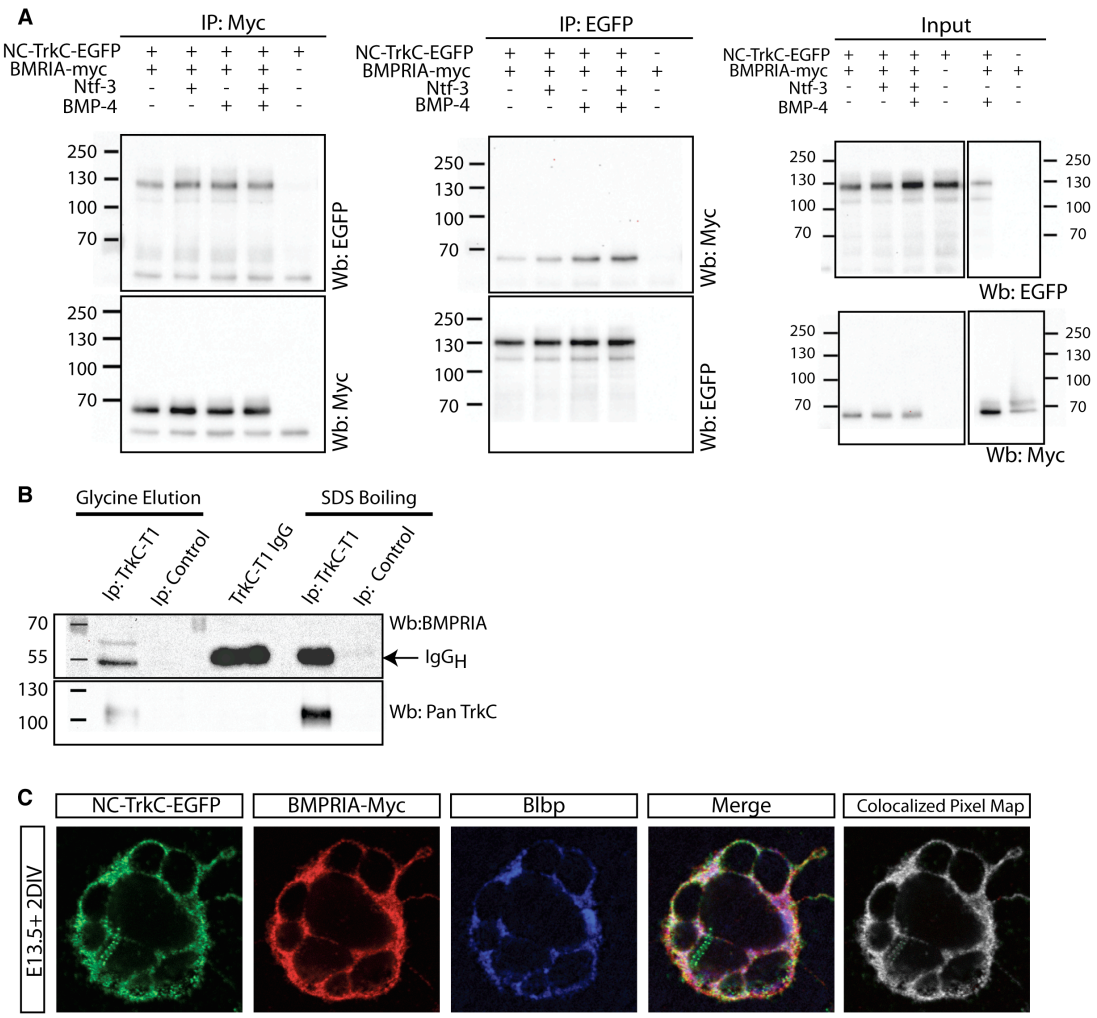

Figure 16. NC-TrkC and BMPRIA interact *in vivo* and *in vitro*.
(A) EGFP tagged *NC-TrkC* and Myc-tagged *BMPRIA* were co-transfected in HEK293T cells. 24 hours post transfection, the cells were either stimulated with Ntf-3 or BMP-4 or both for two minutes. Immunoprecipitation of NC-TrkC using an anti-EGFP antibody or BMPRIA using an anti-Myc antibody shows that the two receptors interact *in vitro* constitutively. **(B)** Immunoprecipitation of NC-TrkC using an antibody specifically against the truncated TrkC isoforms (TrkC-T1) shows that BMPRIA co-immunoprecipitates from E13.5 cortical lysates. Glycine elution was used to minimize the amount of IgG released. NC-TrkC was visualized using a pan-TrkC antibody. IP control involved using only PrG sepharose beads without any antibody **(C)** Cultured E13.5 cortical progenitors were transfected with *EGFP* tagged *NC-TrkC* and *Myc-tagged BMPRIA* constructs. Blbp staining confirms the progenitor identity of these cells. A co-localized pixel map, shows that these receptors share a near complete sub-cellular expression domains.

14. The Intracellular Domain of NC-TrkC is required for interaction with BMPRIA

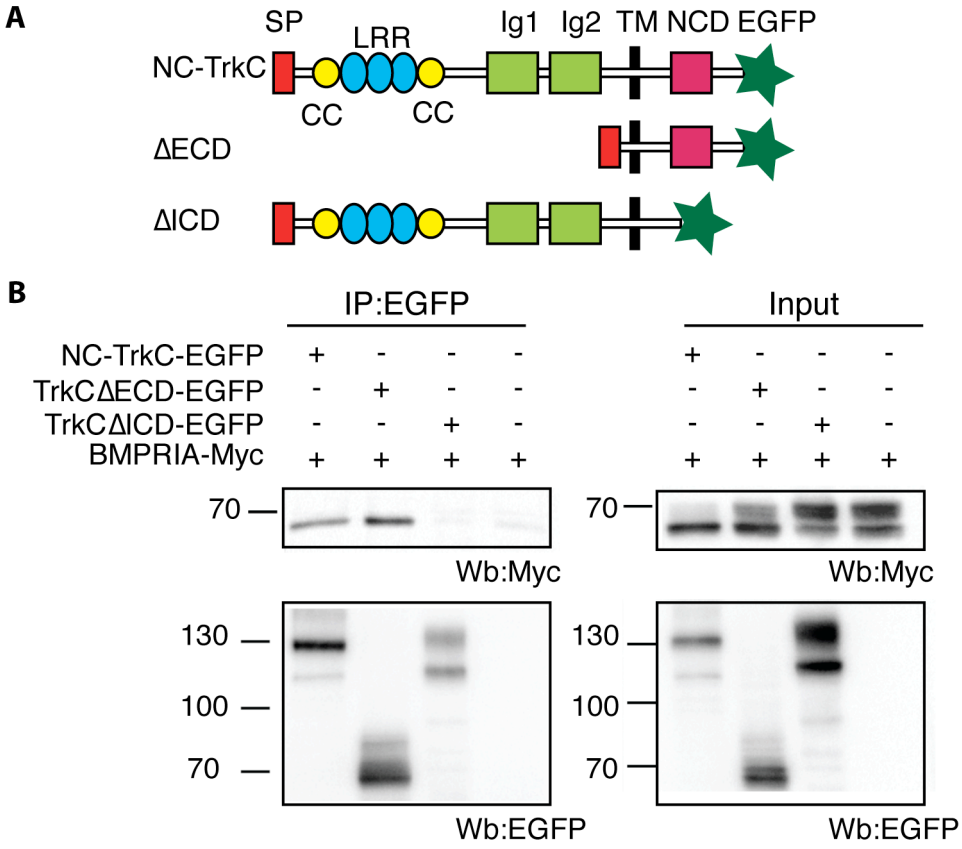

Figure 17. The Intracellular Domain of NC-TrkC is required for interaction with BMPRIA.
(A) Scheme showing the different deletion constructs of NC-TrkC used. ΔECD lacks the entire extracellular domain corresponding to amino acids 33-383 of mouse NC-TrkC. ΔICD similarly lacked the intracellular domain proximal to the juxta-membrane region, corresponding to amino acids 393-614 of mouse NC-TrkC. SP=Signal Peptide, CC= Cysteine cluster LRR= Leucine rich region, Ig=Immunoglobulin like domain, TM=Transmembrane region, NCD= Non catalytic domain **(B)** The EGFP tagged deletion constructs of *NC-TrkC* were co-transfected with *BMPRIA* in HEK293T cells. Immunoprecipitation of NC-TrkC using an anti EGFP antibody shows that while the ΔECD mutant could still bind to BMPRIA, the ΔICD mutant could not bind any longer.

In order to identify the domain within NC-TrkC that interacts with BMPRIA, we cloned deletion constructs of NC-TrkC, that either lacks the extracellular domain (ΔECD-Δaa 33-383) or the intracellular domain (ΔICD-Δaa 393-614) (Figure 17A, Takahashi et al., 2011). We transfected these deletion constructs along with Myc tagged-*BMPRIA* in HEK293T cells and immunoprecipitated NC-TrkC using an anti-EGFP antibody. We found that the ΔECD-NC-TrkC binds BMPRIA with

an affinity very similar to the full length NC-TrkC. The ΔICD-NC-TrkC however did not bind to BMPRIA (Figure 17B). These results thus show that NC-TrkC and BMPRIA interact with their intracellular domains, which might have implications for down-streaming signaling.

15. NC-TrkC Y516F also binds to BMPRIA

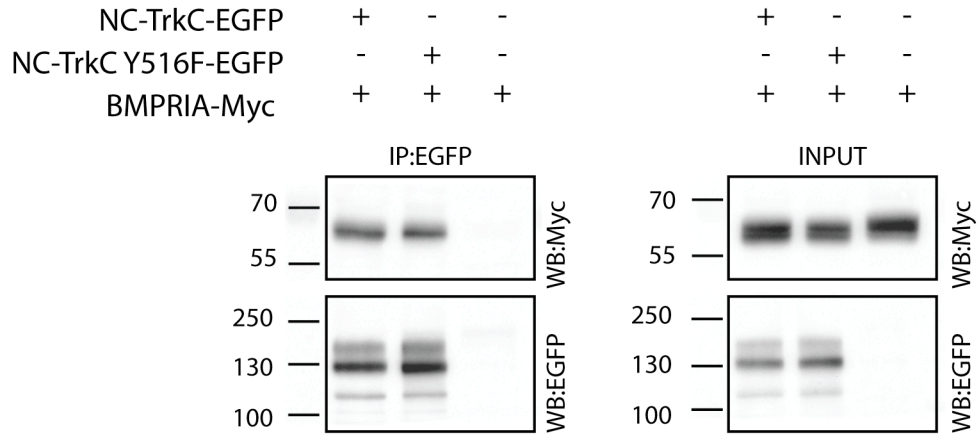

Figure 18. NC-TrkC Y516F also binds to BMPRIA.
NC-TrkC-EGFP or *NC-TrkC Y516F –EGFP* constructs were co-transfected with Myc tagged BMPRIA in N2A cells. Immunoprecipitation of NC-TrkC and NC-TrkC Y516F using an anti EGFP antibody shows that the Y516F mutation has no effect on the binding properties of the receptor with BMPRIA.

Since, the over-expression of the *NC-TrkC* Y516F mutant did not alter the cell fate in the developing cortex, we questioned if this could be a result of its inability to interact with BMPRIA. To answer this, we cloned a NC-TrkC Y516F-*EGFP* fusion construct and co-transfected it with a *BMPRIA*- myc tagged construct in N2A cells. We found that NC-TrkC Y516F could also interact with BMPRIA and the interaction was comparable to the interaction of wildtype NC-TrkC and BMPRIA (Figure 18).

16. *BMPRIA* is expressed throughout neurogenesis in the VZ of the developing cortex

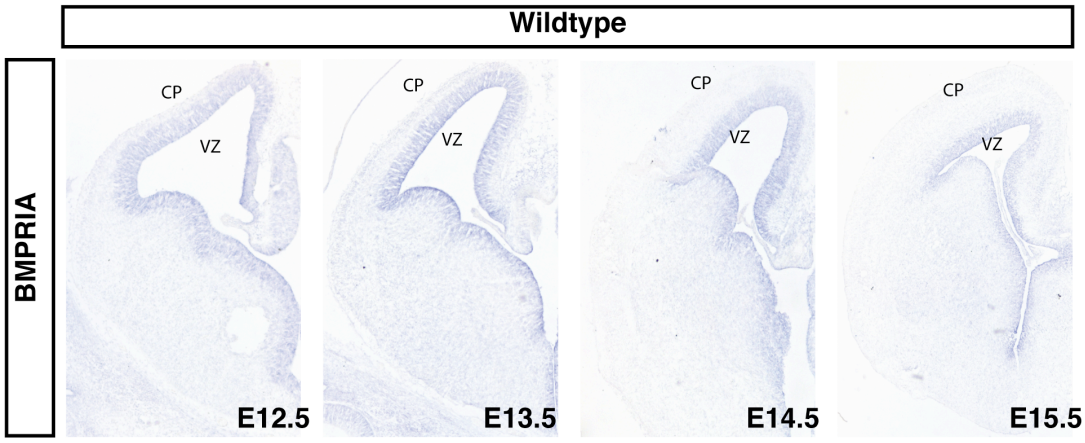

Figure 19. Expression pattern of *BMPRIA*.
In situ hybridization against the *BMPRIA* mRNA shows that *BMPRIA* has a consistent pattern of expression in the VZ between E12.5 and E15.5. VZ=ventricular zone, CP=cortical plate

In order to understand the relevance of the interaction of BMPRIA with NC-TrkC, we studied the expression pattern of *BMPRIA* during different stages of embryonic neurogenesis. Using a riboprobe against the *BMPRIA* mRNA, we found that *BMPRIA* is continuously expressed in the ventricular zone of the cortex from E12.5 till E15.5 (Figure 19). Since *NC-TrkC* is also expressed in the VZ, atleast from E12.5 to E14.5, we believed that this interaction could have important implications for cortical cell fate determination.

17. *BMPRII* and *NC-TrkC* share opposing expression patterns

Since BMPRIA interacts with NC-TrkC, we wondered if this could interfere with its interaction with BMPRII, which is required for activating BMPRIA in a ligand dependent manner. We initially studied the expression pattern of *BMPRII* to examine the degree of overlap in expression between the three genes. We found that *BMPRII* was expressed at very low levels in the VZ and follows a high lateral to low

medial gradient at E13.5 and E14.5 (Figure 20). This expression pattern is opposite to that of *NC-TrkC*. Further, at E15.5, when the expression of *NC-TrkC* is lost from the VZ; *BMPRII* was expressed more uniformly throughout the cortical VZ (Figure 20). This data thus suggests that the interaction of NC-TrkC and BMPRIA is largely independent of the interaction of BMPRIA and BMPRII and thus might not directly influence BMPRIA mediated BMP signaling/Smad phosphorylation.

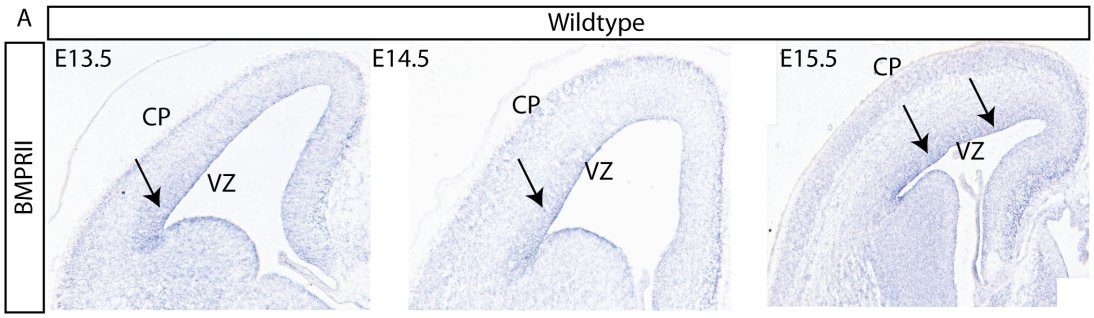

Figure 20. Expression pattern of *BMPRII*.
BMPRII is expressed at low levels at E13.5 and E14.5 in the lateral edges of the cortical VZ. At E15.5, though the expression is still low, the expression is uniformly present throughout the VZ. Stronger expression can also be seen in the cortical plate, particularly at E14.5 and 15.5. VZ= ventricular zone, CP=cortical plate

18. NC-TrkC enhances the kinase activity of BMPRIA in a ligand independent manner

To understand the implications of the interaction between NC-TrkC and BMPRIA, we studied the influence of NC-TrkC on the intrinsic kinase activity of BMPRIA. Normally, ligand binding to BMPRII leads to phosphorylation and activation of BMPRIA, leading to further activation of the downstream signaling molecules but spontaneous mutations in the GS domain of BMPRIA, which precedes the kinase domain, have also been known to enhance the kinase activity of BMPRIA independent of ligand activation (Wieser et al., 1995).

Thus, we asked if the interaction between the NC-TrkC and BMPRIA receptors could in a similar manner influence the kinase activity of

BMPRIA in a ligand independent way. To study this, we used the phosphorylation of Smad1, a physiological downstream effector of BMPRIA activation, as a measure of the kinase activity.

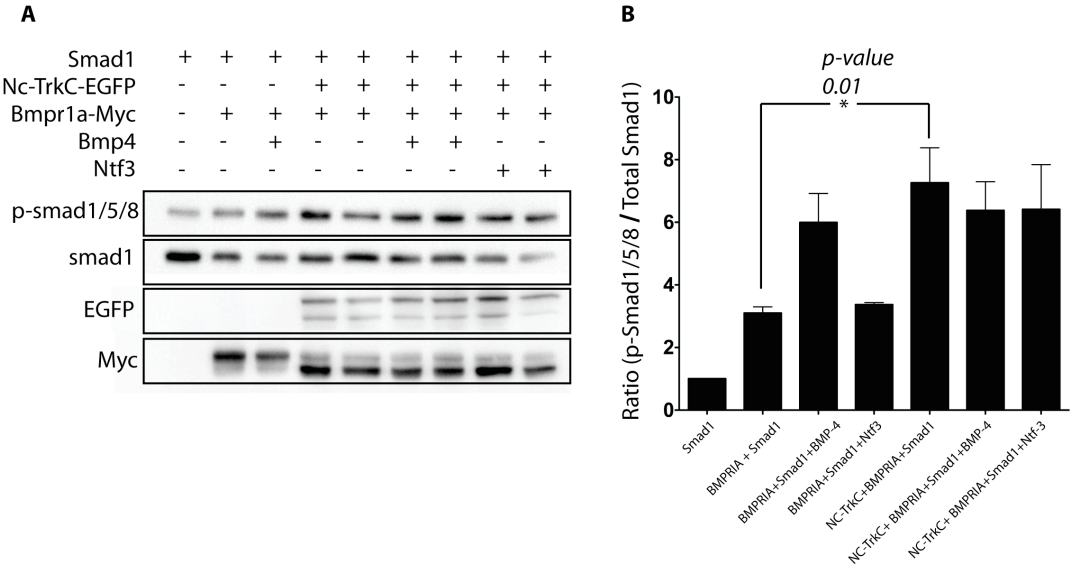

Figure 21. NC-TrkC enhances the kinase activity of BMPRIA.
(A) *Smad1* along with myc tagged *BMPRIA* and EGFP tagged *NC-TrkC* was transfected in HEK293T cells. The cells were either not stimulated or stimulated with 10ng/ml BMP-4 or 50ng/ml Ntf-3 for five minutes. Western blot analysis for p-Smad1/5/8, total Smad1 and EGFP and Myc was performed **(B)** Quantification of the relative amounts of p-Smad1/5/8 to total Smad1 shows that NC-TrkC increases the intrinsic kinase activity of BMPRIA by 2.3 fold (p-value=0.01). The extent of NC-TrkC mediated increase in Smad1 phosphorylation was ligand independent.

We transfected *BMPRIA, NC-TrkC* and *Smad1* in HEK293T cells and investigated the extent of Smad1 phosphorylation. We found that the extent of Smad1 phosphorylation increased by 2.3 fold when *NC-TrkC* was co-transfected with *BMPRIA* (Figure 21A,B, p-value=0.01). Interestingly, the extent of Smad1 phosphorylation did not increase on the addition of BMP-4, a ligand for BMPRIA. These results collectively show that the interaction of NC-TrkC with BMPRIA can enhance the intrinsic kinase activity of BMPRIA, which is independent of the class II receptor or a ligand.

19. Generation of shRNA constructs to knock-down the expression of BMPRIA

In order to study the role of BMPRIA in cell fate decisions in the developing cortex, we prepared four different shRNA clones against the mouse *BMPRIA* coding region. The shRNA clones were cloned into pSUPER.retro.neo-GFP (oligoengine).

The shRNA clones were transfected along with a *BMPRIA*-myc tagged construct in HEK293T cells. The protein samples were subjected to western blot analysis. Amongst the four clones, we found that shRNA 3 and 4 gave a very high knockdown efficiency (Figure 22). GAPDH served as the loading control. Clones 3 and 4 were used for subsequent analysis.

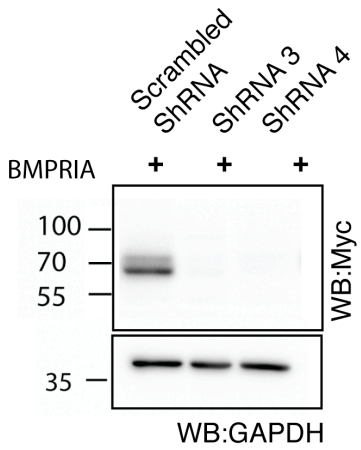

Figure 22. Generation of shRNA clones for the knock-down of *BMPRIA* expression.
Myc tagged *BMPRIA* was transfected along with either one of the four shRNA clones in HEK293T cells. Equal amounts of the total protein were loaded on a SDS-PAGE gel. Immunoblotting using an anti Myc antibody shows that shRNA clones 3 and 4 give a high efficiency knock down. GAPDH served as the loading control.

20. Down-regulating BMPRIA leads to a premature production of upper layer neurons

In order to study the role of *BMPRIA* in cortical development, we down-regulated its expression using shRNAs introduced by *in utero* electroporation at E12.5. When we analyzed the brains at E16.5, we

observed a significant decrease in the number of GFP positive cells that co-localized with the deeper layer marker Ctip2 (Figure 23A). A scrambled shRNA co-electroporated with *EGFP* served as the control (Figure 23A,C 25.5±3.2% of GFP positive cells were also Ctip2 positive in control electroporation compared to 13.99±5.7% upon *BMPRIA* down-regulation, n=6 each, p-value= 0.0027; student's t-test). This decrease in the number of deeper layer neurons generated upon down-regulation of *BMPRIA*, coincided with an increase in the number of upper layer neurons marked by Cux1 (Figure 23A,C 36.05±2.9% of GFP positive cells were also Cux1 positive in control electroporation compared to 57.09±7.5% upon *BMPRIA* down-regulation, n=6 for the control and 5 for BMPRIA shRNA electroporation, p-value= 0.002; student's t-test). These results thus suggest that cortical progenitors that down-regulate *BMPRIA* preferentially produce upper layer neurons over deep layer neurons.

21. NC-TrkC and BMPRIA controlled pathways interact genetically to control cortical cell fate

Since we have shown that NC-TrkC and BMPRIA interact *in vivo* and *in vitro*, we hypothesized that the signaling pathways controlled by them could also interact to determine cortical cell fate. Further, our experiments have shown that over-expression of NC-TrkC promotes deeper layer cell fate while down-regulating BMPRIA leads to an increase in upper layer cell fate. To understand if these pathways interact, we over-expressed NC-TrkC and down-regulated BMPRIA simultaneously.

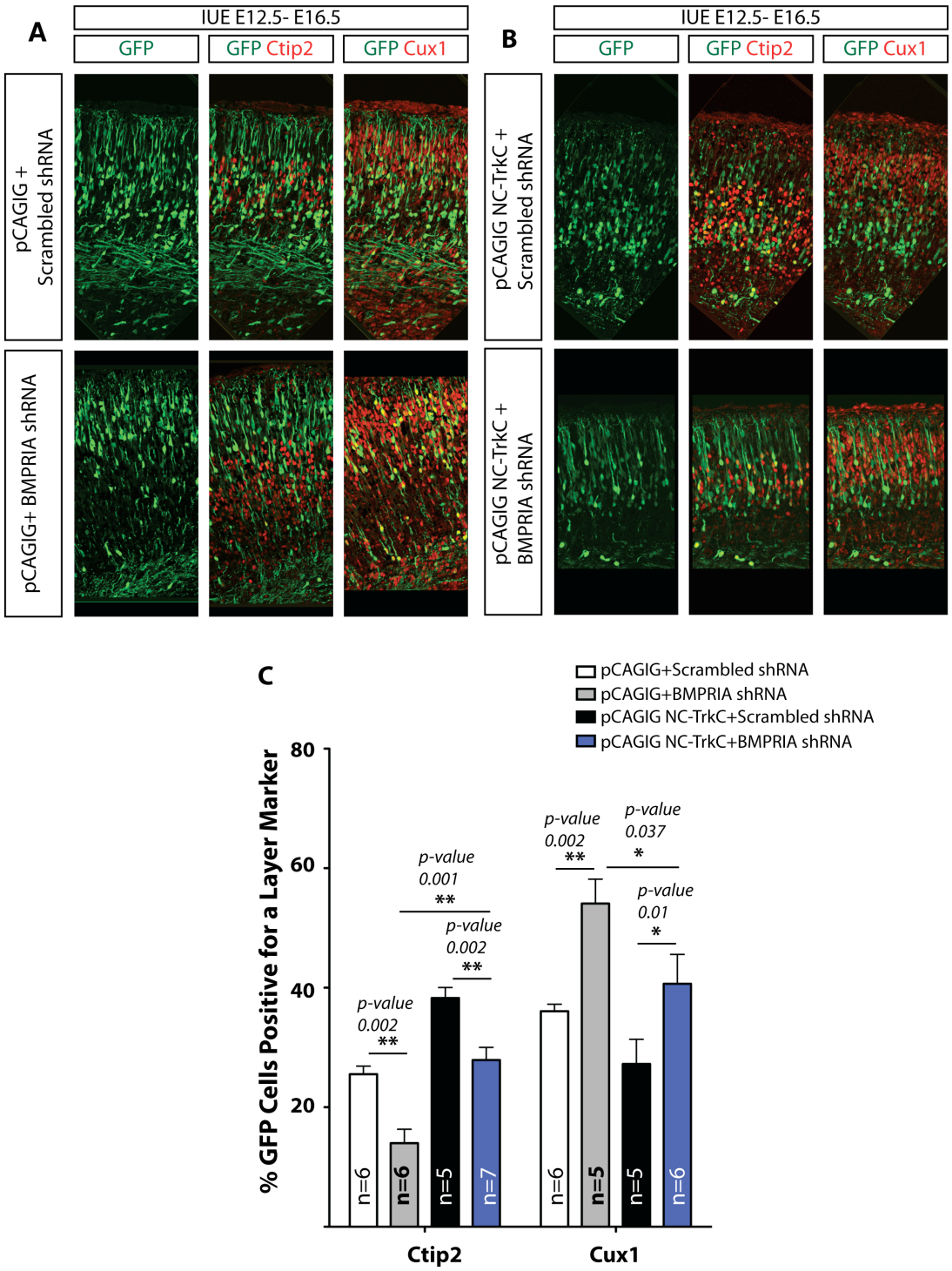

Figure 23. Down-regulation of *BMPRIA* leads to an increased production of upper layer neurons and NC-TrkC-BMPRIA controlled pathways interact genetically.

(A) Down-regulation of *BMPRIA* by introducing shRNA constructs in cortical progenitors at E12.5 leads to a increased production of Cux1+ upper layer neurons from these progenitors and a reduction in the number of Ctip2+ deeper layer neurons **(B)** Over-expression of NC-TrkC and simultaneous down-regulation of *BMPRIA* negates the excess deeper layer Ctip2+ neurons generated upon *NC-TrkC* alone over-expression. The excess number of Cux1+ upper layer neurons generated upon *BMPRIA* down-regulation is also lowered when *NC-TrkC* is over-expressed along with the down-regulation of *BMPRIA* **(C)** Percentage of GFP positive cells that were either positive for the deeper layer marker Ctip2 or upper layer marker Cux1. P-

values and number of samples analyzed are labeled within the figure. Error bars indicate mean± S.E.M.

We reasoned that if these two molecules do control genetic pathways that control cell fate determination, then the over-expression of one and the down-regulation of the other should restore the equilibrium in the system. Supporting our hypothesis, we observed that when *NC-TrkC* was over-expressed and *BMPRIA* down-regulated, the proportion of both the percentage of GFP positive cells that were Ctip2 positive or Cux1 positive were restored to control levels (Figure 23 A-C). The percentage of GFP positive cells upon *NC-TrkC* over-expression and *BMPRIA* down-regulation that were also Ctip2 positive was 27.89±5.6% (n=7) compared to 13.99±5.7% when *BMPRIA* was down-regulated (n=6, p-value=0.001, student's t-test) and 38.27±3.9% with *NC-TrkC* over-expression (n=5, p-value=0.004). On the other hand the percentage of Cux1 positive cells was 44.2±9.9% (n=6) compared to 57.09±7.5% when *BMPRIA* was down-regulated (n=5, p-value=0.037; student's t-test) and 27.2±9.2% when *NC-TrkC* was over-expressed (n=5, p-value= 0.016; student's t-test).

22. FL-TrkC also interacts with BMPRIA

Finally, we were also interested in studying if FL-TrkC could also interact with BMPRIA. Since FL-TrkC and BMPRIA do not have over-lapping expression patterns in the developing cortex, this interaction would not be of relevance *in vivo* for the developing cortex. This interaction could nevertheless be important in other systems where these receptors are co-expressed. Further, a small region within the intracellular domain of NC-TrkC and FL-TrkC is common, supporting a probable interaction between FL-TrkC and BMPRIA. We transfected tagged versions of FL-TrkC and BMPRIA in HEK293T cells. Immunoprecipitation of either one of the two receptors again showed

that they could interact *in vitro* (Figure 24). The interaction was again not affected by the addition of Ntf3 (Figure 24).

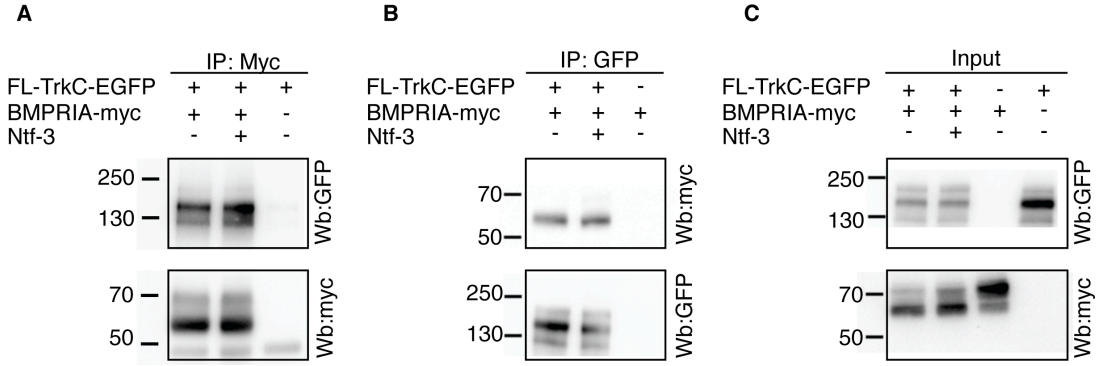

Figure 24. FL-TrkC can also interact with BMPRIA.
EGFP tagged *FL-TrkC* and Myc tagged *BMPRIA* were co-transfected in HEK293T cells. The cells were either not stimulated or stimulated with 50ng/ml Ntf3 for two minutes. Upon Immunoprecipitation using an antibody against EGFP or Myc, we observed that that the two receptors co-immunoprecipitate. The interaction was unaffected by the addition of Ntf3.

Thus, our results conclusively establish the importance of the truncated TrkC receptor- NC-TrkC in regulating cell fate decision-making in the developing cortex. NC-TrkC most likely influences this process via its negative regulation of ERK signaling. On the other hand, NC-TrkC and BMPRIA interact both *in vitro* and *in vivo*. We also showed that the downstream genetic programs controlled by these two receptors interact to determine cell fate in the cortex. Our data also suggests that Ntf3, which mediates feedback signaling from cortical postmitotic neurons to progenitors, may act through NC-TrkC in influencing cell fate.

We next asked, if pathways other than that controlled by Ntf3 also control cortical feedback signaling.

23. *Cbln4* is also upregulated in the *Sip1* mutant cortex

Since the deletion of *Ntf3* from the *Sip1* mutant cortex did not rescue the *Sip1* mutant phenotype, we wondered if other molecules could also contribute to feedback signaling in the *Sip1* mutant. We found that the transneuronal cytokine-*Cbln4* was upregulated in the *Sip1* mutant cortex at E14.5. This upregulation was restricted to the cortical plate (Figure 25A). We also studied the expression of two other family members- *Cbln1* and *Cbln2*. We did not find expression of either of these two genes at E14.5 in the wildtype or the *Sip1* mutant (Figure 25B).

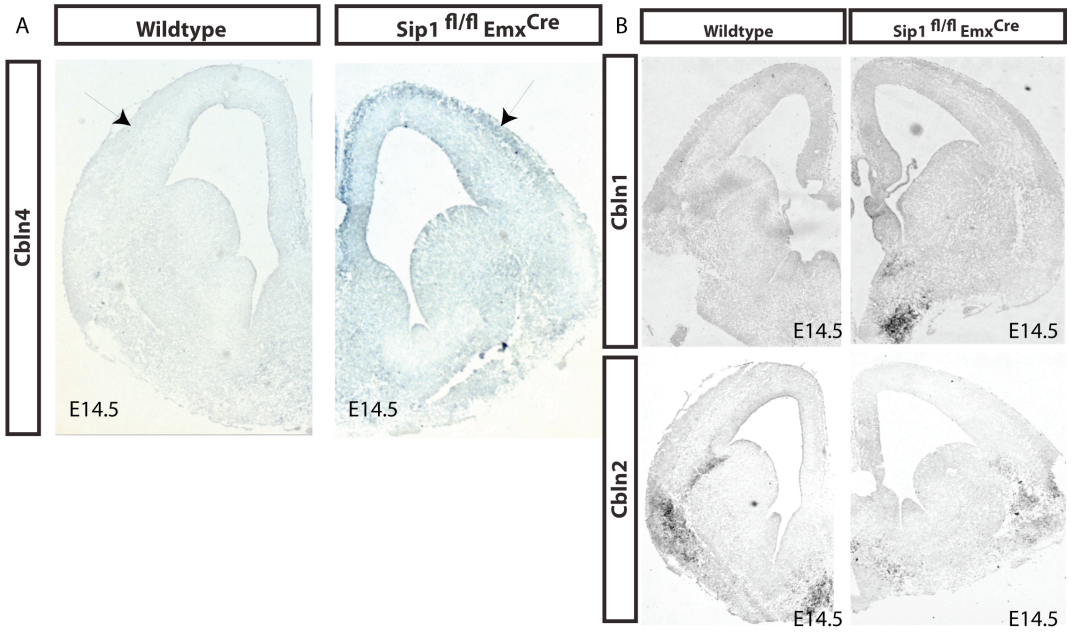

Figure 25. *Cbln4* is upregulated in the *Sip1* mutant cortex.
(A) *Cbln4* was found to be upregulated in the *Sip1* mutant cortical plate at E14.5 **(B)** *Cbln1* and *Cbln2* on the other hand were not expressed at E14.5 in either the wildtype or the *Sip1* mutant cortex.

24. Sip1 can bind to the *Cbln4* enhancer region *in vitro*

Since *Cbln4* was upregulated in the *Sip1* mutant cortex, we considered if Sip1 could directly repress the transcription of *Cbln4*. To test this, we cloned a short region of the *Cbln4* enhancer region upstream of a gaussia luciferase-coding region (Figure 26A).

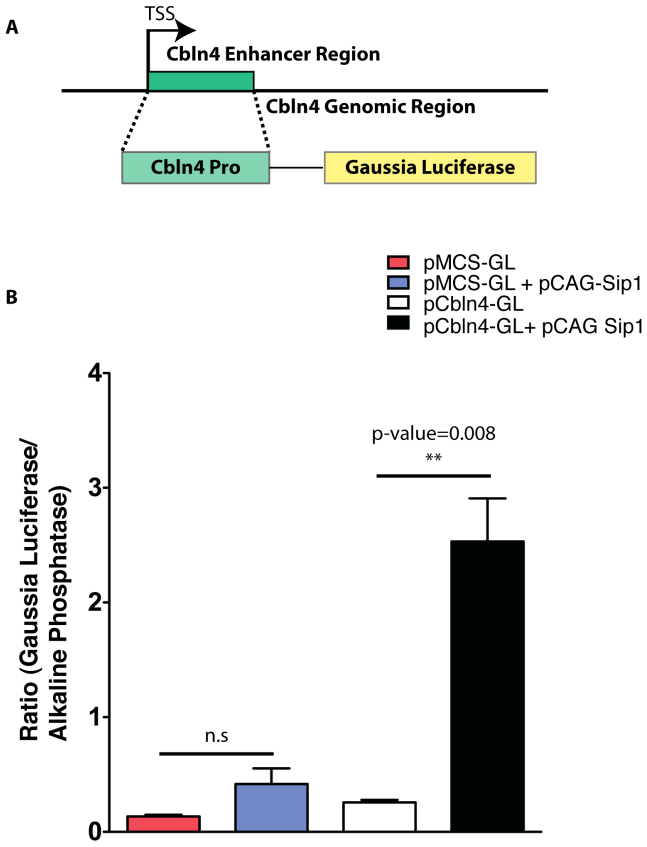

Figure 26. Sip1 can bind to the *Cbln4* enhancer region *in vitro*.
(A) Scheme showing the Cbln4 promoter sequence used for the luciferase assay **(B)** Ratio of Gaussia luciferase to Alkaline phosphatase. Sip1 addition does not alter the enhancer activity of the empty vector (n=3, p-value>0.05). The transcriptional activity of the Cbln4 enhancer was found to be 9.8 fold higher when Sip1 was co-transfected (n=3, p-value= 0.008**).**

We transfected this either alone or with *Sip1* in HEK293T cells and used the ratio of Gaussia Luciferase to Alkaline phosphatase as a measure of the transcriptional regulation of Sip1 over the enhancer region. The sequence contained the bipartite Sip1 consensus binding motif CACCT(G) (Comijn et al., 2001). As expected, the addition of

Sip1 did not alter the transcriptional rate of the control promoter (Figure 26B, ratio of gaussia luciferase to alkaline phosphatase without Sip1=0.13±0.1 and with Sip1=0.41±0.13, p-value>0.05). While we expected a decrease in the transcription of gaussia luciferase upon Sip1 binding to the *Cbln4* enhancer, we observed an increase (Figure 26B, ratio of gaussia luciferase to alkaline phosphatase without Sip1=0.25±0.02 and with Sip1=2.53±0.38, p-value=0.008). While the transcriptional regulation of the *Cbln4* promoter by Sip1 was opposite to what was expected, this result still supports the binding of Sip1 to the promoter region *in vitro*. Indeed Sip1 is known to function both as an activator or repressor depending on the genomic context and environment (Yoshimoto et al., 2005).

25. Cbln4, 1 and 2 can also signal back to influence the proportions of basal and apical progenitors

Since *Cbln4* was upregulated in the *Sip1* mutant cortex, we decided o study its role in feedback signaling by over-expressing it in a wildtype cortex. Further, since Cbln1, 2 and 4 share a high degree of sequence homology; we studied the role of all three Cbln family members. Cbln3 was not included as it is known to be not secreted (Iijima et al., 2007). To examine if *Cbln4, Cbln1* and *Cbln2* affect the ratio of apical to basal progenitor population, we over-expressed these molecules exclusively in postmitotic neurons at E12.5. This was done as described previously (Figure 6A). When analyzed at E14.5, we observed that all three *Cbln* family molecules could enhance the proportion of Tbr2 positive basal progenitors (Figure 27A-D, difference in the proportion of Tbr2 positive cells in the electroporated region versus non-electroporated region- for *EGFP* electroporation =-1.3±0.2%, n=5; *Cbln1-EGFP*= 15±5.7%, n=3, p-value=0.0017; *Cbln2*= 16.3±10.1%, n=3, p-value=0.0076; *Cbln4-EGFP*= 12.1±5.3%, n=4, p-value=0.0009).

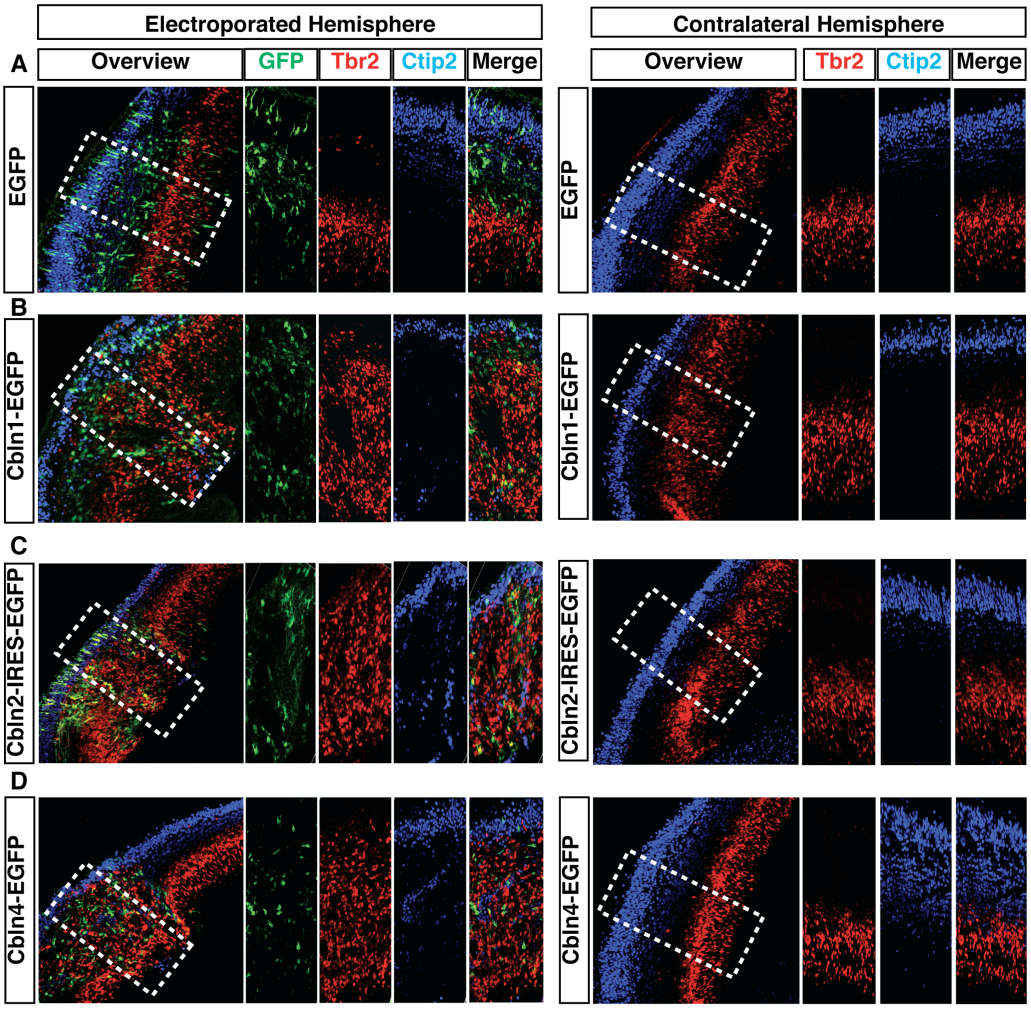
Electroporated Hemisphere
Contralateral Hemisphere
A
Overview
GFP
Tbr2
Ctip2
Merge
Overview
Tbr2
Ctip2
Merge
EGFP
EGFP
B
Cbln1-EGFP
Cbln1-EGFP
C
Cbln2-IRES-EGFP
Cbln2-IRES-EGFP
D
Cbln4-EGFP
Cbln4-EGFP

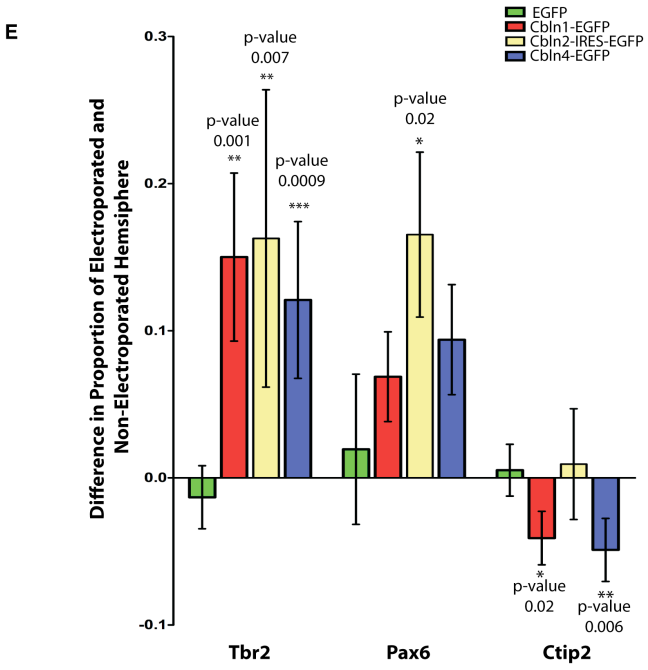
E
EGFP
Cbln1-EGFP
Cbln2-IRES-EGFP
Cbln4-EGFP
Difference in Proportion of Electroporated and Non-Electroporated Hemsiphere
0.3
0.2
0.1
0.0
-0.1
p-value 0.007
**
p-value 0.001
**
p-value 0.0009
***
p-value 0.02
*
*
p-value 0.02
**
p-value 0.006
Tbr2
Pax6
Ctip2

Figure 27. Over-expression of *Cbln1*, 2 and 4 leads to an increase in Tbr2 positive basal progenitor population.
Cbln1-EGFP, *Cbln2* and *Cbln4-EGFP* were over-expressed at E12.5 and the brains were analyzed at E14.5. **(A, E)** Differences between the electroporated and non-electroporated hemispheres upon *EGFP* over-expression with respect to the proportion of Tbr2+ cells = 1.3± 2.1% n=5, Pax6+ cells= 1.9± 5.1%, n=3 and Ctip2+ cells= -0.5± 1.7%, n=5 **(B, E)** Over-expression of *Cbln1-EGFP* leads to a 15±5.7% increase in Tbr2+ cells compared to the contralateral hemisphere (n=3, p-value compared to EGFP over-expression= 0.0017). Pax6+ cells were not significantly changed between *Cbln1* and empty vector over-expression (n=3, p>0.05). Ctip2+ cells were reduced by -4±1.8% upon *Cbln1* over-expression (n=3, p-value=0.02) **(C, E)** Over-expression of *Cbln2* leads to a 16.3±10.1% increase in Tbr2+ cells compared to the contralateral hemisphere (n=3, p-value compared to EGFP over-expression = 0.0076). Pax6+ cells were also significantly higher in the electroporated hemisphere (16.5±5.6%, n=3, p=0.03). Ctip2+ cells were not significantly changed upon *Cbln2* over-expression (n=3, p-value>0.05) **(D, E)** Over-expression of *Cbln4-EGFP* leads to a 12.1±5.3% increase in Tbr2+ cells compared to the contralateral hemisphere (n=4, p-value compared to EGFP over-expression= 0.0009). Pax6+ cells were not significantly changed between *Cbln4* and empty vector over-expression (n=3, p>0.05). Ctip2+ cells were reduced by -5±2% upon *Cbln4* over-expression (n=4, p-value=0.006)

This increase in Tbr2 positive cells resembled the increase caused by *Ntf3* over-expression. However, unlike *Ntf3* we did not observe any decrease in Pax6 positive cells (Figure 27A-D, difference in the proportion of Pax6 positive cells in the electroporated region versus non-electroporated region for *EGFP* electroporation = 1.9±5.1%, n=3; *Cbln1-EGFP*= 6.8±3%, n=3, p-value>0.05; *Cbln2*= 16.5±5.6%, n=3, p-value=0.03; *Cbln4-EGFP*= 9.4±3.7%, n=4, p-value>0.05). In fact, there was a slight increase in Pax6 positive cells upon over-expression of all three *Cbln* family members, indicating that these molecules and Ntf3 act on independent pathways. These results may explain as to why the *Sip1* mutant phenotype was not rescued in the *Sip1-Ntf3* double mutant. Up-regulation of *Cbln4* may also be one of the important reasons for the enhanced feedback signaling observed in the *Sip1* mutant.

26. Cbln4 also promotes premature upper layer neurogenesis

We found a decrease in the number of Ctip2 positive deep layer neurons already at E14.5 upon over-expression of both *Cbln1* and *Cbln4* (Figure 27A, C, D, difference in the proportion of Ctip2 positive cells in the electroporated region versus non-electroporated region for *EGFP* electroporation = -0.5±1.7%, n=5; *Cbln1-EGFP*= -4±1.8%, n=3, p-value=0.02; *Cbln2*= 0.9±3.7%, n=3, p-value>0.05; *Cbln4-EGFP*= -4.9±2.1%, n=4, p-value=0.006). Hence, we wanted to study the effects of Cbln4 over-expression on laminar fate in the developing cortex. To do so, we over-expressed *Cbln4* with *EGFP* or *EGFP* alone at E12.5 in wildtype cortices by *in utero* electroporation. To determine the final position of the neurons born at E13.5, we injected BrdU into the mother intraperitonially. When we analyzed the brains at P4, a stage at which migration is mostly complete, we observed that in the *EGFP* alone expressing brains; most of the cells born at E13.5 occupied deeper layers of the cortex, with few cells reaching the upper layers (Figure 28, upper panel). However, with *Cbln4* over-expression, majority of the neurons occupied the upper layers (Figure 28, lower panel). This indicates that when *Cbln4* is over-expressed in the cortex, a vast majority of neurons born at E13.5 within the electroporated region are upper layers neurons. This data supports our hypothesis that *Cbln4* upregulation in the *Sip1* mutant cortex is one of the reasons for the premature generation of upper layer neurons at the expense of deeper layer neurons.

Further, a general increase in the number of BrdU positive cells can be observed with the over-expression of *Cbln4* (Figure 28). This might co-relate to an increase in both the number of Pax6 positive and Tbr2 positive cells observed at earlier stages (Figure 27).

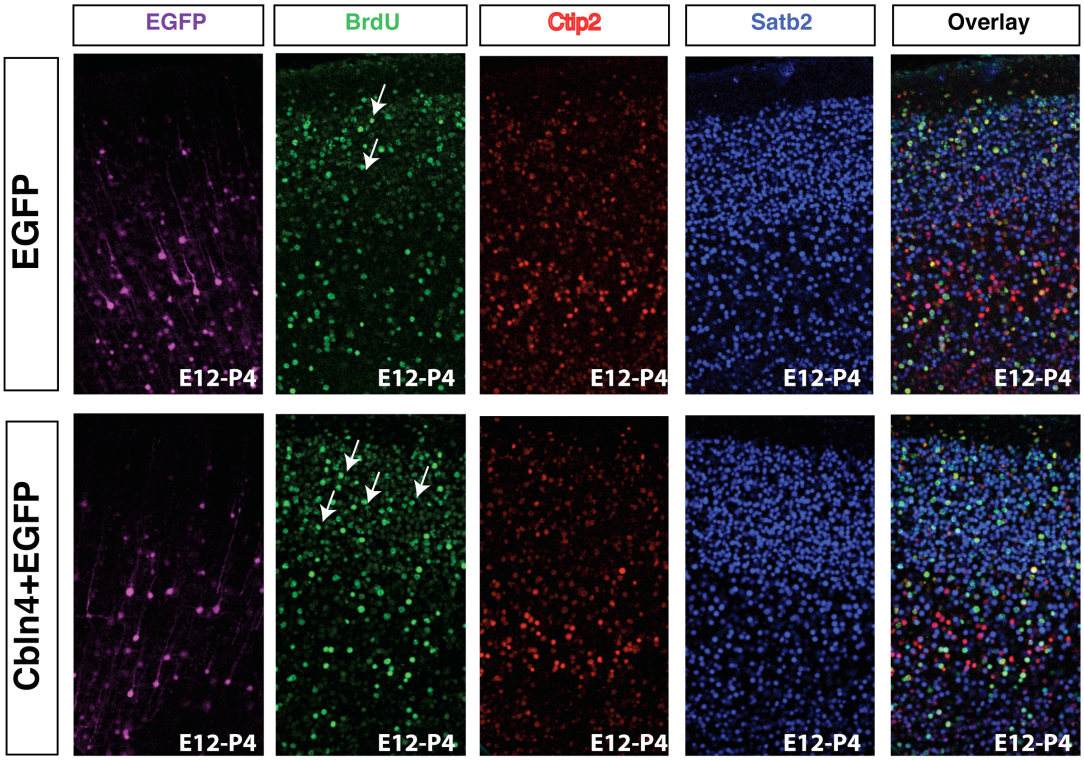

Figure 28. Cbln4 promotes premature upper layer neurogenesis.
A *Cbln4* over-expressing plasmid along with *EGFP* or *EGFP* alone was over-expressed in neocortical neurons at E12.5. A BrdU pulse was given at E13.5 and the brains analyzed at P4. While in control plasmid electroporated brains, only a moderate number of neurons born at E13.5 occupy the upper layers of the cortex, upon *Cbln4* over-expression the number increased significantly (arrows). Also, a decrease in the number of Ctip2+ layer V cells can be seen in upon *Cbln4* over-expression.

27. Receptors for Cbln4 are located along the radial glial process

Since there are few cognate receptors known for the Cbln family, we decided to screen for putative receptor(s). In order to do so, we first wanted to localize the receptor in the developing cortex. We hence cloned a *Cbln4-Alkaline phosphatase* fusion construct and expressed it in HEK293T cells (Figure 29A). We later collected the supernatant from these cells and used the recombinant ligand to identify the location of the receptor (Figure 29B).

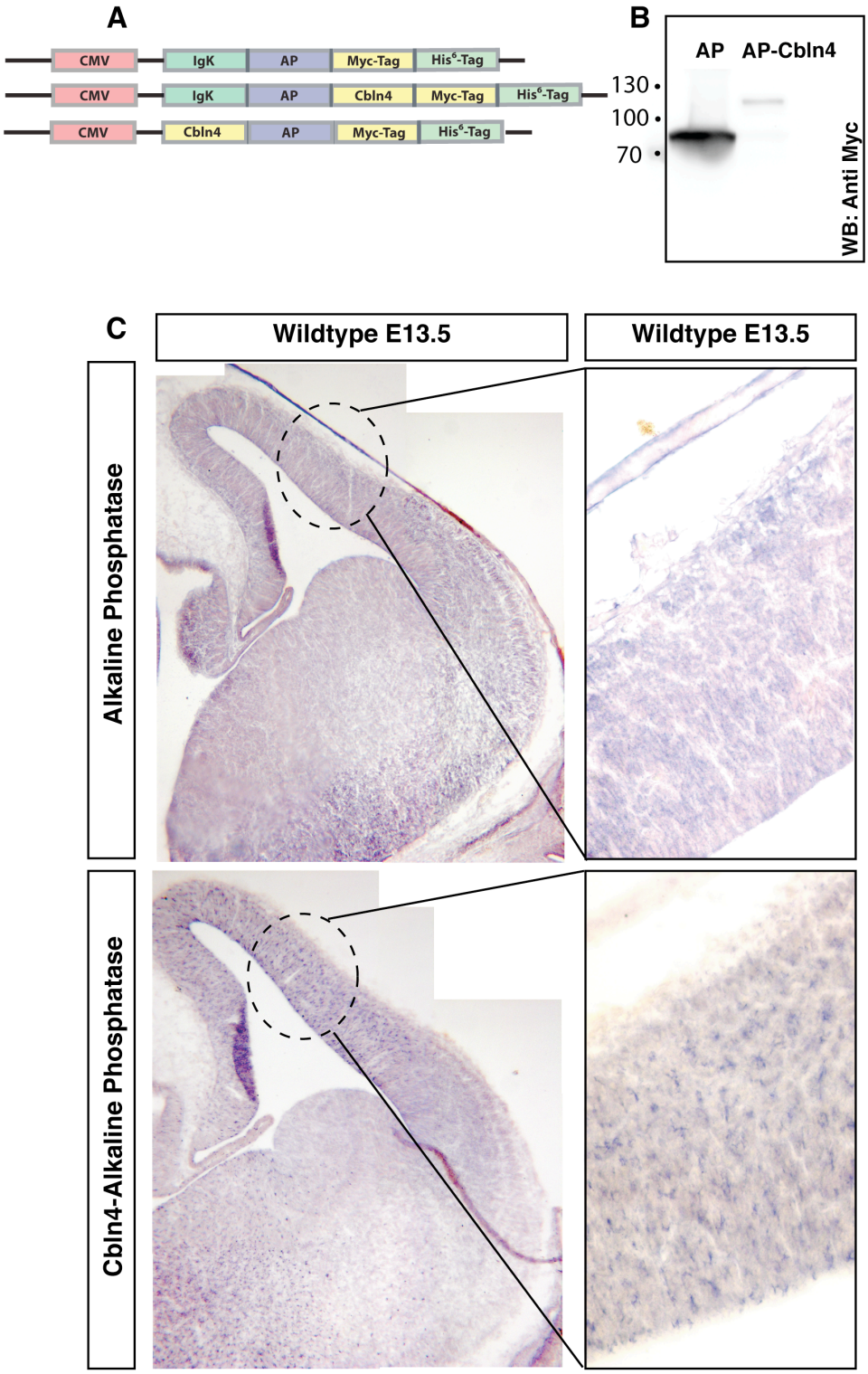

Figure 29. Receptor for Cbln4 is located within the developing cortex
(A) Scheme showing the different Cbln4-Alkaline phosphatase constructs used **(B)** Western blot image showing the presence of the AP tagged Cbln4 in the supernatant of transfected HEK293T cells **(C)** E13.5 wildtype sections were incubated with the untagged AP or the Cbln4-tagged AP. While AP alone does not give any specific signal, Cbln4-AP gave a distinct pattern within the cortex. Staining was not observed in any other part of the tissue. Within the cortex, the staining pattern was radial and segmented.

Untagged Alkaline phosphatase, which served as the negative control did not give any specific staining. Cbln4 tagged Alkaline phosphatase however, showed a dispersed staining pattern within the dorsal cortex (Figure 29C). Specific staining was absent from other areas in the forebrain. Within the cortex, interrupted staining was observed from the ventricular surface till the marginal zone (Figure 29C). Since, at E13.5 the cortex largely comprises of progenitor cells, we believe that this staining most likely represents the presence of receptors on the progenitors. Additionally, since the pattern of staining is radial, we believe that this could represent small segments of the radial glial process (Figure 29C). However, further co-localization studies will be required to confirm this assumption.

28. Preparation of an E14.5 cortical cDNA library

Since the over-expression of *Cbln4* at E12.5 had an effect on the progenitors when analyzed at E14.5, we concluded the cognate receptor must be present between E13.5 and E14.5 in the cortex. We hence decided to construct a full-length cortex specific E14.5 cDNA library. The E14.5 cortical cDNA library was prepared using the full-length cDNA library construction kit (Invitrogen). Post electroporation of two different fractions, representing cDNA clones of different sizes, into electrocompetent bacteria; the culture was plated in serial dilutions to estimate the total number of clones. Fraction 2 cDNA library in pDONR222 contained 5x10*5 cfu with an average insert size of 1.2Kb and 100% recombinants (Figure 30). Fraction 3 cDNA library in pDONR222 contained 1.2x10*6 cfu with an average insert size of 0.8Kb and 100% recombinants (Figure 30). Based on the average size and the percentage of total recombinants, these values indicate that the cDNA library preparation was successful. To transfer the cDNA library into an expression system, the LR cloning system was used to shuttle the library into a Gateway expression plasmid- pDEST 40

(Invitrogen). The total number of clones in pDEST 40 was found to be 6.7x10*5 cfu with an average size of 1.02Kb and 70% recombinants, from fraction 2 (Figure 30). Thus, this library can be used for screening for a Cbln4 cognate receptor in the developing cortex.

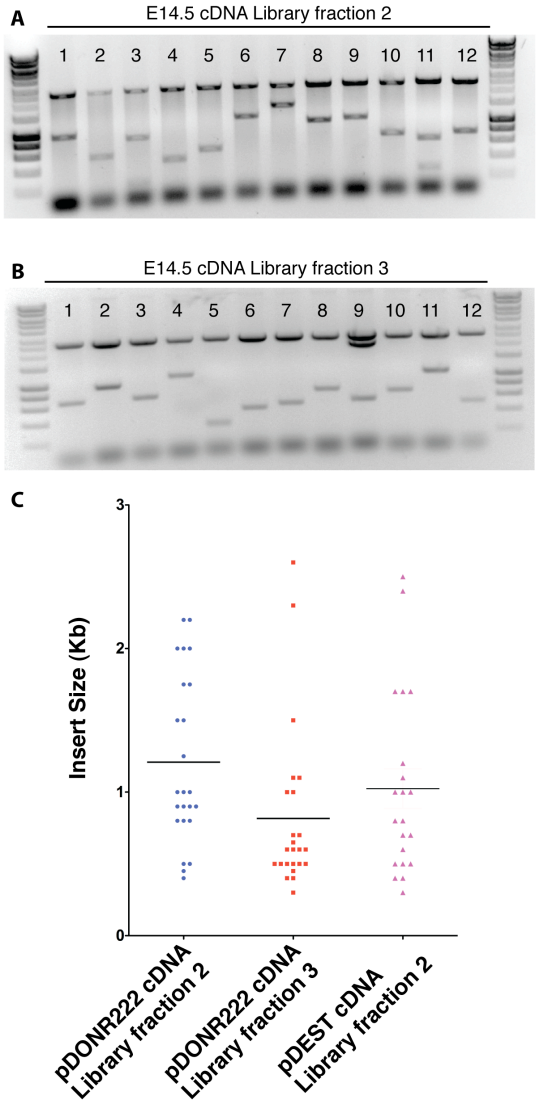

Figure 30. Construction of an E14.5 cortex specific cDNA library
(A) Examples of clones selected from the pDONR 222 cDNA library fraction 2, digested with the enzyme BsrG1 **(B)** Examples of clones selected from the pDONR 222 cDNA library fraction 3, digested with the enzyme BsrG1 **(C)** Quality assessment of the cDNA library. The library in pDONR222, fraction 2 contained 5 x 10*5 cfu with an average insert size of 1.2Kb. The library in pDONR222, fraction 3 contained 1.2 x 10*6 cfu with an average size of 0.8 Kb. Both libraries had 100% recombinants. The library in pDEST, fraction 2 had 6.7 x 10*5 cfu with an average size of 1.02 Kb and 70% recombinants.

Thus we demonstrate that the Cbln family of transneuronal cytokines can also signal to cortical progenitors when expressed in postmitotic neurons. To better understand the molecular pathway controlling this feedback signaling, it would be necessary to identify the cognate receptor for Cbln4 during cortical development. Here, we report the construction of a high quality, full-length E14.5 cDNA library. Receptor screening, by expressing pools of cDNA clones in mammalian cells and using recombinant Cbln4-AP fusion protein, would yield candidate receptors that could control important mechanisms that govern cell fate switch in the developing neocortex.

DISCUSSION

1. Ntf3 mediated feedback signaling

Cortical progenitors cultured *in vitro* can faithfully recapitulate the entire sequence of corticogenesis suggesting a hardwired cellular program (Shen et al., 2006). However, when younger progenitors are transplanted into an older brain, they adapt to their new environment and immediately start producing late born neurons (Frantz and McConnell, 1996; Desai and McConnell, 2000). These two findings thus predict that though progenitors possess all the necessary genetic components to take them through the various stages of neurogenesis, environmental fine-tuning mechanisms must exist that control the timing of cell fate switch.

These environmental cues could originate from multiple sources like the meninges, thalamus or the cerebro-spinal fluid (CSF), all of which have been shown to have important implications on cortical progenitors (Dehay et al., 2001; Zarbalis et al., 2007; Lehtinen et al., 2011; Siegenthaler and Pleasure, 2011). We previously showed that deletion of *Sip1* in postmitotic neurons has severe effects on cortical development (Miquelajauregui et al., 2007; Seuntjens et al., 2009). During neocortical development *Sip1* controls feedback signaling that influences glia versus neuronal cell fate choice. We identified Fgf9 as an important player downstream of *Sip1* that initiates gliogenesis (Seuntjens et al., 2009b). This study also suggested that a similar feedback mechanism might exist within the time span of neurogenesis wherein postmitotic neurons signal back to the progenitors and prevent the over-production of a subtype of neocortical neurons. However, such a feedback mechanism was proposed based on circumstantial evidence. It was neither corroborated with direct evidence, nor was the precise signal governing the switch from deep layer to upper layer cell fate identified.

Here, using mosaic loss-of-function of *Sip1*, we demonstrate that Sip1 controls lamination via non-cell autonomous mechanism. We previously identified *Ntf3* as a Sip1 target in the neocortex. In the current study we show that the binding of Sip1 to the *Ntf3* promoter is functional. Moreover, using *in vivo* gain of function assay, we show that *Ntf3* increases both, the proportion of basal progenitors and the proportion of upper layer neurons. These results, to our knowledge, for the first time conclusively show the presence of cortical feedback signals in neocortical layer specification. Our results also highlight that postmitotic neurons can influence the apical to basal progenitor balance leading to a radial expansion of the cortex. A radial expansion of the cortex has been previously reported with such a shift from apical to basal progenitor population (Nonaka-Kinoshita et al., 2013; Stahl et al., 2013).

Although to our knowledge, *Ntf3* expression has not been conclusively detected in the early developing cortex, our results indicate that there still might be a direct implication of the importance of neurotrophin-Trk signaling pathway in the process of cell fate switch. For instance, over-expression of dominant negative TrkB/C has been shown to reduce the total number of proliferating cortical progenitors (Bartkowska et al., 2007). This finding directly implies that signaling via these receptors is necessary for governing cell cycle parameters. It is possible that in the wildtype scenario, in order to cause cell fate switch, the activation of the Trk receptors is not dependent on their natural ligands but rather on non-classical signaling mechanisms. For example, recent work has shown that EGFR can transactivate both TrkB and TrkC and that the phosphorylation of TrkB and TrkC was unchanged in *BDNF* and *Ntf3* mutants (Ernfors et al., 1994; Puehringer et al., 2013) clearly showing that mechanisms beyond the classical ligand dependent activation of Trk receptors exist in the developing cortex. In such a scenario, we could explain the cell fate switch initiated by Ntf3 in *Sip1* mutants as a hyper-activation of a

system that is normally controlled by other stimuli. It is also possible that Ntf3 is present in the developing cortex but has not been detected. Possible sources of Ntf3 could be incoming thalamo-cortical axons or the CSF both of which have been shown to bring important information to the developing cortex (Dehay et al., 2001; Lehtinen et al., 2011). Additionally, the marginal increase in the proportion of Sox5 positive layer VI neurons in *Ntf3* mutants indicate that Ntf3 is required for controlling important aspects of cortical lamination. However, since the deletion of *Ntf3* from the *Sip1* cortex does not rescue the *Sip1* mutant phenotype, it is probable that multiple pathways exist for controlling cortical feedback signaling.

Recent work points to the existence of lineage specific progenitors (Franco et al., 2012). One hypothesis for the switch from deep layer to upper layer neuron production in the *Sip1* mutant and in the *Ntf3* over-expression studies, would be the preferential effect of Ntf3 on upper layer specific progenitors (Franco and Muller, 2013). In such a scenario, *Ntf3* over-expression could promote early differentiation of upper layer specific progenitors. Since this would prematurely exhaust the progenitor pool, the increase in basal progenitor population seen with *Ntf3* over-expression could be an additional step in order to prevent such a situation.

The presence of secreted molecules like Ntf3 in the cortical plate (CP) that act as feedback signals influencing progenitors located within the ventricular zone (VZ) and sub-ventricular zone (SVZ) raises another intriguing question about how these signals reach the VZ-SVZ from the CP. Signals originating from the CP could either bind to their cognate receptor along the radial glial process or diffuse into the VZ and bind to the receptor on the radial glial cell body (Seuntjens et al., 2009). In the first scenario the effect of Ntf3 over-expression should be local since radial glial processes are widespread and thus signaling would be restricted to a smaller number of progenitors. In the second scenario, signals diffusing to the VZ should produce a widespread

effect, since the area occupied by radial glial cell bodies is much smaller than the size of the cortex they produce (Figure 31). Our results do not provide evidence to support one or the other hypothesis, however we believe that using such a system in combination with optical methods like FRET could address this issue (Figure 31).

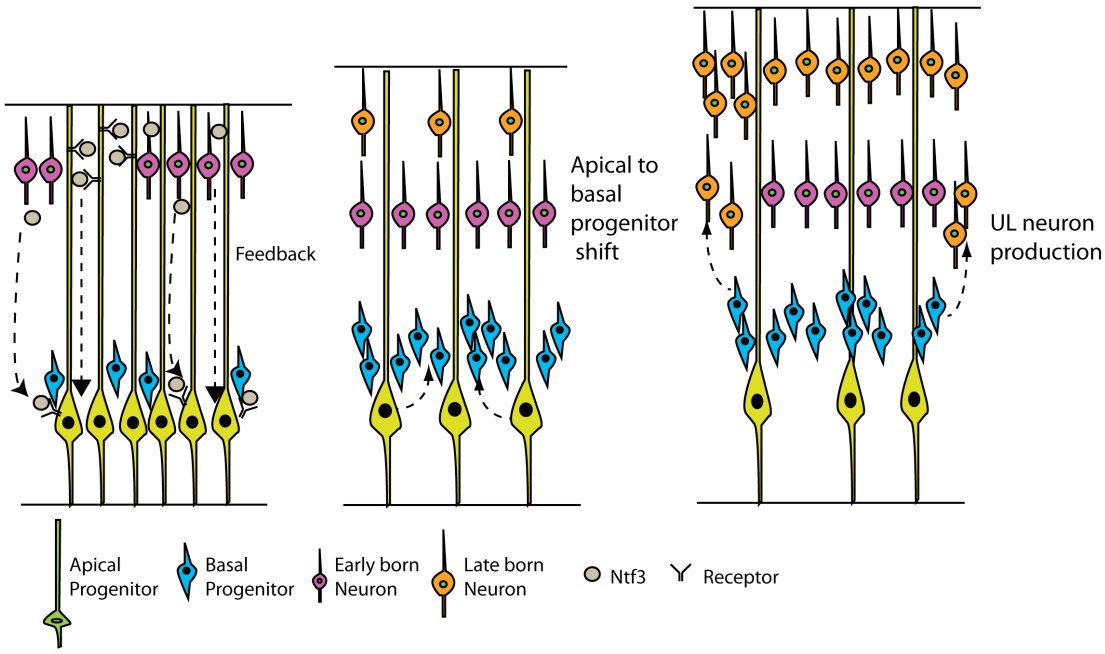

Figure 31. Model depicting the two possible modes of Ntf3 mediated signaling. Receptors located along the radial glial process or on the cell body could sense Ntf3 released by postmitotic neurons. Such a signaling initiates the generation of basal progenitors, which in turn could lead to the expansion of UL neurons.

We believe that we have provided the first evidence for the presence of postmitotic neuron to progenitor feedback signaling in laminar cell fate determination, Ntf3 being one such signal that influences both the ratio of apical to basal progenitors and deep layer to upper layer neurons.

2. Expression Pattern of *NC-TrkC* mirrors the transition from deep layer to upper layer production.

Generation of cortical neurons occurs between E11.5 and E16.5 in the mouse. Each layer has a distinct peak of production- layer VI at E12.5, layer V at E13.5, layer IV at E14.5 and layers II-III at E15.5 (Molyneaux et al., 2007). Further, the onset of neurogenesis begins in rostrolateral positions and progresses caudomedially (Sanderson and Weller, 1990; Hill and Walsh, 2005; Bayatti et al., 2008). This implies that neurogenesis at the lateral edge of the neocortex is developmentally more advanced than the medial regions. Thus, molecules displaying such a pattern of expression may govern the transition from deeper layer to upper layer neuronal production. The POU-III family of transcription factors has been shown to be necessary for upper-layer neurogenesis (Dominguez et al., 2013). Correspondingly, their expression pattern was shown to mirror the generation of upper layer neurons in the VZ, by showing a high lateral-low medial expression at mid corticogenesis. Similarly, *Tbr2*, a T-box transcription factor essential for basal progenitor mediated upper layer neurogenesis, shows a high lateral-low medial gradient of expression (Bulfone et al., 1999; Englund et al., 2005). The non-coding RNA *svet1*, whose expression first appears around E13.5 in the SVZ, was also shown to increase with the onset of upper layer neurogenesis. The expression of *svet1* persists later in upper layer neurons suggesting a lineage relationship between the SVZ progenitors and the upper layer neurons they generate (Tarabykin et al., 2001). Similarly the transcription factor *Cux2* has been shown to be expressed in dividing SVZ cells and also later on in upper layer neurons (Zimmer et al., 2004). *Cux2* also appears around E13.5 and the expression levels increase as upper layer neurogenesis begins. More recently, *Cux2* was also shown to mark upper layer specific apical progenitors, the numbers of which increase with corticogenesis (Franco et al., 2012).

Surprisingly even the mutant for the apical progenitor marker *Pax6* (*Pax6$^{sey/sey}$* mutant) displays problems only with specification of upper layer neurons and not deep layer neurons (Stoykova and Gruss, 1998; Tarabykin et al., 2001; Nieto et al., 2004; Zimmer et al., 2004).

While many molecules appear later during development at the germinal zone and parallel the generation of upper layer neurogenesis, not many molecules with the opposite pattern of expression have been identified. Expression of such molecules should peak during deep layer neurogenesis and drop during upper layer neuronal production. To our knowledge, so far, no molecule with such a pattern of expression has been identified. Here, we show that the non-catalytic isoform of the neurotrophin receptor *TrkC (NC-TrkC)* is expressed at high levels in the ventricular zone during early neurogenesis (E12.5-E13.5). At E14.5, when the lateral boundaries of the neocortical VZ have already started generating upper layer neurons, *NC-TrkC* is down regulated and expression persists only in the dorso-medial cortex. At E15.5, when the progenitor zone of the neocortex is mostly producing only upper layer neurons, *NC-TrkC* expression is completely lost. Thus, we believe that *NC-TrkC* is one of the first molecules to have been shown to possess an expression pattern that would suggest a role in determining deeper layer cell fate.

Receptors lacking a kinase domain have long been thought to act as dominant negatives to the full-length receptor (Dorsey et al., 2012; Fenner, 2012; Yanpallewar et al., 2012b). This assumption however would not hold true when the different isoforms have divergent expression patterns (Menn et al., 1998b, 2000b; Rose et al., 2003). In the context of the developing neocortex, both isoforms of *TrkB* and *TrkC* have well defined and segregated expression patterns. While *NC-TrkC* is expressed both in the germinal zone and the cortical plate, *FL-TrkC* is expressed only in the cortical plate. This suggests that *NC-TrkC* has a unique role, which goes beyond acting as a dominant negative of *FL-TrkC*, within cortical progenitors. On the other hand,

since both the isoforms are co-expressed in postmitotic neurons, it is possible that within these cells, *NC-TrkC* acts as a dominant negative. However, since there is little or no *Ntf3* expression within the developing cortex, what is the role of such a dominant negative NC-TrkC, still remains unanswered.

The two different isoforms of *TrkB* also display mutually exclusive expression domains. *FL-TrkB* is expressed in postmitotic neurons and *NC-TrkB* in the lateral VZ. Numerous pieces of work have shown the importance of TrkB mediated signaling during corticogenesis (Medina et al., 2004; Bartkowska et al., 2007; Puehringer et al., 2013). Unfortunately, none of this work differentiates between the importance of the individual isoforms and their functions in controlling cortical development. Work done in other systems have attributed unique functions to the truncated Trk isoforms. For example, truncated TrkB has been shown to control Ca^{2+} signaling within glial populations (Rose et al., 2003). It is also known that waves of calcium propagate through radial glial cells and the amplitude and frequency of these waves increases as neurogenesis progresses (Weissman et al., 2004). Thus, it would be reasonable to study the role of NC-TrkB in governing radial glial proliferation and cell fate determination.

3. NC-TrkC influences cell fate by favoring deep layer neurogenesis

To study the role of NC-TrkC in cortical cell fate switch, we employed gain-of-function experiments. By doing so, we showed that *NC-TrkC* over-expression could shift neurogenesis in favor of deeper layer neuronal production. This supported our hypothesis based on the expression pattern of *NC-TrkC* that it could be a deep layer neuronal fate determinant.

NC-TrkC expression drops as upper layer neurogenesis begins. This poses the question about the cause and the consequence. Does *NC-*

TrkC down-regulation pave the way for upper layer neurogenesis or does the progressive commitment to upper layer fate lead to a down-regulation of *NC-TrkC*? Our experiments here do not support either hypothesis and analysis of TrkC mutants would be needed to answer this question. Alternatively, one could over-express the NC-TrkC at later stages to study if the fate of older progenitors can be reversed.

Apart from the over expression studies with NC-TrkC, another interesting evidence that helped further our understanding about how NC-TrkC may control cell fate was the over-expression of the Y516F NC-TrkC mutant which is incapable of binding to the signaling molecule Shc. This mutant carries a tyrosine to phenylalanine Y516F mutation, thereby rendering the receptor incapable of being phosphorylated at this residue, thus preventing the recruitment of Shc to the receptor. Since the over-expression of this mutant *NC-TrkC* did not lead to changes in cell fate, it can be concluded that signaling via this tyrosine is essential for cell fate determination.

The FL-TrkC upon ligand binding autophosphorylates and subsequently phosphorylates the tyrosine at the 516th position. This leads to Shc recruitment and downstream signaling. However, in the context of the NC-TrkC, since the receptor has no kinase domain, it is not clear as to which kinase phosphorylates this tyrosine and what happens downstream of this tyrosine phosphorylation. Recent work has shown that in cortical progenitors, Trk receptors are transactivated by the EGF-receptor via Src kinases (Puehringer et al., 2013b). This work also shows that Trk receptors expressed in embryonic cortical precursors are non-responsive to Ntf3 or BDNF. One possible explanation for this is that since only the non-catalytic isoforms of the Trk receptors are expressed by cortical progenitors, they are incapable of carrying out signaling by direct ligand binding. However, EGF mediated transactivation could lead to the phosphorylation of both NC-TrkC and NC-TrkB. Under this circumstance, Shc should be recruited to the phosphorylated NC-TrkC receptor. Further, it remains to be answered as to what happens

downstream of Shc recruitment by NC-TrkC. It is counter intuitive and highly unlikely that the recruitment of Shc by NC-TrkC would lead to the activation of the MAP kinase pathway, because of the following reasons:

a) NC-TrkC has no kinase domain to phosphorylate Shc
b) It would seem redundant to activate the same pathway as that activated directly downstream of EGFR activation, since EGFR can also directly recruit Shc and activate the MAP Kinase (MAPK) pathway.

On the other hand, it could be suggested that NC-TrkC recruitment of Shc leads to a dampening of MAP kinase signaling. Indeed, pERK1/2 is expressed in a high lateral-low medial pattern, which is opposite to that of *NC-TrkC* at E14.5. This is further supported by the appearance of p-ERK1/2 throughout the VZ at E15.5, when *NC-TrkC* has been downregulated. It is also interesting to note that the phenotype of the *ERK1/2* double mutant is very similar to the over-expression of *NC-TrkC*, which involves producing lesser upper layer neurons and more deep layer neurons (Pucilowska et al., 2012). Further, in the *Sip1* mutant, which generates upper layer neurons prematurely, p-ERK1/2 expression at E14.5 extends further medially as compared to wild type controls, suggesting that appearance of p-ERK1/2 is correlative to upper layer neurogenesis (Seuntjens et al., 2009c).

Our data also suggests that *in vitro,* NC-TrkC can dampen ERK signaling. The negative regulation of MAPK signaling by NC-TrkC could perhaps be explained by the sequestering of Shc by NC-TrkC post transactivation by EGFR. However, if this were the only reason, then NC-TrkB, which overlaps with p-ERK1/2 expression at E13.5 and 14.5, should also have dampened MAPK signaling.

It is also unclear if *NC-TrkC* promotes deeper layer neurogenesis only by negatively regulating ERK signaling or if it has independent functions during early corticogenesis. This could be answered by co-

expressing NC-TrkC and constitutively active ERK, which would allow us dissect out the NC-TrkC- MAPK dependent and independent role.

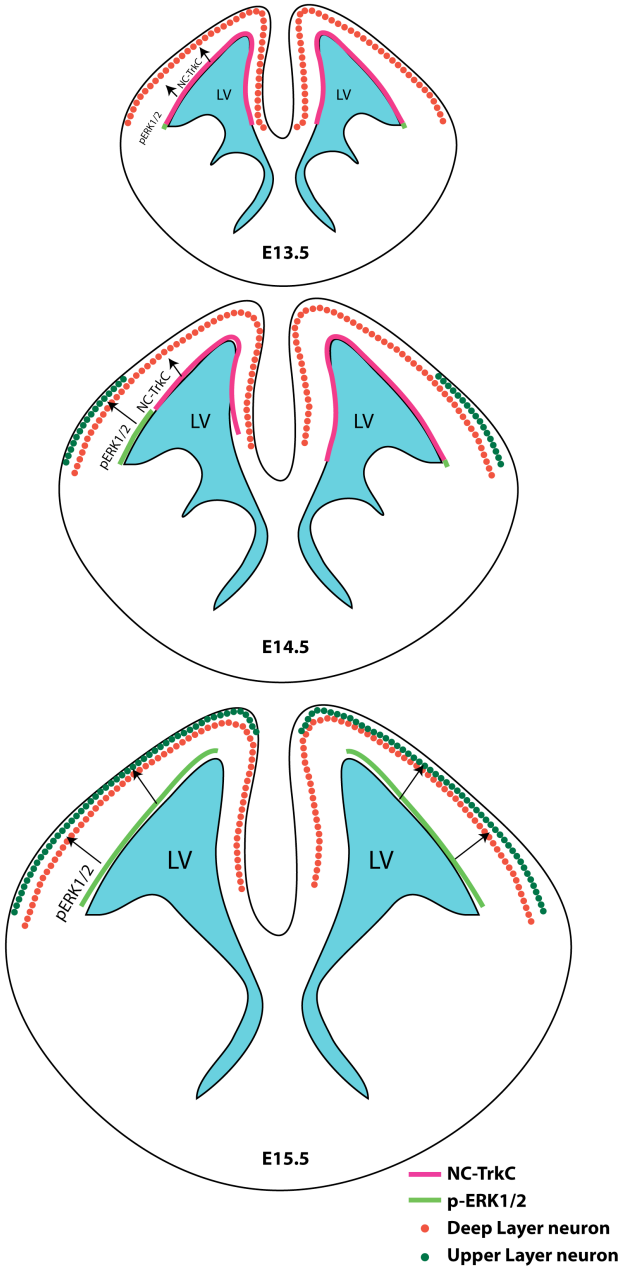

Figure 32. Expression pattern of *NC-TrkC* and p-ERK1/2.
During early corticogenesis (E13.5), *NC-TrkC* is expressed throughout the cortical VZ promoting deep layer neurogenesis. At the same time p-ERK1/2 is present at very low levels, close to the lateral edge of the cortical VZ. At E14.5, when the expression of *NC-TrkC* is restricted to more medial regions of the cortical VZ, p-ERK1/2 shifts further medially, which corresponds to the shift in deep layer to upper layer neuronal production. At E15.5, when *NC-TrkC* is absent from the cortical VZ, p-ERK1/2 is present throughout the dorsal progenitor zone and promotes upper layer neurogenesis.

4. A Ligand for the receptor?

During cortical development, expression of important signaling molecules such as BDNF, NTf3 or EGF has not been detected (Ernfors et al., 1994; Puehringer et al., 2013a). EGF expression in the embryonic striatum has although been reported. However, mice lacking their cognate receptors show a wide variety of defects including proliferation, migration and maturation (Medina et al., 2004; Puehringer et al., 2013a)

Recent work done by Puehringer et al. suggests that EGFR transactivation leads to TrkB/C phosphorylation (Puehringer et al., 2013a). Using cortical progenitor cultures the authors show that *in vitro* EGF stimulation leads to Trk phosphorylation and downstream signaling including ERK1/2 activation (Puehringer et al., 2013a). It is also important to note that while *in vitro*, EGF activation leads to ERK1/2 phosphorylation in early progenitors, pERK1/2 levels normally do not rise *in vivo* in the cortex before E15.5. Thus, EGF dependent signaling may also not be intrinsic to very early progenitors.

The lack of these above-mentioned ligands during development raises the question as to why would a system evolve to retain functional receptors without any ligand. This would then suggest a ligand independent role for these receptors, including NC-TrkC. Indeed, our experiments involving the over-expression of the NC-TrkC ΔECD mutant demonstrate that NC-TrkC by itself does not need to respond to extracellular cues for controlling cell fate switch. This poses an important question for the Ntf3 mediated feedback signaling. If NC-TrkC does not require its extracellular domain for cell fate determination, how does Ntf3 mediate its feedback effect on NC-TrkC expressing progenitors?

It is also noteworthy that Ntf3 mediated feedback-signaling leads to the opposite outcome as that of NC-TrkC over-expression. Thus, one may hypothesize that Ntf3 leads to down-regulation of NC-TrkC levels.

One possible mechanism for this can be explained on the basis of work done by Mateos et al. This work describes the shedding of the extracellular domain of NC-TrkC in response to Ntf3 stimulation (Mateos et al., 2003). This phenomenon was not observed in the full-length receptor. This could lead to the internalization of the remaining receptor thus down-regulating NC-TrkC levels. This work also showed the involvement of metalloproteinase in the shedding of the extracellular domain of NC-TrkC. Metalloproteinase such as ADAM10 have been also shown to be important for cortical development via the regulation of Notch signaling (Muraguchi et al., 2007; Jorissen et al., 2010). Thus a possible pathway linking Ntf3 to NC-TrkC and ADAM10 may connect cortical feedback signaling to cell fate decision-making.

5. NC-TrkC interacts with BMPRIA

One of the central reasons for our hypothesis that NC-TrkC functions as more than a dominant negative receptor, was based on its interaction with BMPRIA. While there has been a lot of work focusing on the interaction of the signaling pathways controlled by Trk receptors and BMP receptors, few pieces of work have studied the physical interaction of these receptors (Aubin et al., 2004; Guo and Wang, 2009). FL-TrkC is known to interact with BMPRII in cancer cell lines and prevents the interaction of the BMP class I and class II receptors, thereby preventing BMP signaling (Jin et al., 2007). We thus, wondered if the interaction of NC-TrkC and BMPRIA could also similarly prevent the association of BMPRIA and II, thereby preventing BMP signaling. However, the expression pattern of BMPRII and NC-TrkC is, to a large extent, non-overlapping. While BMPRII is expressed high laterally and low medially, NC-TrkC is expressed high medially and low laterally at E14.5. Thus, we proposed that the interaction of BMPRIA and NC-TrkC could be relevant in activating a different pathway. Our finding that NC-TrkC and BMPRIA interact with their

intracellular domains further supports a possible role for controlling downstream signaling with respect to this interaction.

One possible outcome of this interaction could be the usage of the kinase activity of BMPRIA in the NC-TrkC mediated signaling. Here, BMPRIA would serve as a co-receptor for NC-TrkC, thus initiating the signaling cascade. Indeed our results demonstrate that NC-TrkC can enhance the kinase activity of BMPRIA in a ligand independent manner. The classical BMP signaling requires ligand binding to class II BMP receptors, which in turn activate class I BMP receptors, which then activate downstream effectors (Liu and Niswander, 2005). Using an *in vitro* system we asked whether the interaction of BMPRIA with NC-TrkC could enhance its intrinsic kinase activity. Single amino acid mutations within the GS domain of the class I BMPR have been shown to dramatically enhance its kinase activity (Wieser et al., 1995). Along the same lines, the constitutive association of BMPRIA with NC-TrkC could enhance its kinase activity. Indeed, when we analyzed ligand independent Smad1 phosphorylation by BMPRIA in the absence of the class II receptors, we observed that NC-TrkC could greatly enhance the kinase activity of BMPRIA.

Since the over-expression of the Shc binding mutant of *NC-TrkC* (Y516F) did not influence cell fate, it can be assumed that signaling via this tyrosine is essential. Or in other words, Shc recruitment to NC-TrkC is necessary for cell fate determination. However, NC-TrkC itself cannot further phosphorylate Shc. Since NC-TrkC interacts with BMPRIA, Shc would be brought in close proximity of BMPRIA. This could serve to phosphorylate several possible Serine/Threonine sites on Shc, which have distinct functions compared to the tyrosine activated Shc (Zheng et al., 2013). This kind of a signaling mechanism would lead to the integration of signaling pathways and perhaps increase the repertoire of responses a cell could initiate using the same number of receptors.

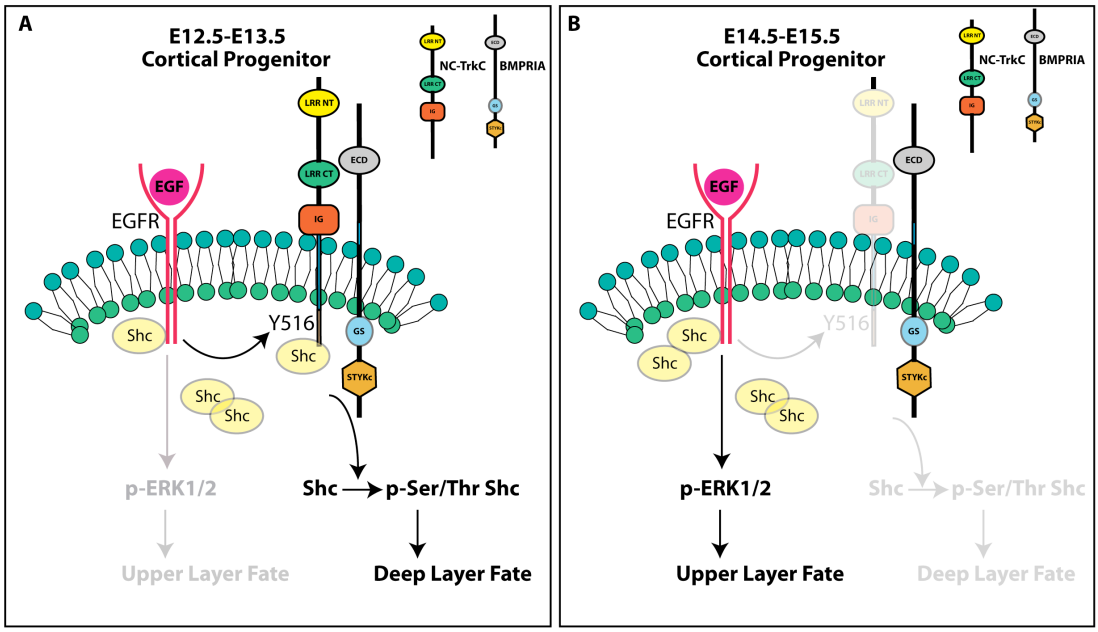

Figure 33. Model proposing NC-TrkC control over cell fate determination.
(A) During early corticogenesis, EGFR transactivation of NC-TrkC leads to the recruitment of Shc to NC-TrkC, thereby lowering free Shc available for EGFR mediates MAPK pathway activation. NC-TrkC enhances BMPRIA kinase activity and thereby promotes phosphorylation of Shc on Serine/Threonine residues. The final outcome of lowered ERK phosphorylation and Ser/Thr phosphorylation of Shc leads to a deep layer cell fate. **(B)** During late neurogenesis, NC-TrkC levels decline, thereby allowing Shc activation downstream of EGFR and hence ERK phosphorylation. The absence of Ser/Thr phosphorylated Shc accompanied by an increase in ERK phosphorylation leads to the promotion of upper layer cell fate.

6. Multiple pathways control cortical feedback signaling

Since the deletion of *Ntf3* from the *Sip1* mutant cortex does not rescue the *Sip1* mutant phenotype, it implied that either Ntf3 was not involved in feedback signaling or that multiple pathways are involved in feedback signaling. Our results with the over-expression of *Ntf3* clearly demonstrate the important role of *Ntf3* in feedback signaling. Thus, we postulated that multiple pathways may exist downstream of Sip1 that contribute to cortical feedback signaling.

Using microarray data collected from comparing *Sip1* mutant cortices to wildtype cortices, we narrowed in on a family of transneuronal cytokines. *Cbln4*, a member of this family, was upregulated in the *Sip1* mutant. This was further verified with *in situ* hybridization. While

Cbln4 is upregulated in the *Sip1* mutant cortex, *in vitro Sip1* activates transcription of a *Cbln4* enhancer region. This was surprising given that Sip1 normally functions as a transcriptional repressor (Comijn et al., 2001). However, is certain systems and genomic contexts, Sip1 is known to function as an activator too (Yoshimoto et al., 2005). Thus, while we cannot assign a direct role to Sip1 in regulating the expression of *Cbln4*, we found that Sip1 can bind to the enhancer region *in vitro* and thus making it likely that it does so *in vivo* too.

Since the various member of the Cbln family of proteins share a high degree of homology, we studied the role of all of them in feedback signaling (Iijima et al., 2007; Yuzaki, 2008). However, since Cbln3 is not secreted by itself, it was omitted from our functional studies. Over-expression of *Cbln1*, *2* and *4* lead to an increase in the number of Tbr2 positive basal progenitors, similar to that achieved on *Ntf3* over-expression. However, the effect of the Cbln family on the apical Pax6 positive population differed from that of Ntf3. While Ntf3 lowered the number of Pax6 positive cells, all three Cbln family members caused an increase in the number of VZ progenitors. Thus, while Ntf3 shifts the balance between apical and basal progenitors, the Cbln family causes a general increase in proliferation of cortical progenitors. This is also confirmed by the increase in BrdU positive cells observed in the cortical plate after Cbln4 *in utero* electroporation. More detailed phenotypic analysis of the effects of Cbln family over-expression would be required to understand the role of this family in cell fate switch.

Another experiment that hints towards a different signaling pathway employed by Ntf3 and the Cbln family is the location of their cognate receptors. The receptor for Ntf3- NC-TrkC is located in the VZ and the protein localizes to the ventricular lumen. Using alkaline phosphatase tagged Cbln4, we localized the receptor for Cbln4 within the cortical plate. The pattern of signal produced resembled segments of radial glia processes. While the E14.5 cDNA library still needs to be screened

for candidate receptors, the location of the cognate receptor supports the usage of two alternate pathways by these molecules.

The Cbln family is also interesting from another point of view. Cbln1, the most studied member of this family, has been known to function as a bi-directional signaling molecule during synaptic development (Uemura et al., 2010). Cbln1 binds to GluR∂2 post-synaptically and Neurxin1 pre-synaptically. It is thus possible that the Cbln family plays a similar role in the developing cortex, wherein they bind to receptors on the radial glial process and cortical postmitotic neurons. This kind of a signaling mechanism may regulate feedback signaling and postmitotic maturation of neurons. This might be necessary for coupling neuronal differentiation to neuronal production.

REFERENCES

Anderson GJ, Darshan D (2008) Small-molecule dissection of BMP signaling. Nat Chem Biol 4:15–16.

Angevine JB, Sidman RL (1961) Autoradiographic study of cell migration during histogenesis of cerebral cortex in the mouse. Nature 192:766–768.

Anthony TE, Klein C, Fishell G, Heintz N (2004) Radial glia serve as neuronal progenitors in all regions of the central nervous system. Neuron 41:881–890.

Arnold SJ, Huang G-J, Cheung AFP, Era T, Nishikawa S-I, Bikoff EK, Molnár Z, Robertson EJ, Groszer M (2008) The T-box transcription factor Eomes/Tbr2 regulates neurogenesis in the cortical subventricular zone. Genes Dev 22:2479–2484.

Aubin J, Davy A, Soriano P (2004) In vivo convergence of BMP and MAPK signaling pathways: impact of differential Smad1 phosphorylation on development and homeostasis. Genes Dev 18:1482–1494.

Barnabé-Heider F, Wasylnka JA, Fernandes KJL, Porsche C, Sendtner M, Kaplan DR, Miller FD (2005) Evidence that embryonic neurons regulate the onset of cortical gliogenesis via cardiotrophin-1. Neuron 48:253–265.

Bartkowska K, Paquin A, Gauthier AS, Kaplan DR, Miller FD (2007) Trk signaling regulates neural precursor cell proliferation and differentiation during cortical development. Development 134:4369–4380.

Bayatti N, Sarma S, Shaw C, Eyre J a, Vouyiouklis D a, Lindsay S, Clowry GJ (2008b) Progressive loss of PAX6, TBR2, NEUROD and TBR1 mRNA gradients correlates with translocation of EMX2 to the cortical plate during human cortical development. Eur J Neurosci 28:1449–1456.

Bodmer J-L, Schneider P, Tschopp J (2002) The molecular architecture of the TNF superfamily. Trends Biochem Sci 27:19–26.

Brennan C, Fabes J (2003) Alkaline phosphatase fusion proteins as affinity probes for protein localization studies. Sci STKE 2003:PL2.

Bulfone a, Martinez S, Marigo V, Campanella M, Basile a, Quaderi N, Gattuso C, Rubenstein JL, Ballabio a (1999) Expression pattern of the Tbr2 (Eomesodermin) gene during mouse and chick brain development. Mech Dev 84:133–138.

Carim-Todd L, Bath KG, Fulgenzi G, Yanpallewar S, Jing D, Barrick CA, Becker J, Buckley H, Dorsey SG, Lee FS, Tessarollo L (2009) Endogenous truncated TrkB.T1 receptor regulates neuronal complexity and TrkB kinase receptor function in vivo. J Neurosci 29:678–685.

Chao M V (2003) Neurotrophins and their receptors: a convergence point for many signalling pathways. Nat Rev Neurosci 4:299–309.

Choe Y, Siegenthaler J a, Pleasure SJ (2012) A cascade of morphogenic signaling initiated by the meninges controls corpus callosum formation. Neuron 73:698–712.

Comijn J, Berx G, Vermassen P, Verschueren K, Van Grunsven L, Bruyneel E, Mareel M, Huylebroeck D, Van Roy F (2001) The two-handed E box binding zinc finger protein SIP1 downregulates E-cadherin and induces invasion. Mol Cell 7:1267–1278.

Conti L, De Fraja C, Gulisano M, Migliaccio E, Govoni S, Cattaneo E (1997) Expression and activation of SH2/PTB-containing ShcA adaptor protein reflects the pattern of neurogenesis in the mammalian brain. Proc Natl Acad Sci U S A 94:8185–8190.

Conti L, Sipione S, Magrassi L, Bonfanti L, Rigamonti D, Pettirossi V, Peschanski M, Haddad B, Pelicci P, Milanesi G, Pelicci G, Cattaneo E (2001) Shc signaling in differentiating neural progenitor cells. Nat Neurosci 4:579–586 Available at: http://www.ncbi.nlm.nih.gov/pubmed/11369938.

Cordon-Cardo C, Tapley P, Jing SQ, Nanduri V, O'Rourke E, Lamballe F, Kovary K, Klein R, Jones KR, Reichardt LF (1991) The trk tyrosine protein kinase mediates the mitogenic properties of nerve growth factor and neurotrophin-3. Cell 66:173–183.

De Vries L, Finana F, Cachoux F, Vacher B, Sokoloff P, Cussac D (2010) Cellular BRET assay suggests a conformational rearrangement of preformed TrkB/Shc complexes following BDNF-dependent activation. Cell Signal 22:158–165.

Dehay C, Savatier P, Cortay V, Kennedy H (2001a) Cell-cycle kinetics of neocortical precursors are influenced by embryonic thalamic axons. J Neurosci 21:201–214.

Dehay C, Savatier P, Cortay V, Kennedy H (2001b) Cell-cycle kinetics of neocortical precursors are influenced by embryonic thalamic axons. J Neurosci 21:201–214.

Desai AR, McConnell SK (2000) Progressive restriction in fate potential by neural progenitors during cerebral cortical development. Development 127:2863–2872.

Dickinson ME, Selleck MA, McMahon AP, Bronner-Fraser M (1995) Dorsalization of the neural tube by the non-neural ectoderm. Development 121:2099–2106.

Dominguez MH, Ayoub AE, Rakic P (2013) POU-III transcription factors (Brn1, Brn2, and Oct6) influence neurogenesis, molecular identity, and migratory destination of upper-layer cells of the cerebral cortex. Cereb Cortex 23:2632–2643.

Dorsey SG et al. (2012) Genetic deletion of trkB.T1 increases neuromuscular function. AJP Cell Physiol 302:C141–C153.

Englund C, Fink A, Lau C, Pham D, Daza RAM, Bulfone A, Kowalczyk T, Hevner RF (2005a) Pax6, Tbr2, and Tbr1 are expressed sequentially by radial glia, intermediate progenitor cells, and postmitotic neurons in developing neocortex. J Neurosci 25:247–251.

Ernfors P, Lee KF, Jaenisch R (1994) Mice lacking brain-derived neurotrophic factor develop with sensory deficits. Nature 368:147–150.

Esteban PF, Yoon H-Y, Becker J, Dorsey SG, Caprari P, Palko ME, Coppola V, Saragovi HU, Randazzo PA, Tessarollo L (2006) A kinase-deficient TrkC receptor isoform activates Arf6-Rac1 signaling through the scaffold protein tamalin. J Cell Biol 173:291–299.

Fenner BM (2012) Truncated TrkB: Beyond a dominant negative receptor. Cytokine Growth Factor Rev 23:15–24.

Fishell G, Hanashima C (2008) Pyramidal neurons grow up and change their mind. Neuron 57:333–338.

Flanagan BJG, Lu Q, Vanderhaeghen P (1990) [2] Alkaline Phosphatase Fusions of Ligands or Receptors as in Situ Probes for Staining of Cells , Tissues , and Embryos. 321.

Flanagan JG, Cheng HJ (2000) Alkaline phosphatase fusion proteins for molecular characterization and cloning of receptors and their ligands. Methods Enzymol 327:198–210.

Franco SJ, Gil-Sanz C, Martinez-Garay I, Espinosa A, Harkins-Perry SR, Ramos C, Muller U (2012a) Fate-restricted neural progenitors in the mammalian cerebral cortex. Science (80-) 337:746–749.

Franco SJ, Muller U (2013) Shaping our minds: stem and progenitor cell diversity in the mammalian neocortex. Neuron 77:19–34 Available at: http://www.ncbi.nlm.nih.gov/pubmed/23312513.

Frantz GD, McConnell SK (1996) Restriction of late cerebral cortical progenitors to an upper-layer fate. Neuron 17:55–61.

Goebbels S, Bormuth I, Bode U, Hermanson O, Schwab MH, Nave K-A (2006) Genetic targeting of principal neurons in neocortex and hippocampus of NEX-Cre mice. Genesis 44:611–621.

Gomes JR, Costa JT, Melo C V., Felizzi F, Monteiro P, Pinto MJ, Inacio AR, Wieloch T, Almeida RD, Graos M, Duarte CB (2012) Excitotoxicity Downregulates TrkB.FL Signaling and Upregulates the Neuroprotective Truncated TrkB Receptors in Cultured Hippocampal and Striatal Neurons. J Neurosci 32:4610–4622.

Gorski JA, Talley T, Qiu M, Puelles L, Rubenstein JLR, Jones KR (2002) Cortical excitatory neurons and glia, but not GABAergic neurons, are produced in the Emx1-expressing lineage. J Neurosci 22:6309–6314.

Götz M, Huttner WB (2005) The cell biology of neurogenesis. Nat Rev Mol Cell Biol 6:777–788.

Guo C, Eckler MJ, McKenna WL, McKinsey GL, Rubenstein JLR, Chen B (2013) Fezf2 expression identifies a multipotent progenitor for neocortical projection neurons, astrocytes, and oligodendrocytes. Neuron 80:1167–1174.

Guo X, Wang X (2009) Signaling cross-talk between TGF- β / BMP and other path- ways. :71–88.

Haubensak W, Attardo A, Denk W, Huttner WB (2004a) Neurons arise in the basal neuroepithelium of the early mammalian

telencephalon: a major site of neurogenesis. Proc Natl Acad Sci U S A 101:3196–3201.

Heins N, Malatesta P, Cecconi F, Nakafuku M, Tucker KL, Hack M a, Chapouton P, Barde Y-A, Götz M (2002) Glial cells generate neurons: the role of the transcription factor Pax6. Nat Neurosci 5:308–315 Available at: http://www.ncbi.nlm.nih.gov/pubmed/11896398 [Accessed January 24, 2014].

Higashi Y, Maruhashi M, Nelles L, Putte T Van De, Verschueren K, Miyoshi T, Yoshimoto A, Kondoh H, Huylebroeck D (2002) Generation of the Floxed Allele of the SIP1 (Smad-Interacting Protein 1) Gene for Cre-Mediated Conditional Knockout in the Mouse. 84:82–84.

Hill RS, Walsh C a (2005) Molecular insights into human brain evolution. Nature 437:64–67.

Iacopetti P, Michelini M, Stuckmann I, Oback B, Aaku-Saraste E, Huttner WB (1999) Expression of the antiproliferative gene TIS21 at the onset of neurogenesis identifies single neuroepithelial cells that switch from proliferative to neuron-generating division. Proc Natl Acad Sci U S A 96:4639–4644.

Iijima T, Miura E, Matsuda K, Kamekawa Y, Watanabe M, Yuzaki M (2007) Characterization of a transneuronal cytokine family Cbln--regulation of secretion by heteromeric assembly. Eur J Neurosci 25:1049–1057.

Jin W, Yun C, Kim H-S, Kim S-J (2007) TrkC binds to the bone morphogenetic protein type II receptor to suppress bone morphogenetic protein signaling. Cancer Res 67:9869–9877 Available at: http://www.ncbi.nlm.nih.gov/pubmed/17942918 [Accessed January 27, 2014].

Jing S, Tapley P, Barbacid M (1992) Nerve growth factor mediates signal transduction through trk homodimer receptors. Neuron 9:1067–1079.

Jorissen E, Prox J, Bernreuther C, Weber S, Schwanbeck R, Serneels L, Snellinx A, Craessaerts K, Thathiah A, Tesseur I, Bartsch U, Weskamp G, Blobel CP, Glatzel M, De Strooper B, Saftig P (2010) The disintegrin/metalloproteinase ADAM10 is essential for the establishment of the brain cortex. J Neurosci 30:4833–4844.

Kishore U, Gaboriaud C, Waters P, Shrive AK, Greenhough TJ, Reid KBM, Sim RB, Arlaud GJ (2004) C1q and tumor necrosis factor superfamily: modularity and versatility. Trends Immunol 25:551–561.

Klein R, Conway D, Parada LF, Barbacid M (1990) The trkB tyrosine protein kinase gene codes for a second neurogenic receptor that lacks the catalytic kinase domain. Cell 61:647–656.

Klein R, Nanduri V, Jing SA, Lamballe F, Tapley P, Bryant S, Cordon-Cardo C, Jones KR, Reichardt LF, Barbacid M (1991) The trkB tyrosine protein kinase is a receptor for brain-derived neurotrophic factor and neurotrophin-3. Cell 66:395–403.

Kowalczyk T, Pontious A, Englund C, Daza RAM, Bedogni F, Hodge R, Attardo A, Bell C, Huttner WB, Hevner RF (2009) Intermediate neuronal progenitors (basal progenitors) produce pyramidal-projection neurons for all layers of cerebral cortex. Cereb Cortex 19:2439–2450.

Lamballe F, Klein R, Barbacid M (1991) trkC, a new member of the trk family of tyrosine protein kinases, is a receptor for neurotrophin-3. Cell 66:967–979.

Lehtinen MK, Zappaterra MW, Chen X, Yang YJ, Hill AD, Lun M, Maynard T, Gonzalez D, Kim S, Ye P, D'Ercole AJ, Wong ET, LaMantia AS, Walsh CA (2011) The cerebrospinal fluid provides a proliferative niche for neural progenitor cells. Neuron 69:893–905.

Lemmon MA, Schlessinger J (1994) Regulation of signal transduction and signal diversity by receptor oligomerization. Trends Biochem Sci 19:459–463.

Liu A, Niswander L a (2005) Bone morphogenetic protein signalling and vertebrate nervous system development. Nat Rev Neurosci 6:945–954.

Mabie PC, Mehler MF, Kessler J a (1999) Multiple roles of bone morphogenetic protein signaling in the regulation of cortical cell number and phenotype. J Neurosci 19:7077–7088.

Malatesta P, Hartfuss E, Götz M (2000) Isolation of radial glial cells by fluorescent-activated cell sorting reveals a neuronal lineage. Development 127:5253–5263 Available at: http://www.ncbi.nlm.nih.gov/pubmed/11076748.

Martin-Zanca D, Barbacid M, Parada LF (1990) Expression of the trk proto-oncogene is restricted to the sensory cranial and spinal ganglia of neural crest origin in mouse development. Genes Dev 4:683–694.

Martínez-Cerdeño V, Noctor SC, Kriegstein AR (2006) The role of intermediate progenitor cells in the evolutionary expansion of the cerebral cortex. Cereb Cortex 16 Suppl 1:i152–i161.

Mateos S, Calothy G, Lamballe F (2003) The noncatalytic TrkCNC2 receptor is cleaved by metalloproteases upon neurotrophin-3 stimulation. Oncogene 22:740–745.

Matsuda K, Miura E, Miyazaki T, Kakegawa W, Emi K, Narumi S, Fukazawa Y, Ito-Ishida A, Kondo T, Shigemoto R, Watanabe M, Yuzaki M (2010) Cbln1 is a ligand for an orphan glutamate receptor delta2, a bidirectional synapse organizer. Science 328:363–368.

McConnell SK, Ghosh A, Shatz CJ (1989) Subplate neurons pioneer the first axon pathway from the cerebral cortex. Science 245:978–982.

Medina DL, Sciarretta C, Calella AM, Von Bohlen Und Halbach O, Unsicker K, Minichiello L (2004) TrkB regulates neocortex formation through the Shc/PLCgamma-mediated control of neuronal migration. EMBO J 23:3803–3814.

Menn B, Timsit S, Calothy G, Lamballe F (1998a) Differential expression of TrkC catalytic and noncatalytic isoforms suggests

that they act independently or in association. J Comp Neurol 401:47–64.

Menn B, Timsit S, Represa A, Mateos S, Calothy G, Lamballe F (2000a) Spatiotemporal expression of noncatalytic TrkC NC2 isoform during early and late CNS neurogenesis: a comparative study with TrkC catalytic and p75NTR receptors. Eur J Neurosci 12:3211–3223.

Middlemas DS, Lindberg RA, Hunter T (1991) trkB, a neural receptor protein-tyrosine kinase: evidence for a full-length and two truncated receptors. Mol Cell Biol 11:143–153.

Minichiello L (2009) TrkB signalling pathways in LTP and learning. Nat Rev Neurosci 10:850–860.

Miquelajauregui A, Van de Putte T, Polyakov A, Nityanandam A, Boppana S, Seuntjens E, Karabinos A, Higashi Y, Huylebroeck D, Tarabykin V (2007) Smad-interacting protein-1 (Zfhx1b) acts upstream of Wnt signaling in the mouse hippocampus and controls its formation. Proc Natl Acad Sci U S A 104:12919–12924 Available at: http://www.ncbi.nlm.nih.gov/pubmed/17644613.

Miura E, Iijima T, Yuzaki M, Watanabe M (2006) Distinct expression of Cbln family mRNAs in developing and adult mouse brains. Eur J Neurosci 24:750–760.

Miyata T, Kawaguchi A, Okano H, Ogawa M (2001) Asymmetric inheritance of radial glial fibers by cortical neurons. Neuron 31:727–741.

Mizutani K, Saito T (2005) Progenitors resume generating neurons after temporary inhibition of neurogenesis by Notch activation in the mammalian cerebral cortex. Development 132:1295–1304.

Molyneaux BJ, Arlotta P, Menezes JRL, Macklis JD (2007) Neuronal subtype specification in the cerebral cortex. Nat Rev Neurosci 8:427–437 Available at: http://www.ncbi.nlm.nih.gov/pubmed/17514196 [Accessed February 20, 2014].

Muraguchi T, Takegami Y, Ohtsuka T, Kitajima S, Chandana EPS, Omura A, Miki T, Takahashi R, Matsumoto N, Ludwig A, Noda M, Takahashi C (2007) RECK modulates Notch signaling during cortical neurogenesis by regulating ADAM10 activity. Nat Neurosci 10:838–845.

Nguyen VH, Trout J, Connors SA, Andermann P, Weinberg E, Mullins MC (2000) Dorsal and intermediate neuronal cell types of the spinal cord are established by a BMP signaling pathway. Development 127:1209–1220.

Nieto M, Monuki ES, Tang H, Imitola J, Haubst N, Khoury SJ, Cunningham J, Gotz M, Walsh C a (2004) Expression of Cux-1 and Cux-2 in the subventricular zone and upper layers II-IV of the cerebral cortex. J Comp Neurol 479:168–180.

Nityanandam A (2009) Investigation of Sip1 gene interactions in the development of the mammalian telencephalon. PhD thesis.

Noctor SC, Flint a C, Weissman T a, Dammerman RS, Kriegstein a R (2001) Neurons derived from radial glial cells establish radial units in neocortex. Nature 409:714–720.

Noctor SC, Martínez-Cerdeño V, Ivic L, Kriegstein AR (2004) Cortical neurons arise in symmetric and asymmetric division zones and migrate through specific phases. Nat Neurosci 7:136–144.

Nonaka-Kinoshita M, Reillo I, Artegiani B, Martinez-Martinez MA, Nelson M, Borrell V, Calegari F (2013a) Regulation of cerebral cortex size and folding by expansion of basal progenitors. EMBO J 32:1817–1828.

Panchision DM, Pickel JM, Studer L, Lee SH, Turner P a, Hazel TG, McKay RD (2001) Sequential actions of BMP receptors control neural precursor cell production and fate. Genes Dev 15:2094–2110.

Pucilowska J, Puzerey P a, Karlo JC, Galán RF, Landreth GE (2012) Disrupted ERK signaling during cortical development leads to abnormal progenitor proliferation, neuronal and network excitability and behavior, modeling human neuro-cardio-facial-cutaneous and related syndromes. J Neurosci 32:8663–8677.

Puehringer D, Orel N, Luningschror P, Subramanian N, Herrmann T, Chao M V, Sendtner M (2013a) EGF transactivation of Trk receptors regulates the migration of newborn cortical neurons. Nat Neurosci 16:407–415.

Rakic P (1974) Neurons in rhesus monkey visual cortex: systematic relation between time of origin and eventual disposition. Science 183:425–427.

Rakic P (2003) Developmental and evolutionary adaptations of cortical radial glia. Cereb Cortex 13:541–549.

Ravichandran KS (2001) Signaling via Shc family adapter proteins. Oncogene 20:6322–6330.

Renn CL, Leitch CC, Dorsey SG (2009) In vivo evidence that truncated trkB.T1 participates in nociception. Mol Pain 5:61.

Rose CR, Blum R, Pichler B, Lepier A, Kafitz KW, Konnerth A (2003) Truncated TrkB-T1 mediates calcium signalling in glia cells. 426.

Saito T (2006) In vivo electroporation in the embryonic mouse central nervous system. Nat Protoc 1:1552–1558.

Samanta J, Burke GM, McGuire T, Pisarek AJ, Mukhopadhyay A, Mishina Y, Kessler J a (2007) BMPR1a signaling determines numbers of oligodendrocytes and calbindin-expressing interneurons in the cortex. J Neurosci 27:7397–7407.

Sanderson KJ, Weller WL (1990) Gradients of neurogenesis in possum neocortex. Brain Res Dev Brain Res 55:269–274 Available at: http://www.ncbi.nlm.nih.gov/pubmed/2253327.

Seuntjens E, Nityanandam A, Miquelajauregui A, Debruyn J, Stryjewska A, Goebbels S, Nave K-A, Huylebroeck D, Tarabykin V (2009a) Sip1 regulates sequential fate decisions by feedback signaling from postmitotic neurons to progenitors. Nat Neurosci 12:1373–1380.

Shen Q, Wang Y, Dimos JT, Fasano CA, Phoenix TN, Lemischka IR, Ivanova NB, Stifani S, Morrisey EE, Temple S (2006) The timing of cortical neurogenesis is encoded within lineages of individual progenitor cells. Nat Neurosci 9:743–751.

Siegenthaler JA, Pleasure SJ (2011) We have got you "covered": how the meninges control brain development. Curr Opin Genet Dev 21:249–255 Available at: http://www.ncbi.nlm.nih.gov/pubmed/21251809.

Soppet D, Escandon E, Maragos J, Middlemas DS, Reid SW, Blair J, Burton LE, Stanton BR, Kaplan DR, Hunter T, Nikolics K, Parada LF (1991) The neurotrophic factors brain-derived neurotrophic factor and neurotrophin-3 are ligands for the trkB tyrosine kinase receptor. Cell 65:895–903.

Stahl R, Walcher T, De Juan Romero C, Pilz GA, Cappello S, Irmler M, Sanz-Aquela JM, Beckers J, Blum R, Borrell V, Götz M (2013) Trnp1 regulates expansion and folding of the mammalian cerebral cortex by control of radial glial fate. Cell 153:535–549.

Stoykova A, Gruss P (1998) Pax6 Controls Radial Glia Differentiation. 21:1031–1044.

Takahashi H, Arstikaitis P, Prasad T, Bartlett TE, Wang YT, Murphy TH, Craig AM (2011) Postsynaptic TrkC and presynaptic PTPσ function as a bidirectional excitatory synaptic organizing complex. Neuron 69:287–303.

Takahashi T (1995) The Cell Cycle of the Pseudostratified Embryonic Murine Cerebral Wall Ventricular Epithelium of the. 15:6046–6057.

Tarabykin V, Stoykova A, Usman N, Gruss P (2001) Cortical upper layer neurons derive from the subventricular zone as indicated by Svet1 gene expression. Development 128:1983–1993.

Timmer JR, Wang C, Niswander L (2002) BMP signaling patterns the dorsal and intermediate neural tube via regulation of homeobox and helix-loop-helix transcription factors. Development 129:2459–2472.

Tsoulfas P, Soppet D, Escandon E, Tessarollo L, Mendoza-Ramirez J-L, Rosenthal A, Nikolics K, Parada LF (1993) The rat trkC locus encodes multiple neurogenic receptors that exhibit differential response to neurotrophin-3 in PC12 cells. Neuron 10:975–990.

Uemura T, Lee S-J, Yasumura M, Takeuchi T, Yoshida T, Ra M, Taguchi R, Sakimura K, Mishina M (2010) Trans-synaptic interaction of GluRdelta2 and Neurexin through Cbln1 mediates synapse formation in the cerebellum. Cell 141:1068–1079.

Valenzuela DM, Maisonpierre PC, Glass DJ, Rojas E, Nuez L, Kong Y, Gies DR, Stitt TN, Ip NY, Yancopoulos GD (1993) Alternative Forms of Rat TrkC with Different Functional Capabilities. 10:963–974.

Van de Putte T, Maruhashi M, Francis A, Nelles L, Kondoh H, Huylebroeck D, Higashi Y (2003) Mice lacking ZFHX1B, the gene that codes for Smad-interacting protein-1, reveal a role for multiple neural crest cell defects in the etiology of Hirschsprung

disease-mental retardation syndrome. Am J Hum Genet 72:465–470.

Verstappen G, van Grunsven LA, Michiels C, Van de Putte T, Souopgui J, Van Damme J, Bellefroid E, Vandekerckhove J, Huylebroeck D (2008) Atypical Mowat-Wilson patient confirms the importance of the novel association between ZFHX1B/SIP1 and NuRD corepressor complex. Hum Mol Genet 17:1175–1183.

Wei P, Pattarini R, Rong Y, Guo H, Bansal PK, Kusnoor S V, Deutch AY, Parris J, Morgan JI (2012) The Cbln family of proteins interact with multiple signaling pathways. J Neurochem 121:717–729

Weissman T a, Riquelme P a, Ivic L, Flint AC, Kriegstein AR (2004) Calcium waves propagate through radial glial cells and modulate proliferation in the developing neocortex. Neuron 43:647–661.

Wieser R, Wrana JL, Massagué J (1995) GS domain mutations that constitutively activate T beta R-I, the downstream signaling component in the TGF-beta receptor complex. EMBO J 14:2199–2208.

Yanpallewar SU, Barrick CA, Buckley H, Becker J, Tessarollo L (2012a) Deletion of the BDNF Truncated Receptor TrkB.T1 Delays Disease Onset in a Mouse Model of Amyotrophic Lateral Sclerosis. PLoS One 7:e39946.

Yoshimoto A, Saigou Y, Higashi Y, Kondoh H (2005) Regulation of ocular lens development by Smad-interacting protein 1 involving Foxe3 activation. Development 132:4437–4448.

Yuzaki M (2008) Cbln and C1q family proteins: new transneuronal cytokines. Cell Mol Life Sci 65:1698–1705.

Zarbalis K, Siegenthaler JA, Choe Y, May SR, Peterson AS, Pleasure SJ (2007) Cortical dysplasia and skull defects in mice with a Foxc1 allele reveal the role of meningeal differentiation in regulating cortical development. Proc Natl Acad Sci U S A 104:14002–14007.

Zheng Y, Zhang C, Croucher DR, Soliman M a, St-Denis N, Pasculescu A, Taylor L, Tate S a, Hardy WR, Colwill K, Dai AY, Bagshaw R, Dennis JW, Gingras A-C, Daly RJ, Pawson T (2013) Temporal regulation of EGF signalling networks by the scaffold protein Shc1. Nature 499:166–171.

Zimmer C, Tiveron M-C, Bodmer R, Cremer H (2004a) Dynamics of Cux2 expression suggests that an early pool of SVZ precursors is fated to become upper cortical layer neurons. Cereb Cortex 14:1408–1420.